Supporting Information

Native Carboxylate-Assisted Enantioselective C–H Annulations with Allenes and 1,3-Dienes on Ferrocene

Devendra Parganiha, Yagya Dutt Upadhyay, Sumit Khevariya,[#] Pruthviraj Amar Patil,[#] Svastik Jaiswal, Yogesh Dhasmana, and Sangit Kumar[*]

Department of Chemistry, Indian Institute of Science Education and Research (IISER) Bhopal, Bhopal By-pass Road, Bhauri, Bhopal, Madhya Pradesh, India, 462 066

E-mail: sangitkumar@iiserb.ac.in

General Experimental Details

Starting materials were prepared under an inert atmosphere (N_2, Ar), and Pd-catalyzed ferrocene fused isochroman derivatives were prepared under dry air. Primary analyses were carried out using thin-layer chromatography (TLC) with silica-coated plates. Reagents were procured from commercial sources, including Sigma Aldrich, Alfa Aesar, BLD Pharma, and Spectrochem. The solvents were meticulously dried following standard procedures. Nuclear Magnetic Resonance (NMR) spectral data were collected using Bruker 400, 500, and 700 MHz spectrometers, with chemical shift values reported in parts per million (ppm) relative to $CDCl_3$ as an internal standard (7.26 ppm for ^1H, 77.16 ppm for ^{13}C). ^{19}F NMR data are reported in δ units (ppm) and were measured relative to the signals for residual $CFCl_3$ (0.00 ppm) in the deuterated chloroform solvent unless otherwise stated. Multiplicity was denoted using the following abbreviations: s (singlet), d (doublet), t (triplet), q (quartet), dd (doublet of doublet), td (triplet of doublet), and m (multiplet). High-resolution mass spectrometric (HRMS) analyses were performed using a quadrupole time-of-flight mass spectrometry (Q-TOF-MS) instrument with an electrospray ionization (ESI) technique. Chiral analysis was carried out using high-performance liquid chromatography (HPLC) equipment from Agilent Technologies and PerkinElmer for compounds **3a** and **3h** only employing CHIRALCELL OZ-3, AD-H, and AD-3 chiral HPLC columns. The weighing balance utilized was from Sartorius (model BSA224S-CW). Single crystal X-ray data were collected using a Bruker APEX-II CCD diffractometer equipped with a CMOS Photon 100 detector. Crystal structures were refined using the Olex2 and WinGX Program System package with the SHELXL-2019/2 program. The starting material and amines were freshly prepared by following a reported procedure with slight modifications, while ferrocene carboxylic acid and its derivatives[1] were directly purchased from BLD Pharm India and used without further purification or synthesized according to the literature. Amino acids and *R*-BINOL were directly purchased from commercial sources and further modified using the reported procedure.

Synthesis of precursors 2a-2m

Allenes **2a-2k**, and diene **(2l-2m)** were synthesized according to the previously reported literature procedure[2], and allene **2g** was purchased commercially.

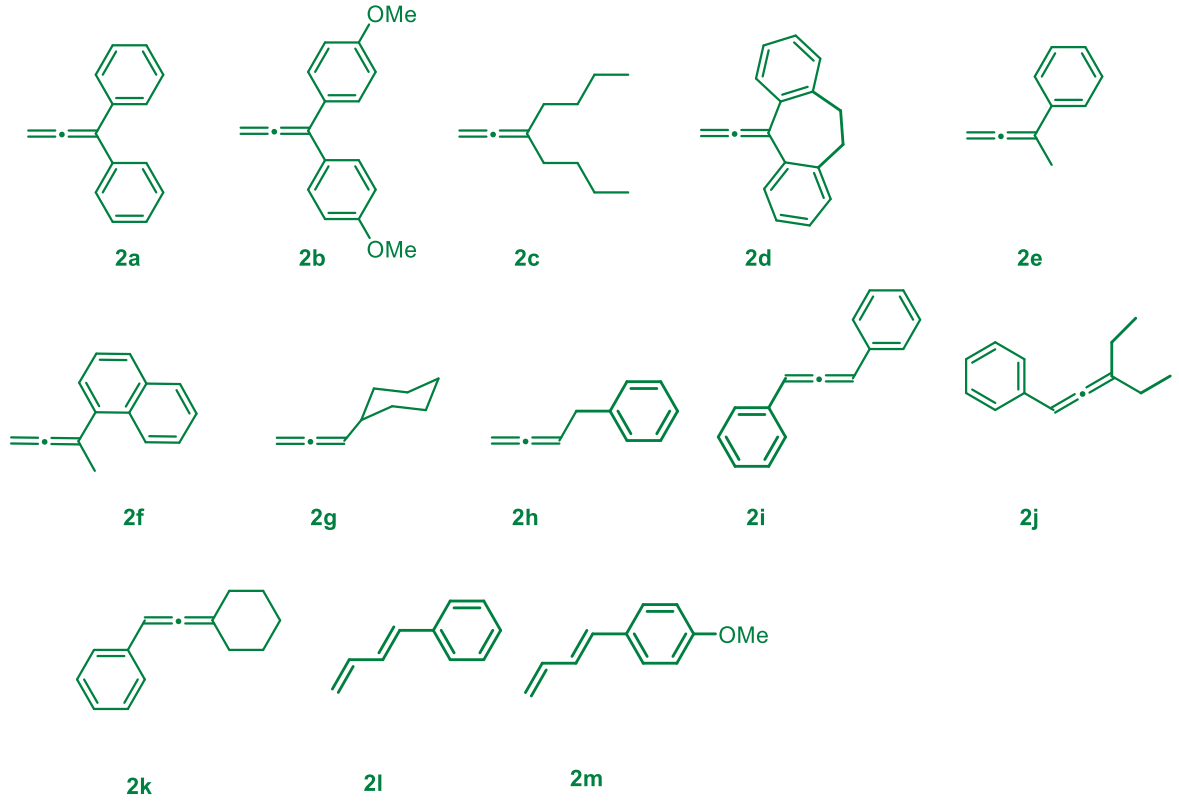

Figure S1. Synthesis of allenes and dienes **2a-2m.**

Synthesis of ligand L1-L12

Monoprotected amino acid-derived ligand **L1-L9, L11** was synthesized according to the reported literature[3] procedure and **L10, L12** was purchased commercially.

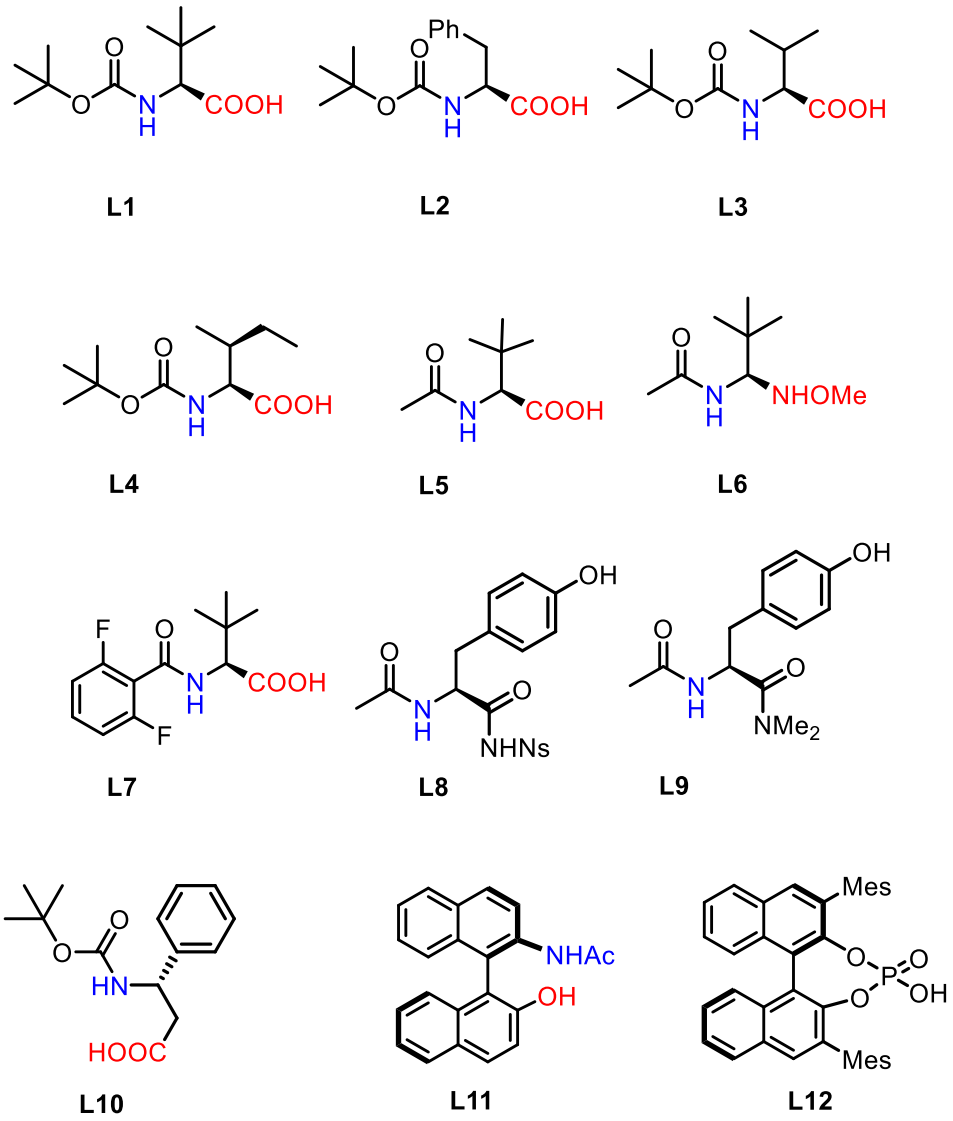

Figure S2. List of ligand **L1-L12**

Reaction Optimization

Reaction optimization for enantioselective synthesis of ferrocene fused isochroman derivatives

Table S1. Reaction optimization by varying the solvents, time, and temperature [a]

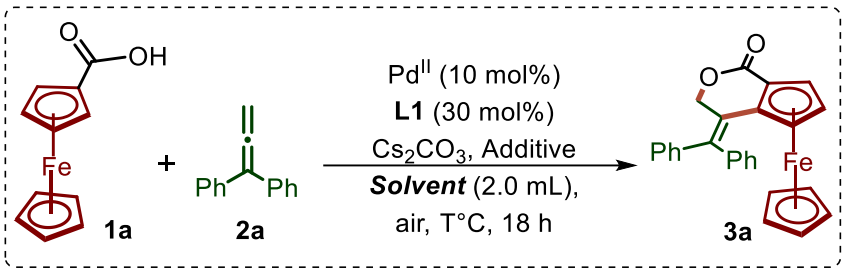

Entry	Solvent	Additive	Temp. (°C)	Yield (%)[b]	*er* (%)[c]
1	THF	-	60	40	82:18
2	Toluene	-	60	18	60:40
3	DMF	-	60	NR	-
4	DMSO	-	60	8	78:22
	TFE	-	60	NR	-
	HFIP	-	60	NR	-
5	*tert*-amyl alcohol	-	60	72	85:15
6	***tert*-amyl alcohol**	**-**	**35**	**65**	**90:10**
7	*tert*-amyl alcohol	TBAB	35	66	88:12

Reaction conditions: (a) **1a** (30 mg, 0.13 mmol, 1 equiv), **2a** (2 equiv), $Pd(OAc)_2$ (10 mol%), **L1** (30 mol%), Additive (0.5 equiv), Cs_2CO_3 (1.2 equiv), solvent (2 mL), air, T °C, 18h. (b) Crude yield of **3a** is determined by ^1H NMR with CH_2Br_2 as an internal standard. (c) *er* of **3a** was determined by HPLC analysis.

Table S2. Base Optimization [a]

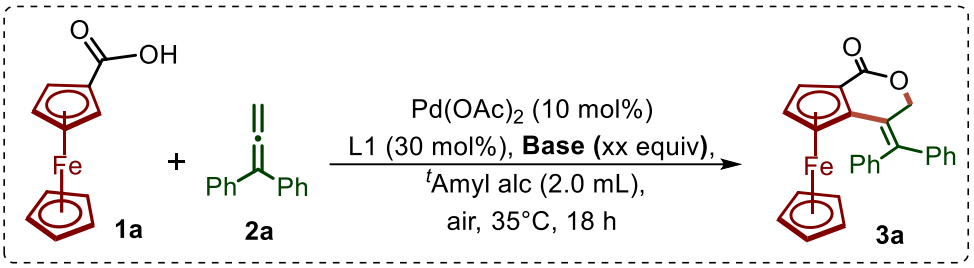

Entry	Base	Equiv	Yield (%)[b]	*er* (%)[c]
1	**Cs_2CO_3**	**1.2**	**65**	**90:10**
2	K_2CO_3	1.2	55	84:16
3	Na_2CO_3	1.2	57	78:22
4	Li_2CO_3	1.2	NR	-
5	CsOAc	1.2	66	70:30
6	KF	1.2	62	87:13
7	CsF	1.2	71	91:9
8	NEt_3	1.2	NR	-
9	**CsF**	**1.5**	**72**	**92:8**
10	CsF	2	72	91:9
11	CsF	2.5	72	90:10
12[d]	**CsF**	**1.8**	**80**	**93:7**

Reaction conditions: (a) **1a** (30 mg, 0.13 mmol, 1 equiv), **2a** (2 equiv), $Pd(OAc)_2$ (10 mol%), **L1** (30 mol%), **Base** (xx equiv), tert amyl alc (2 mL), air, 35 °C, 18h. (b) Crude yield of **3a** is determined by ^1H NMR with CH_2Br_2 as an internal standard. (c) *er* of **3a** was determined by HPLC analysis.(d) 0.6 equiv of **L1** was used instead of 0.3 equiv with 1.8 equiv CsF.

Table S3. Ligand Screening [a]

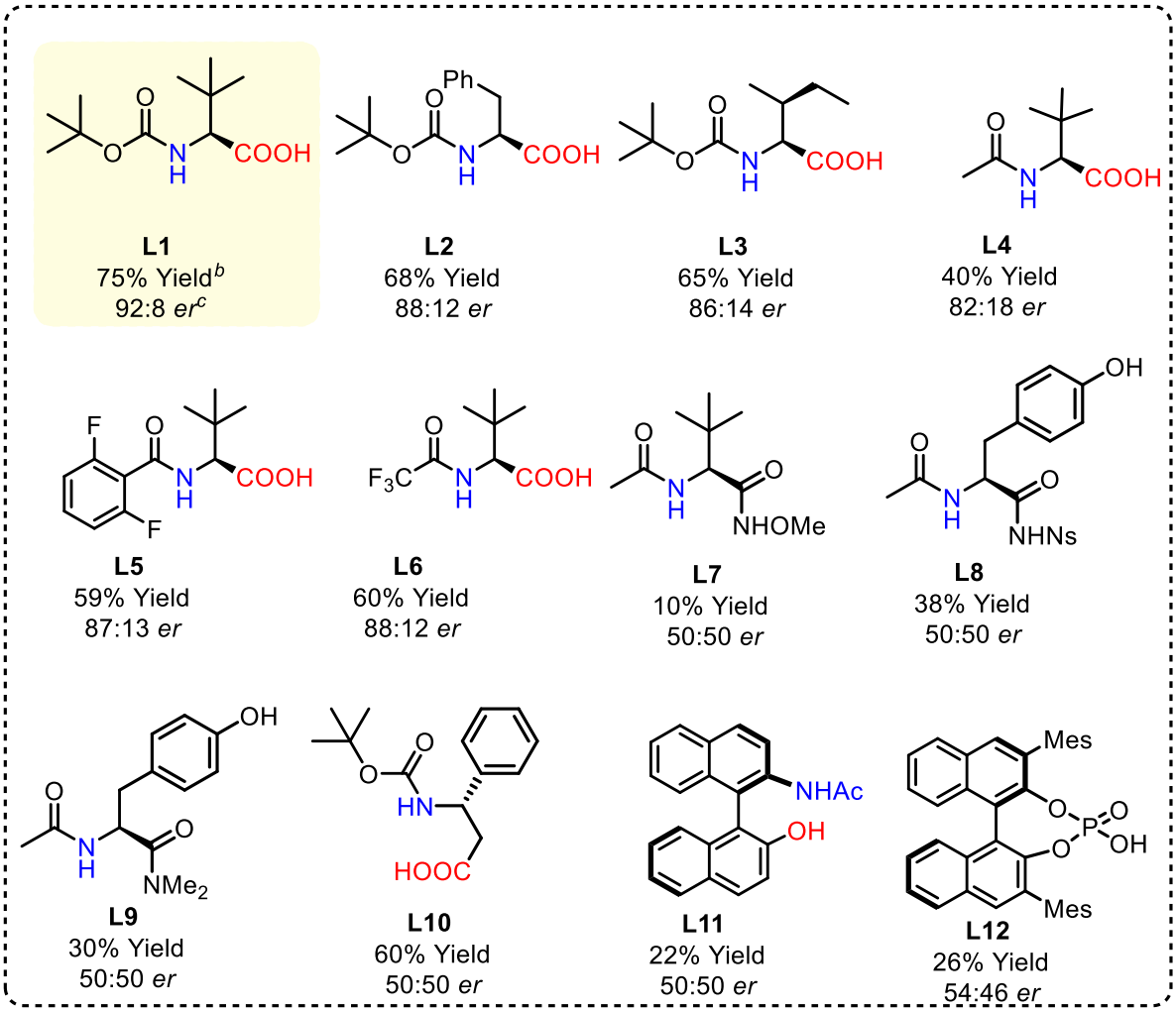

Reaction conditions: (a) **1a** (30 mg, 0.13 mmol, 1 equiv), **2a** (2 equiv), $Pd(OAc)_2$ (10 mol%), **L1** (30 mol%), **CsF** (1.5 equiv), tert amyl alc (2 mL), air, 35 °C, 18h. (b) Crude yield of **3a** is determined by ^1H NMR with CH_2Br_2 as an internal standard. (c) *er* of **3a** was determined by HPLC analysis.

General procedure for the enantioselective synthesis of ferrocene fused isochromans with allenes and dienes

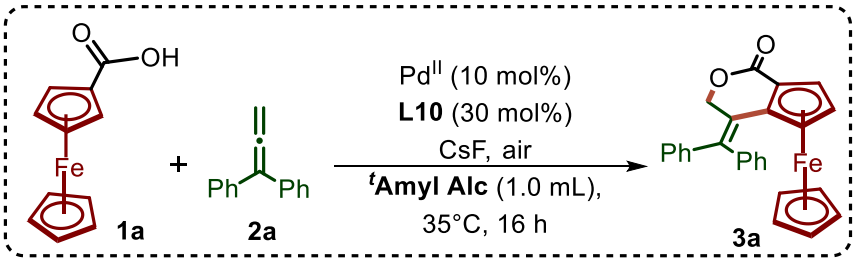

Scheme S1. Pd-catalyzed C-H activation oxidative deamination of ferrocene carboxylic acid **1a** with allene **2a**

In a Schlenk tube, $Pd(OAc)_2$ (6 mg, 0.026 mmol, 10 mol%), **L1** (18 mg, 0.078 mmol, 30 mol %), CsF (50 mg, 0.32 mmol, 1.2 equiv), and ferrocene carboxylic acid **1a** (60 mg, 0.26 mmol, 1 equiv) were added in dry *tert*-amyl alcohol (1.5 mL) under an inert atmosphere and solution was stirred for 10 min. After pre-stirring, allene **2a** (100 µL, 0.52 mmol, 2 equiv) was added to the resulting reaction mixture. The tube was sealed with a rubber septum, and a air atmosphere was maintained in the flask with a balloon. The reaction was stirred at 35 °C, for 18 h. The crude reaction mixture was passed through a celite pad, evaporation, and column chromatography on silica gel (mesh 100-200) using a hexane: ethyl acetate solvent system to afford Chiral ferrocene fused formaldehyde derivative (**3a)**.

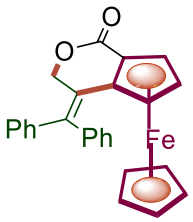

Chiral ferrocene fused isochroman 3a was purified on silica gel (mesh 100-200) in (hexanes: ethylacetate; 80:20), obtained as an orange solid, mp:130-131 ºC. Yield: 77 mg (70%).^{1}H NMR (400 MHz, $CDCl_3$) δ 7.40 – 7.33 (m, 6H), 7.21 (s, 2H), 7.13 (d, *J* = 7.0 Hz, 2H), 5.46 (d, *J* = 12.9 Hz, 1H), 5.05 (d, *J* = 12.9 Hz, 1H), 4.97 (s, 1H), 4.39 (s, 1H), 4.30 (s, 5H), 3.62 (s, 1H). ^{13}C{^{1}H} NMR (101 MHz, $CDCl_3$) δ 171.0 (C), 141.5 (C), 140.5 (C), 140.0 (CH), 129.8 (CH), 129.3 (CH), 128.6 (CH), 128.4 (CH), 128.0 (CH), 127.8 (C), 124.7 (C), 84.1 (C), 71.9 (C), 71.3 (CH), 70.9 (CH), 70.0 (CH), 68.0 (CH), 67.6 (CH_2). HRLCMS (ESI) *m/z*: $[M+H]^+$ Calcd for $C_{26}H_{21}FeO_2$ 421.0886, found 421.0897. Enantioselectivity 93:7 of **3a** was determined by chiral HPLC analysis on OZ-3 (hexane: isopropanol = 80:20, 1 mL/min, λ=254 nm).

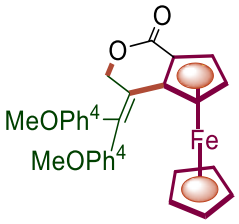

Chiral ferrocene fused isochroman 3b was purified on silica gel (mesh 100-200) in (hexanes: ethylacetate; 80:20), obtained as an orange solid, mp:135-136 ºC. Yield: 82 mg (66%). ^{1}H NMR (400 MHz, $CDCl_3$) δ 7.09 (d, *J* = 8.3 Hz, 2H), 7.02 (d, *J* = 8.2 Hz, 2H), 6.88 (dd, *J* = 13.0, 8.4 Hz, 4H), 5.46 (d, *J* = 12.7 Hz, 1H), 5.05 (d, *J* = 12.8 Hz, 1H), 4.96 (s, 1H), 4.40 (t, *J* = 2.8 Hz, 1H), 4.29 (s, 5H), 3.85 (s, 6H), 3.73 (s, 1H).^{13}C NMR (101 MHz, $CDCl_3$) δ 171.2 (C), 159.3 (C), 159.2 (C), 139.6 (C), 134.0 (C), 133.3 (CH), 131.3 (CH), 130.8 (CH), 123.0 (CH), 113.8 (C), 113.6 (C), 85.2 (C), 71.6 (C), 71.7(CH), 70.9 (CH), 70.0 (CH), 67.6 (CH), 67.5 (CH_2), 55.3 (CH_3), 55.2 (CH_3). HRLCMS (ESI) *m/z*: $[M+H]^+$ Calcd for $C_{28}H_{25}FeO_4$ 481.1097, found 481.1091. Enantioselectivity 90:10 of **3b** was determined by chiral HPLC analysis on OZ-3 (hexane: isopropanol = 80:20, 1 mL/min, λ=254 nm).

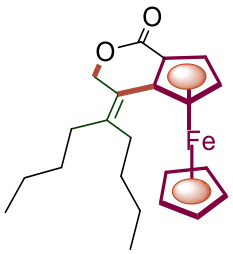

Chiral ferrocene fused isochroman 3c was purified on silica gel (mesh 100-200) in (hexanes: ethylacetate; 80:20), obtained as an orange solid, mp:135-136 ºC. Yield: 66 mg (70%). ^{1}H NMR (700 MHz, $CDCl_3$) δ 5.59 (s, 1H), 5.09 (s, 1H), 5.04 (dd, *J* = 2.7, 1.3 Hz, 1H), 4.86 (dd, *J* = 2.6, 1.3 Hz, 1H), 4.58 (t, *J* = 2.6 Hz, 1H), 4.21 (s, 5H), 1.97 (tt, *J* = 15.7, 6.5 Hz, 2H), 1.66 (tt, *J* = 16.2, 6.9 Hz, 4H), 1.49 – 1.39 (m, 2H), 1.14 (dd, *J* = 21.5, 6.0 Hz, 4H), 1.00 (t, *J* = 7.4 Hz, 3H), 0.80 (t, *J* = 7.1 Hz, 3H). ^{13}C NMR (176 MHz, $CDCl_3$) δ 170.7 (C), 141.8 (C), 108.4 (C), 91.0 (C), 83.5 (C), 71.9 (CH), 71.9 (CH), 69.2 (CH), 66.2 (CH), 64.7 (CH_2), 42.9 (CH_2), 37.5 (CH_2), 26.0 (CH_2), 25.9 (CH_2), 23.0 (CH_2), 22.7 (CH_2), 14.1 (CH_3), 13.8 (CH_3). HRLCMS (ESI) *m/z*: $[M+H]^+$ Calcd for $C_{22}H_{29}FeO_2$ 381.1512, found 381.1518. Enantioselectivity 85:15 of **3c** was determined by chiral HPLC analysis on OZ-3 (hexane: isopropanol = 90:10, 1 mL/min, λ=254 nm).

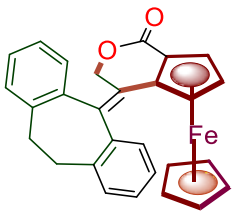

Chiral ferrocene fused isochroman 3d was purified on silica gel (mesh 100-200) in (hexanes: ethylacetate; 80:20), obtained as an orange solid, mp:145-146 ºC. Yield: 85 mg (68%). ^{1}H NMR (400 MHz, $CDCl_3$) δ 7.24 (dq, *J* = 5.8, 2.9 Hz, 6H), 7.16 – 7.09 (m, 2H), 5.32 (s, 1H), 5.27 (s, 1H), 5.23 (s, 1H), 4.98 (s, 1H), 4.23 (s, 5H), 3.59 (d, *J* = 3.0 Hz, 1H), 3.55 – 3.40 (m, 2H), 2.98 (q, *J* = 9.0, 8.2 Hz, 2H). ^{13}C NMR (176 MHz, $CDCl_3$) δ 171.3 (C), 140.0 (C), 139.2 (C), 138.9 (C), 137.7 (CH), 137.5 (CH), 129.9 (CH), 129.4 (CH), 128.0 (CH), 127.9 (CH), 127.8 (CH), 127.3 (CH), 126.4 (CH), 126.3 (C), 124.0 (C), 83.5 (C), 71.8 (C), 70.7 (CH), 70.2 (CH), 70.0 (CH), 68.0 (CH), 67.8 (CH_2), 32.4 (CH_2), 32.0 (CH_2). HRLCMS (ESI) *m/z*: $[M+H]^+$ Calcd for $C_{28}H_{23}FeO_2$ 447.1042, found 447.1015. Enantioselectivity 92:8 of **3d** was determined by chiral HPLC analysis on OZ-3 (hexane: isopropanol = 80:20, 1 mL/min, λ=254 nm).

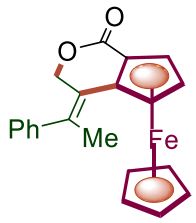

Chiral ferrocene fused isochroman 3e was purified on silica gel (mesh 100-200) in (hexanes: ethylacetate; 85:15), obtained as an orange solid, mp:131-132 ºC. Yield: 70 mg (71%). ^{1}H NMR (400 MHz, $CDCl_3$) δ 7.40 (d, *J* = 7.5 Hz, 2H), 7.36 (d, *J* = 7.2 Hz, 1H), 7.17 (d, *J* = 7.0 Hz, 2H), 5.09 (dd, *J* = 12.6, 0.9 Hz, 1H), 5.05 (d, *J* = 1.6 Hz, 1H), 4.90 (d, *J* = 1.4 Hz, 1H), 4.78 (d, *J* = 12.6 Hz, 1H), 4.69 (t, *J* = 2.5 Hz, 1H), 4.32 (s, 5H), 2.33 (s, 3H). ^{13}C NMR (176 MHz, $CDCl_3$) δ 171.2 (C), 142.3 (C), 136.9 (CH), 128.5 (CH), 127.8 (CH), 127.6 (C), 122.8 (C), 84.7 (C), 71.7 (C), 71.1 (CH), 71.0 (CH), 70.8 (CH), 70.0 (CH), 68.5 (CH_2), 22.6 (CH_3). HRLCMS (ESI) *m/z*: $[M+H]^+$ Calcd for $C_{28}H_{23}FeO_2$ 359.0729, found 359.0703. Enantioselectivity 92:8 of **3e** was determined by chiral HPLC analysis on OD-H (hexane: isopropanol = 95:5, 1 mL/min, λ=254 nm).

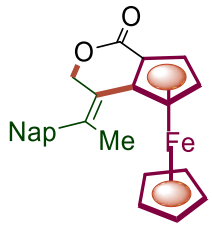

Chiral ferrocene fused isochroman 3f was purified on silica gel (mesh 100-200) in (hexanes: ethylacetate; 85:15), obtained as an orange solid, mp:135-136 ºC. Yield: 70 mg (66%). ^{1}H NMR (400 MHz, $CDCl_3$) δ 7.94 – 7.84 (m, 3H), 7.60 (s, 1H), 7.58 – 7.52 (m, 2H), 7.33 (d, *J* = 8.4 Hz, 1H), 5.16 (d, *J* = 12.6 Hz, 1H), 5.08 (d, *J* = 3.0 Hz, 1H), 4.94 (d, *J* = 2.9 Hz, 1H), 4.85 (d, *J* = 12.6 Hz, 1H), 4.72 (t, *J* = 3.1 Hz, 1H), 4.37 (s, 5H), 4.20 (s, 1H), 2.42 (s, 3H). ^{13}C NMR (176 MHz, $CDCl_3$) δ 171.2 (C), 139.7 (C), 136.8 (C), 133.0 (CH), 132.6(CH), 128.3 (CH), 127.9 (CH), 127.7 (CH), 126.6 (CH), 126.5 (CH), 126.3 (CH), 125.8 (C), 123.3 (C), 84.7 (C), 71.8 (C), 71.2 (CH), 71.1 (CH), 70.9 (CH), 70.0 (CH), 68.6 (CH), 67.1 (CH_2), 22.6 (CH_3). HRLCMS (ESI) *m/z*: $[M+H]^+$ Calcd for $C_{25}H_{21}FeO_2$ 409.0886, found 409.0884. Enantioselectivity 92:8 of **3f** was determined by chiral HPLC analysis on OZ-3 (hexane: isopropanol = 80:20, 1 mL/min, λ=254 nm).

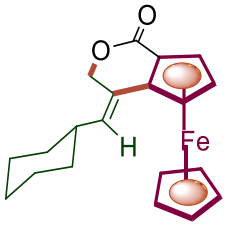

Chiral ferrocene fused isochroman 3g was purified on silica gel (mesh 100-200) in (hexanes: ethylacetate; 85:15), obtained as an orange solid, mp:125-126 ºC. Yield: 72 mg (68%). ^{1}H NMR (700 MHz, $CDCl_3$) δ 5.54 (d, *J* = 2.1 Hz, 1H), 5.18 (d, *J* = 2.1 Hz, 1H), 5.05 (dd, *J* = 2.6, 1.2 Hz, 1H), 4.84 (dd, *J* = 2.6, 1.2 Hz, 1H), 4.75 (dt, *J* = 4.1, 2.1 Hz, 1H), 4.58 (t, *J* = 2.6 Hz, 1H), 4.21 (s, 5H), 2.17 – 2.04 (m, 1H), 1.95 – 1.86 (m, 2H) 1.68 – 1.57 (m, 2H), 1.49 – 1.41 (m, 2H), 1.39 – 1.27 (m, 4H). ^{13}C NMR (176 MHz, $CDCl_3$) δ 170.8 (C), 137.7 (C), 109.0 (CH), 86.0 (C), 84.1 (C), 72.3 (CH), 71.9 (CH), 69.3 (CH), 65.8 (CH), 39.6 (CH_2), 26.6 (CH), 26.4 (CH_2), 26.2 (CH_2), 26.2 (CH_2). HRLCMS (ESI) *m/z*: $[M+H]^+$ Calcd for $C_{25}H_{21}FeO_2$ 409.0886, found 409.0884. Enantioselectivity 93:7 of **3g** was determined by chiral HPLC analysis on OZ-3 (hexane: isopropanol = 90:10, 1 mL/min, λ=254 nm).

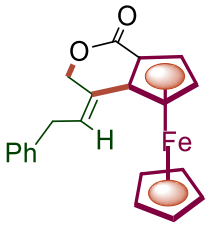

Chiral ferrocene fused isochroman 3h was purified on silica gel (mesh 100-200) in (hexanes: ethylacetate; 85:15), obtained as an orange solid, mp:125-126 ºC. Yield: 59 mg (63%). ^{1}H NMR (400 MHz, $CDCl_3$) δ 7.32 – 7.26 (m, 3H), 7.24 (d, *J* = 6.9 Hz, 1H), 7.18 (d, *J* = 7.3 Hz, 2H), 5.42 (s, 1H), 5.33 (t, *J* = 6.5 Hz, 1H), 5.01 (s, 2H), 4.84 (s, 1H), 4.59 (s, 1H), 4.20 (s, 5H), 3.18 (dd, *J* = 13.9, 6.5 Hz, 1H), 3.03 (dd, *J* = 13.9, 6.6 Hz, 1H). ^{13}C NMR (126 MHz, $CDCl_3$) δ 169.9, 138.7, 136.4, 129.6, 128.3, 126.7, 109.6, 83.7, 82.8, 72.1, 71.9, 69.2, 66.5, 42.0. HRLCMS (ESI) *m/z*: $[M+H]^+$ calcd for $C_{21}H_{19}FeO_2$ 359.0729, found 359.0749. Enantioselectivity 89:11 of **3h** was determined by chiral HPLC analysis on OZ-3 (hexane: isopropanol = 90:10, 1 mL/min, λ=254 nm).

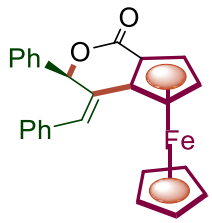

Chiral ferrocene fused isochroman 3i was purified on silica gel (mesh 100-200) in (hexanes: ethylacetate; 80:20), obtained as an orange solid, mp:126-127 ºC. Yield: 68 mg (62%).^{1}H NMR (400 MHz, $CDCl_3$) δ 7.48 (d, *J* = 7.1 Hz, 2H), 7.45 – 7.35 (m, 5H), 7.34 – 7.27 (m, 3H), 6.43 (s, 1H), 6.31 (s, 1H), 5.18 – 4.96 (m, 1H), 4.47 (d, *J* = 15.6 Hz, 1H), 4.28 (s, 6H).^{13}C{^{1}H} NMR (176 MHz, $CDCl_3$) δ 170.7 (C), 137.6 (C), 136.5 (C), 132.7 (C), 129.5 (CH), 128.6 (CH), 128.5 (CH), 128.3 (CH), 127.9 (CH), 127.6 (C), 85.7 (CH), 82.1 (C), 72.0 (C), 72.2 (CH), 71.6 (CH), 70.2 (CH), 68.5 (CH), 67.4 (CH). HRLCMS (ESI) *m/z*: $[M+H]^+$ calcd for $C_{26}H_{21}FeO_2$ 421.0886, found 421.0892.

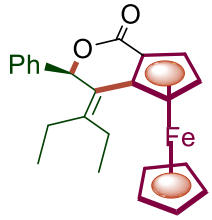

Chiral ferrocene fused isochroman 3j was purified on silica gel (mesh 100-200) in (hexanes: ethylacetate; 80:20), obtained as an orange solid, mp:134-135 ºC. Yield: 54 mg (52%). ^{1}H NMR (400 MHz, $CDCl_3$) δ 7.49 (t, *J* = 7.4 Hz, 2H), 7.40 (d, *J* = 7.6 Hz, 3H), 6.67 (s, 1H), 5.02 (d, *J* = 2.7 Hz, 1H), 4.35 (d, *J* = 2.8 Hz, 1H), 4.17 (s, 5H), 3.86 (d, *J* = 3.0 Hz, 1H), 2.11 (dq, *J* = 22.0, 7.4 Hz, 2H), 1.84 (dd, *J* = 7.5, 3.4 Hz, 2H), 1.29 (t, *J* = 7.2 Hz, 3H), 0.86 (t, *J* = 7.4 Hz, 3H). ^{13}C NMR (176 MHz, $CDCl_3$) δ 171.1 (C), 138.2 (C), 134.3 (CH), 128.6 (CH), 128.5 (CH), 127.5 (C), 126.2 (C), 91.7 (CH), 81.3 (C), 72.3 (C), 72.0 (CH), 71.9 (CH), 69.9 (CH), 68.8 (CH), 36.5 (CH_2), 30.2 (CH_2), 8.7 (CH_3), 8.5 (CH_3). HRLCMS (ESI) *m/z*: $[M+H]^+$ calcd for $C_{24}H_{25}FeO_2$ 401.1196, found 401.1199.

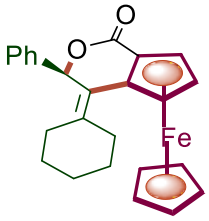

Chiral ferrocene fused isochroman 3k was purified on silica gel (mesh 100-200) in (hexanes: ethylacetate; 80:20), obtained as an orange solid, mp:143-144 ºC. Yield: 53 mg (50%). ^{1}H NMR (400 MHz, $CDCl_3$) δ 7.48 (d, *J* = 7.8 Hz, 2H), 7.39 (t, *J* = 6.6 Hz, 3H), 6.87 (s, 1H), 5.05 – 4.96 (m, 1H), 4.36 (t, *J* = 2.7 Hz, 1H), 4.08 (s, 5H), 3.96 (dd, *J* = 2.7, 1.3 Hz, 1H), 2.29 (dd, *J* = 12.7, 2.3 Hz, 1H), 2.19 – 2.04 (m, 3H), 1.79 (tdq, *J* = 10.6, 7.1, 3.5 Hz, 4H), 1.58 – 1.48 (m, 1H), 1.44 (td, *J* = 13.4, 4.3 Hz, 1H). ^{13}C NMR (176 MHz, $CDCl_3$) δ 170.6 (C), 139.7 (C), 138.1 (CH), 128.6 (CH), 128.4 (CH), 127.4 (CH), 125.2 (C), 86.0 (C), 81.2 (C), 72.3 (CH), 72.2 (CH), 70.8 (CH), 69.0 (CH), 64.9 (CH), 39.5 (CH_2), 34.9 (CH_2), 25.2 (CH_2), 21.6 (CH_2), 21.5 (CH_2). HRLCMS (ESI) *m/z*: $[M+H]^+$ for $C_{25}H_{25}FeO_2$ 413.1199, found 413.1223.

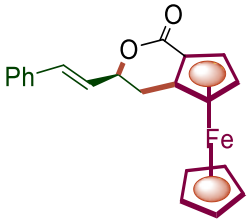

Chiral ferrocene fused isochroman 3l was purified on silica gel (mesh 100-200) in (hexanes: ethylacetate; 80:20), obtained as an orange solid, mp:130-131 ºC. Yield: 58 mg (62%). ^{1}H NMR (400 MHz, $CDCl_3$) δ 7.38 (t, *J* = 7.4 Hz, 3H), 7.34 – 7.29 (m, 2H), 6.85 (d, *J* = 16.1 Hz, 1H), 6.48 – 6.36 (m, 1H), 5.64 – 5.49 (m, 1H), 4.89 (d, *J* = 1.6 Hz, 1H), 4.54 (t, *J* = 2.5 Hz, 1H), 4.50 (s, 1H), 4.35 (s, 5H), 2.79 (dd, *J* = 15.5, 3.6 Hz, 1H), 2.60 (dd, *J* = 15.4, 11.9 Hz, 1H). ^{13}C NMR (101 MHz, $CDCl_3$) δ 170.9 (C), 136.0 (C), 132.5 (CH), 128.7 (CH), 128.2 (CH), 126.7 (CH), 126.5 (CH), 88.0 (C), 80.4 (C), 71.5 (CH), 70.6 (CH), 70.2 (CH), 67.1 (CH), 66.7 (CH), 29.6 (CH_2). HRLCMS (ESI) *m/z*: $[M+H]^+$ for $C_{21}H_{18}FeO_2$ 359.0729, found 359.0716.

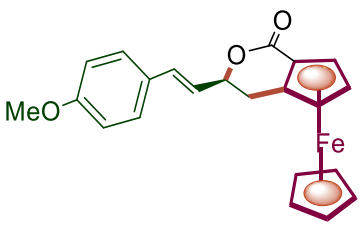

Chiral ferrocene fused isochroman 3m was purified on silica gel (mesh 100-200) in (hexanes: ethylacetate; 80:20), obtained as an orange solid, mp:136-137 ºC. Yield: 60 mg (59%). ^{1}H NMR (400 MHz, $CDCl_3$) δ 7.39 (d, *J* = 8.8 Hz, 2H), 6.91 (d, *J* = 8.8 Hz, 2H), 6.78 (d, *J* = 15.8 Hz, 1H), 6.26 (dd, *J* = 15.9, 6.4 Hz, 1H), 5.59 – 5.46 (m, 1H), 4.88 (d, *J* = 3.0 Hz, 1H), 4.54 (t, *J* = 2.7 Hz, 1H), 4.49 (d, *J* = 2.9 Hz, 1H), 4.34 (s, 5H), 3.85 (s, 3H), 2.77 (dd, *J* = 15.5, 3.6 Hz, 1H), 2.60 (dd, *J* = 15.5, 11.9 Hz, 1H). ^{13}C NMR (176 MHz, $CDCl_3$) δ 171.0 (C), 159.7 (C), 132.2 (CH), 128.7 (CH), 127.9 (CH), 124.2 (CH), 114.1 (CH), 88.1 (C), 80.7 (C), 70.6 (CH), 70.2 (CH), 69.1 (CH), 66.7 (CH), 60.4 (CH), 55.3 (CH_3), 29.7 (CH_2). HRLCMS (ESI) *m/z*: $[M+H]^+$ for $C_{22}H_{21}FeO_3$ 389.0835, found 389.0830.

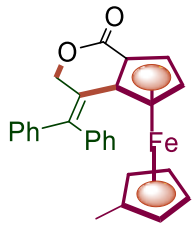

Chiral ferrocene fused isochroman 3n was purified on silica gel (mesh 100-200) in (hexanes: ethylacetate; 80:20), obtained as an orange solid, mp:144-145 ºC. Yield: 66 mg (58%). ^{1}H NMR (400 MHz, $CDCl_3$) δ 7.36 (m, 6H), 7.20 (dd, *J* = 6.4, 2.9 Hz, 2H), 7.13 (d, *J* = 6.3 Hz, 2H), 5.46 (d, *J* = 13.0 Hz, 1H), 5.05 (d, *J* = 13.0 Hz, 1H), 4.89 (d, *J* = 3.0 Hz, 1H), 4.33 (t, *J* = 2.9 Hz, 1H), 4.19 (brs, 2H), 4.15 (brs, 2H), 3.49 (d, *J* = 3.0 Hz, 1H), 1.94 (s, 3H).^{13}C NMR (176 MHz, $CDCl_3$) δ 170.8 (C), 141.7 (C), 140.5 (C), 139.7 (C), 129.8 (CH), 129.2 (CH), 128.6 (CH), 128.4 (CH), 127.9 (CH), 127.7 (CH), 124.7 (C), 86.4 (C), 83.9 (C), 72.8 (C), 71.9 (CH), 71.8 (CH), 71.2 (CH), 71.0 (CH), 70.4 (CH), 70.2 (CH), 68.7 (CH), 67.9 (CH_2), 13.5 (CH_3). HRLCMS (ESI) *m/z*: $[M+H]^+$ calcd for $C_{27}H_{23}FeO_2$ 435.1042, found 435.1053. Enantioselectivity 90:10 of **3n** was determined by chiral HPLC analysis on OZ-3 (hexane: isopropanol = 80:20, 1 mL/min, λ=254 nm).

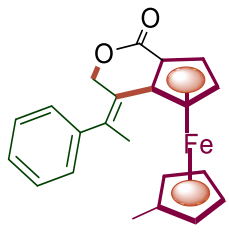

Chiral ferrocene fused isochroman 3o was purified on silica gel (mesh 100-200) in (hexanes: ethylacetate; 80:20), obtained as an orange solid, mp:141-142 ºC. Yield: 50 mg (51%). ^{1}H NMR (400 MHz, $CDCl_3$) δ 7.69 (d, *J* = 8.0 Hz, 2H), 7.47 (t, *J* = 7.6 Hz, 2H), 7.39 (d, *J* = 6.4

Hz, 1H), 5.52 (s, 1H), 5.04 (s, 1H), 4.98 (d, J = 2.8 Hz, 1H), 4.71 (d, J = 2.8 Hz, 1H), 4.55 (t, J = 2.6 Hz, 1H), 3.83 (d, J = 2.5 Hz, 4H), 1.87 (s, 3H), 1.85 (s, 3H). ^{13}C NMR (176 MHz, $CDCl_3$) δ 170.6 (C), 143.2 (C), 128.4 (C), 128.2 (CH), 125.8 (CH), 124.8 (CH), 111.0 (C), 83.9 (C), 73.3 (C), 72.9 (C), 72.5 (CH), 71.5 (CH), 70.0 (CH), 68.1 (CH), 66.8 (CH), 65.3 (CH_2), 29.9 (CH_3), 12.8 (CH_3). HRLCMS (ESI) *m/z*: $[M+H]^+$ calcd for $C_{22}H_{21}FeO_2$ 373.0886, found 373.1002. Enantioselectivity 93:7 of **3o** was determined by chiral HPLC analysis on OX-3 (hexane: isopropanol = 70:30, 1 mL/min, λ=254 nm).

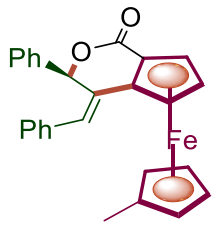

Chiral ferrocene fused isochroman 3p was purified on silica gel (mesh 100-200) in (hexanes: ethylacetate; 80:20), obtained as an orange solid, mp:141-142 ºC. Yield: 55 mg (48%). ^{1}H NMR (400 MHz, $CDCl_3$) δ 7.52 – 7.47 (m, 3H), 7.45 – 7.39 (m, 5H), 7.37 (dd, J = 5.9, 2.6 Hz, 2H), 6.41 (s, 1H), 6.30 (s, 1H), 4.99 – 4.95 (m, 1H), 4.43 (t, J = 2.6 Hz, 1H), 4.15 (d, J = 1.9 Hz, 2H), 4.12 (d, J = 8.9 Hz, 2H), 3.87 (s, 1H), 1.91 (s, 3H). ^{13}C NMR (176 MHz, $CDCl_3$) δ 170.5 (C), 137.7 (C), 136.6 (C), 132.6 (C), 129.2 (CH), 128.6 (CH), 128.4 (CH), 128.4 (CH), 128.0 (CH), 127.6 (CH), 86.5 (CH), 85.6 (C), 82.0 (C), 73.0 (C), 72.5 (CH), 72.3 (CH), 71.0 (CH), 70.9 (CH), 70.7 (CH), 69.2 (CH), 12.9 (CH_3). HRLCMS (ESI) *m/z*: $[M+H]^+$ calcd for $C_{27}H_{23}FeO_2$ 435.1042, found 435.1031.

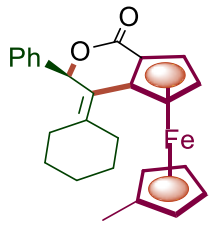

Chiral ferrocene fused isochroman 3q was purified on silica gel (mesh 100-200) in (hexanes: ethylacetate; 80:20), obtained as an orange solid, mp:146-147 ºC. Yield: 49 mg (44%). ^{1}H NMR (400 MHz, $CDCl_3$) δ 7.47 (d, J = 7.3 Hz, 2H), 7.44 – 7.32 (m, 3H), 6.85 (s, 1H), 5.00 – 4.85 (m, 1H), 4.31 (t, J = 2.7 Hz, 1H), 3.99 – 3.93 (m, 2H), 3.94 – 3.87 (m, 3H), 2.26 (dt, J = 9.6, 2.8 Hz, 1H), 2.18 (t, J = 4.4 Hz, 1H), 2.13 – 2.01 (m, 2H), 1.83 (s, 3H), 1.77 (dt, J = 12.8, 3.5 Hz, 3H), 1.58 – 1.50 (m, 2H), 1.44 (td, J = 13.4, 4.4 Hz, 1H). ^{13}C NMR (176 MHz, $CDCl_3$) δ 170.0 (C), 139.4 (C), 138.1 (C), 128.6 (CH), 128.4 (CH), 127.3 (CH), 124.7 (CH), 86.3 (C),

86.0 (C), 81.2 (CH), 73.9 (CH), 72.9 (CH), 72.2 (CH), 71.8 (CH), 70.9 (CH), 70.8 (CH), 69.7 (CH), 65.6 (CH), 39.9 (CH_2), 34.8 (CH_2), 25.2 (CH_2), 21.6 (CH_2), 21.5 (CH_2), 12.1 (CH_3). HRLCMS (ESI) *m/z*: $[M+H]^+$ calcd for $C_{26}H_{27}FeO_2$ 427.1355, found 427.1365.

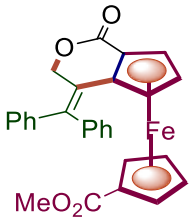

Chiral ferrocene fused isochroman 3r was purified on silica gel (mesh 100-200) in (hexanes: ethylacetate; 70:30), obtained as an orange solid, mp:149-150 ºC. Yield: 39 mg (30%). ^{1}H NMR (400 MHz, $CDCl_3$) δ 7.42 – 7.30 (m, 6H), 7.23 – 7.12 (m, 4H), 5.56 (d, J = 13.1 Hz, 1H), 5.07 (d, J = 13.1 Hz, 1H), 4.94 (s, 2H), 4.81 (s, 1H), 4.48 (dd, J = 15.8, 2.4 Hz, 2H), 4.40 (t, J = 2.8 Hz, 1H), 3.82 (s, 3H), 3.55 (d, J = 3.1 Hz, 1H).^{13}C NMR (176 MHz, $CDCl_3$) δ 170.1 (C), 169.6 (C), 141.8 (C), 141.3 (C), 140.2 (C), 129.7 (CH), 129.5 (CH), 128.6 (CH), 128.4 (CH), 128.2 (CH), 127.9 (CH), 123.2 (C), 85.7 (C), 74.3 (C), 73.3 (C), 73.2 (CH), 73.1 (CH), 72.9 (CH), 72.1 (CH), 71.1 (CH), 68.9 (CH), 68.6 (CH), 60.4 (CH_2), 52.0 (CH_3). HRLCMS (ESI) *m/z*: $[M+Na]^+$ calcd for $C_{28}H_{22}FeO_4Na$ 501.0760, found 501.0744. Enantioselectivity 95:5 of **3r** was determined by chiral HPLC analysis on OX-3 (hexane: isopropanol = 70:30, 1 mL/min, λ=254 nm).

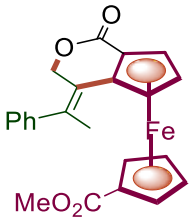

Chiral ferrocene fused isochroman 3s was purified on silica gel (mesh 100-200) in (hexanes: ethylacetate; 70:30), obtained as an orange solid, mp:146-147 ºC. Yield: 32 mg (28%). ^{1}H NMR (400 MHz, $CDCl_3$) δ 7.71 (d, J = 8.1 Hz, 2H), 7.50 (t, J = 7.8 Hz, 2H), 7.41 (t, J = 7.3 Hz, 1H), 5.59 (s, 1H), 5.13 (s, 1H), 5.08 (d, J = 3.1 Hz, 1H), 4.75 (d, J = 3.1 Hz, 1H), 4.65 (d, J = 1.6 Hz, 1H), 4.61 (d, J = 2.8 Hz, 1H), 4.52 (s, 1H), 4.17 (d, J = 3.1 Hz, 1H), 4.00 (d, J = 3.1 Hz, 1H), 3.79 (s, 3H), 1.86 (s, 3H). ^{13}C NMR (176 MHz, $CDCl_3$) δ 170.1 (C), 169.0 (C), 143.0 (C), 142.9 (C), 128.4 (CH), 128.3 (CH), 125.8 (CH), 112.7 (CH), 88.6 (C), 84.8 (C), 75.3 (C), 74.4 (CH), 73.9 (CH), 73.6 (CH), 73.5 (CH), 72.2 (CH), 70.2 (CH), 67.4 (CH), 66.6 (CH_2), 51.7 (CH_3), 29.9 (CH_3). HRLCMS (ESI) *m/z*: $[M+Na]^+$ calcd for $C_{23}H_{20}FeO_4Na$ 439.0603,

found 439.0584. Enantioselectivity 95:5 of **3s** was determined by chiral HPLC analysis on OX-3 (hexane: isopropanol = 70:30, 1 mL/min, λ=254 nm).

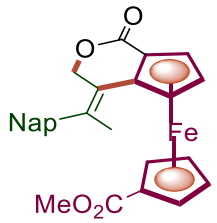

Chiral ferrocene fused isochroman 3t was purified on silica gel (mesh 100-200) in (hexanes: ethylacetate; 70:30), obtained as an orange solid, mp:147-148 ºC. Yield: 34 mg (27%). ^{1}H NMR (400 MHz, $CDCl_3$) δ 7.90 (t, *J* = 7.7 Hz, 3H), 7.69 (s,1H), 7.61 – 7.51 (m, 2H), 7.40 (d, *J* = 8.5 Hz, 1H), 5.21 (d, *J* = 14.5 Hz, 1H), 5.08 (d, *J* = 3.4 Hz, 1H), 4.96 (d, *J* = 5.0 Hz, 1H), 4.88 (d, *J* = 13.0 Hz, 1H), 4.74 (t, *J* = 2.7 Hz, 1H), 4.59 (t, *J* = 3.3 Hz, 1H), 4.55 (t, *J* = 3.3 Hz, 1H), 3.82 (s, 3H), 2.39 (s, 3H). ^{13}C NMR (176 MHz, $CDCl_3$) δ 171.2 (C), 169.9 (C), 139.5 (C), 138.6 (C), 133.0 (C), 132.6 (C), 128.4 (CH), 128.0 (CH), 127.7 (CH), 126.9 (CH), 126.6 (CH), 126.4 (CH), 125.9 (CH), 121.5 (C), 86.0 (C), 74.4 (C), 73.7 (C), 73.3 (CH), 73.1 (CH), 72.1 (CH), 71.0 (CH), 70.9 (CH), 69.4 (CH), 68.3 (CH), 60.4 (CH_2), 51.9 (CH_3), 22.8 (CH_3). HRLCMS (ESI) *m/z*: $[M+Na]^+$ calcd for $C_{27}H_{22}FeO_4Na$ 489.0760, found 489.0763. Enantioselectivity 96:4 of **3t** was determined by chiral HPLC analysis on OX-3 (hexane: isopropanol = 70:30, 1 mL/min, λ=254 nm).

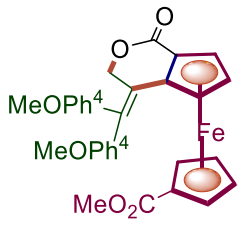

Chiral ferrocene fused isochroman 3u was purified on silica gel (mesh 100-200) in (hexanes: ethylacetate; 70:30), obtained as an orange solid, mp:149-150 ºC. Yield: 35 mg (25%). ^{1}H NMR (700 MHz, $CDCl_3$) δ 7.10 (d, *J* = 8.8 Hz, 2H), 7.05 (d, *J* = 8.8 Hz, 2H), 6.91 (d, *J* = 8.8 Hz, 2H), 6.86 (d, *J* = 8.8 Hz, 2H), 5.56 (d, *J* = 12.8 Hz, 1H), 5.08 (d, *J* = 12zz.8 Hz, 1H), 4.98 – 4.94 (m, 1H), 4.94 – 4.92 (m, 1H), 4.83 – 4.78 (m, 1H), 4.53 – 4.49 (m, 1H), 4.49 – 4.45 (m, 1H), 4.42 (t, *J* = 2.6 Hz, 1H), 3.85 (s, 3H), 3.85 (s, 3H), 3.82 (s, 3H), 3.67 (dd, *J* = 2.7, 1.3 Hz, 1H). ^{13}C NMR (176 MHz, $CDCl_3$) δ 170.2 (C), 169.8 (C), 159.5 (C), 159.3 (C), 141.5 (C), 133.9 (CH), 133.0 (CH), 131.3 (CH), 131.1 (CH), 121.3 (CH), 113.8 (CH), 113.6 (C), 86.7 (C), 74.2 (C), 73.2 (C), 73.2 (CH), 72.9 (CH), 72.8 (CH), 71.9 (CH), 71.5 (CH), 71.1 (CH), 68.8

(CH), 68.2 (CH_2), 55.4 (CH_3), 55.3 (CH_3), 55.2 (CH_3). HRLCMS (ESI) *m/z*: $[M+H]^+$ calcd for $C_{30}H_{27}FeO_6$ 539.1142., found 539.1152. Enantioselectivity 95:5 of **3u** was determined by chiral HPLC analysis on OX-3 (hexane: isopropanol = 70:30, 1 mL/min, λ=254 nm).

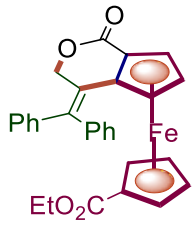

Chiral ferrocene fused isochroman 3v was purified on silica gel (mesh 100-200) in (hexanes: ethylacetate; 70:30), obtained as an orange solid, mp:155-156 ºC. Yield: 24 mg (20%). ^{1}H NMR (400 MHz, $CDCl_3$) δ 7.46 – 7.29 (m, 6H), 7.23 – 7.10 (m, 4H), 5.57 (d, *J* = 13.1 Hz, 1H), 5.06 (d, *J* = 13.1 Hz, 1H), 4.95 (d, *J* = 2.6 Hz, 2H), 4.83 (d, *J* = 2.6 Hz, 1H), 4.58 – 4.44 (m, 2H), 4.41 (t, *J* = 2.7 Hz, 1H), 4.29 (q, *J* = 7.1 Hz, 2H), 3.58 (d, *J* = 2.6 Hz, 1H), 1.34 (t, *J* = 7.1 Hz, 3H). ^{13}C NMR (101 MHz, $CDCl_3$) *δ* 169.6 (C), 141.8 (C), 141.3 (C), 140.3 (C), 129.8 (CH), 129.4 (CH), 128.6 (CH), 128.4 (CH), 128.2 (CH), 127.9 (C), 123.2 (C), 85.7 (C), 74.7 (C), 73.3 (C), 73.2 (CH), 73.0 (CH), 72.7 (CH), 72.1 (CH), 71.1(CH), 71.1 (CH), 68.6 (CH_2), 60.9 (CH_2), 14.4 (CH_3). HRLCMS (ESI) *m/z*: $[M+H]^+$ calcd for $C_{27}H_{22}FeO_4Na$ 489.0760, found 489.0763. Enantioselectivity 96:4 of **3v** was determined by chiral HPLC analysis on OX-3 (hexane: isopropanol = 80:20, 1 mL/min, λ=254 nm).

Synthesis of 1,2-keto acid Ferrocene Derivative under an Oxidizing Atmosphere

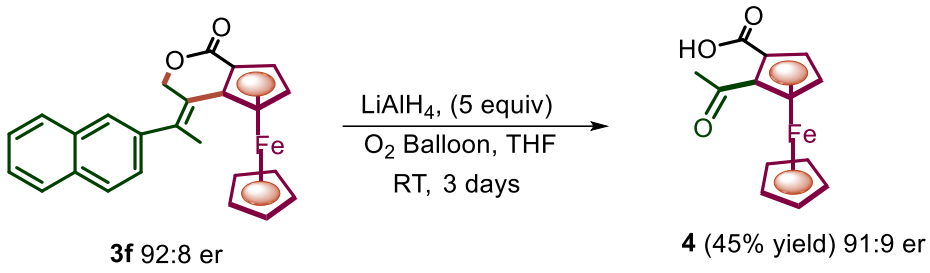

3f 92:8 er

4 (45% yield) 91:9 er

Scheme 2. Oxidation under $LiAlH_4$.

In a Schlenk tube, ferrocene fused isochroman **3f** (36 mg, 0.09 mmol, 1 equiv), $LiAlH_4$ (18 mg, 0.45 mmol, 5 equiv) was mixed in THF at room temperature and stirred for 3 days under an oxygen atmosphere. The crude reaction mixture was passed through a celite pad, quenched with 1N HCl, evaporation, and column chromatography on silica gel (mesh 230-400) using hexane: ethyl acetate solvent system to afford 1,2-keto acid ferrocene **4** as a yellow solid (mp: 133-134 ºC). Yield: 11 mg (45%). ^{1}H NMR (400 MHz, $CDCl_3$) δ 14.27 (s, 1H), 5.59 (d, J = 3.0 Hz, 1H), 4.98 (d, J = 1.6 Hz, 1H), 4.91 (t, J = 3.0 Hz, 1H), 4.40 (s, 5H), 2.61 (s, 3H). ^{13}C NMR (176 MHz, $CDCl_3$) δ 208.9 (C), 170.0 (C), 80.1 (C), 75.1 (C), 74.7 (CH), 74.1 (CH), 72.5 (CH), 27.6 (CH_3). HRLCMS (ESI) *m/z*: $[M+H]^+$ calcd for $C_{13}H_{13}FeO_3$ 273.0209, found 273.0194. Enantioselectivity 91:9 of 4 was determined by chiral HPLC analysis on AD-H (hexane: isopropanol = 70:30, 1 mL/min, λ=254 nm). We performed HRMS analysis of the reaction mixture and found that within the first two hours the expected alcohol intermediate, (Z)-2-(2-(hydroxymethyl)ferrocenyl)-3-(naphthalen-1-yl)but-2-en-1-ol, is formed, confirming that a normal reduction takes place first. When the reaction was run under O_2, we obtained only up to 45% yield of product 4 and no remaining starting material. This indicates that the ferrocene starting material may undergo SET with O_2 to form reactive O_2•– or OOH-type species, which then oxidize the alcohol intermediate to product **4**

HPLC Traces of Compound 3a-3v and 4

Racemic sample of **3a**

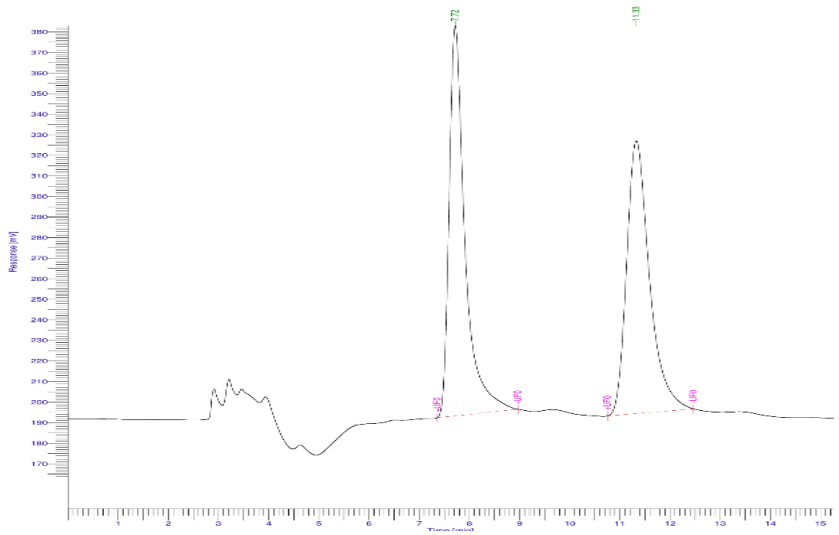

Peak #	Time [min]	Area [µV·s]	Height [µV]	Area [%]	Norm. Area [%]	BL	Area/Height [s]
1	7.717	4179424.59	189651.48	49.88	49.88	MM	22.0374
2	11.327	4200052.81	132717.08	50.12	50.12	MM	31.6467
		8379477.41	322368.56	100.00	100.00		

Asymmetric sample of **3a**

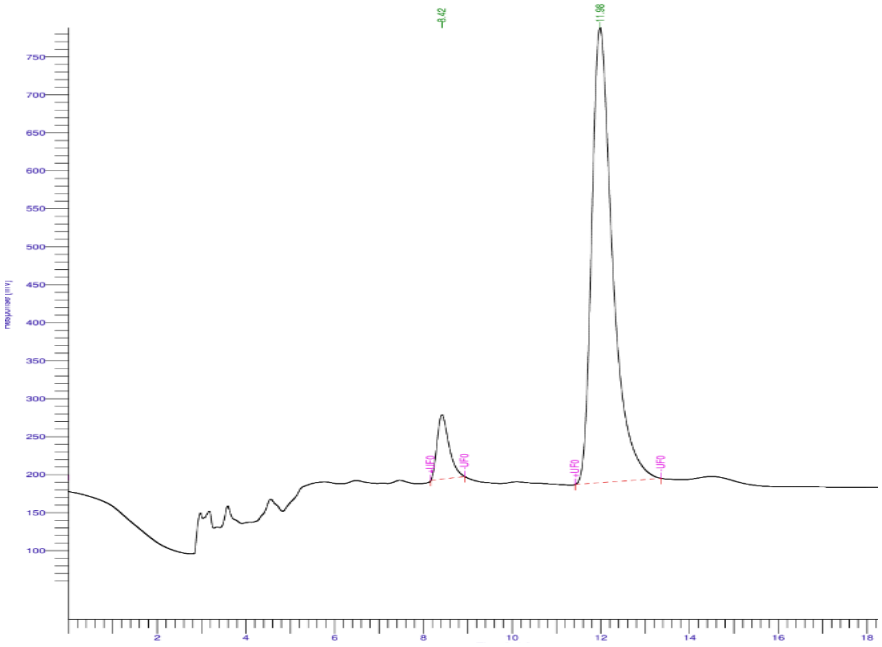

Peak #	Time [min]	Area [µV·s]	Height [µV]	Area [%]	Norm. Area [%]	BL	Area/Height [s]
1	8.417	1581154.15	84517.31	7.48	7.48	MM	18.7081
2	11.983	19559836.98	598832.11	92.52	92.52	MM	32.6633
		21140991.13	683349.42	100.00	100.00		

Racemic sample of **3b**

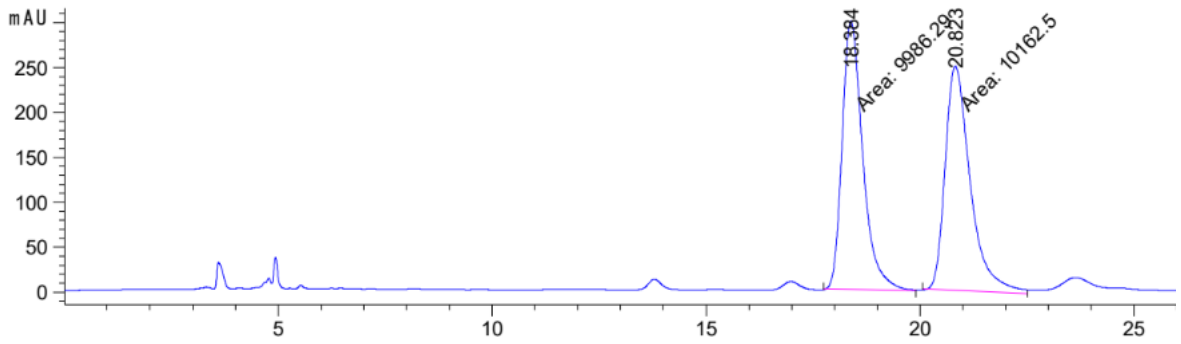

Signal 1: DAD1 A, Sig=254,4 Ref=360,100

Peak #	RetTime [min]	Type	Width [min]	Area [mAU*s]	Height [mAU]	Area %
1	18.384	MM	0.5580	9986.28906	298.27777	49.5628
2	20.823	MM	0.6798	1.01625e4	249.17084	50.4372

Asymmetric sample of **3b**

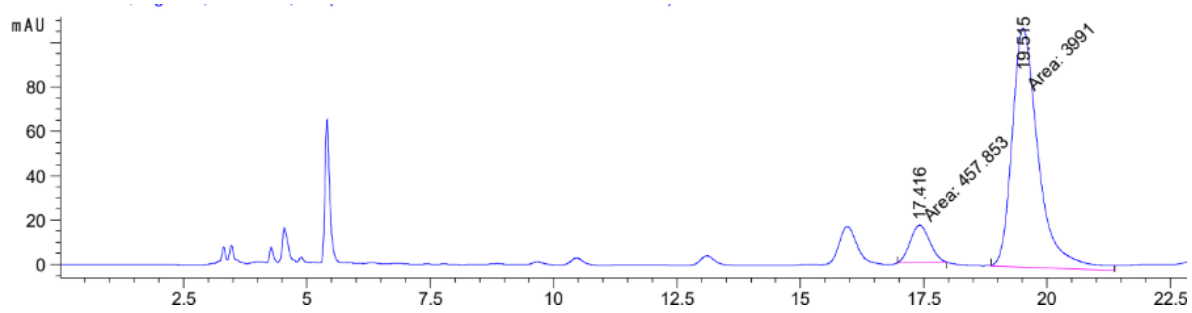

Signal 1: DAD1 A, Sig=254,4 Ref=360,100

Peak #	RetTime [min]	Type	Width [min]	Area [mAU*s]	Height [mAU]	Area %
1	17.416	MM	0.4549	457.85303	16.77549	10.2915
2	19.515	MM	0.6178	3990.99658	107.66175	89.7085

Racemic sample of **3c**

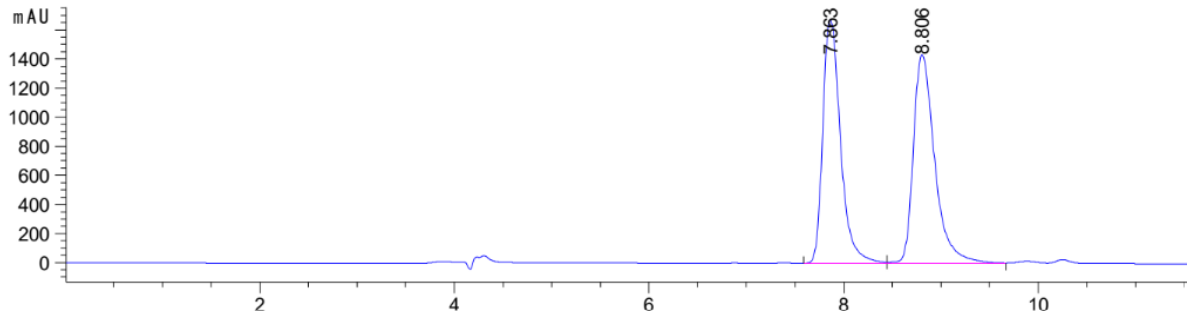

Signal 1: DAD1 A, Sig=254,4 Ref=360,100

Peak #	RetTime [min]	Type	Width [min]	Area [mAU*s]	Height [mAU]	Area %
1	7.863	VV	0.1959	2.12638e4	1677.84192	49.1040
2	8.806	VV	0.2353	2.20398e4	1434.02454	50.8960

Asymmetric sample of **3c**

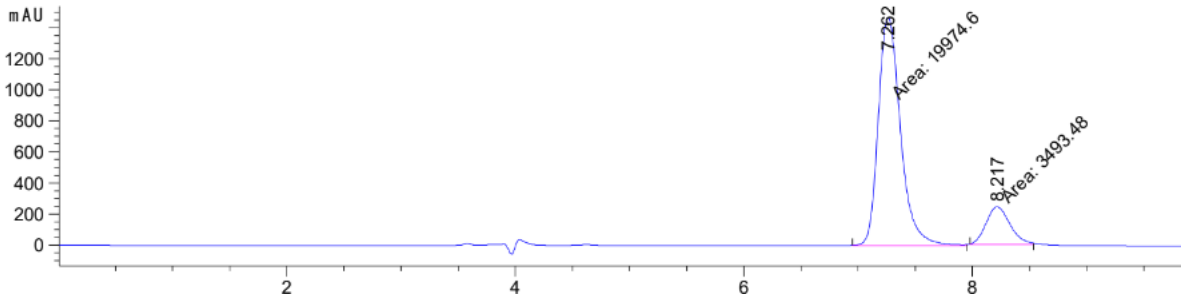

Signal 1: DAD1 A, Sig=254,4 Ref=360,100

Peak #	RetTime [min]	Type	Width [min]	Area [mAU*s]	Height [mAU]	Area %
1	7.262	MM	0.2265	1.99746e4	1469.91406	85.1139
2	8.217	MM	0.2411	3493.48438	241.52734	14.8861

Racemic sample of **3d**

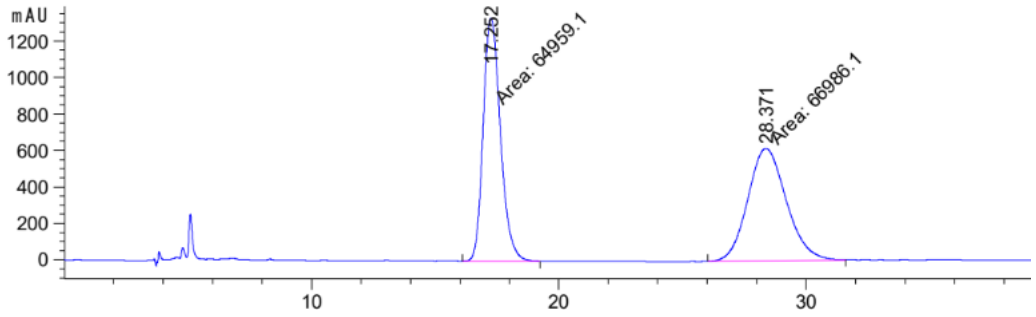

Signal 1: DAD1 A, Sig=254,4 Ref=360,100

Peak #	RetTime [min]	Type	Width [min]	Area [mAU*s]	Height [mAU]	Area %
1	17.252	MM	0.8120	6.49591e4	1333.29773	49.2319
2	28.371	MM	1.8112	6.69861e4	616.39520	50.7681

Asymmetric sample of **3d**

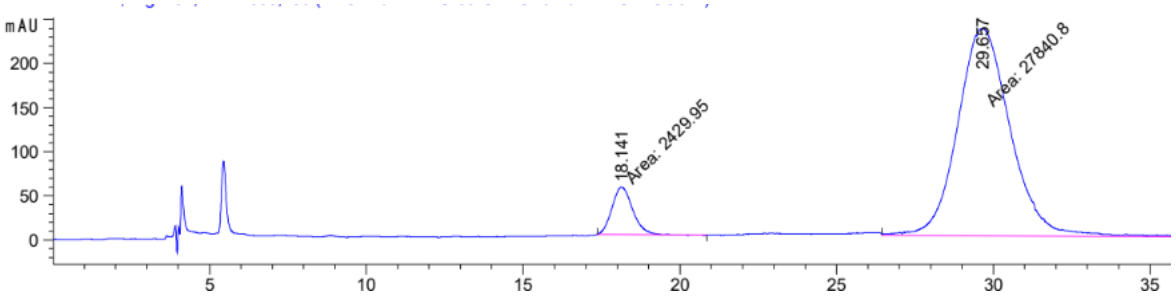

Signal 1: DAD1 A, Sig=254,4 Ref=360,100

Peak #	RetTime [min]	Type	Width [min]	Area [mAU*s]	Height [mAU]	Area %
1	18.141	MM	0.7581	2429.94678	53.42519	8.0274
2	29.657	MM	1.9711	2.78408e4	235.40468	91.9726

Racemic sample of **3e**

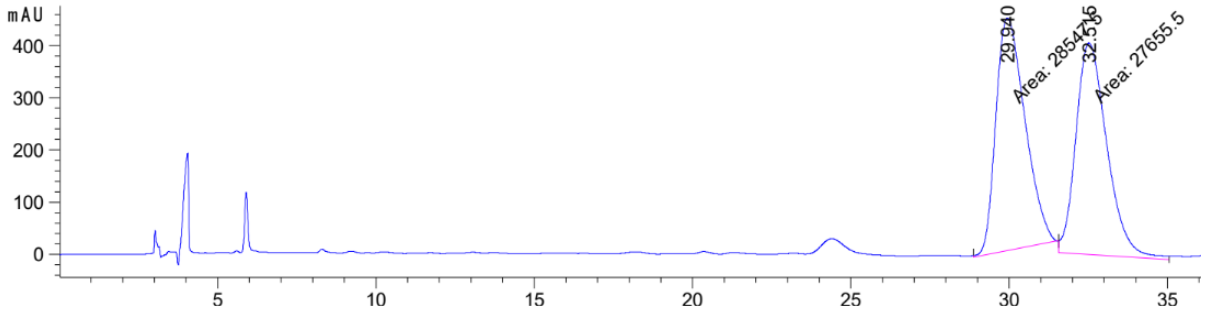

Signal 1: DAD1 A, Sig=254,4 Ref=360,100

Peak #	RetTime [min]	Type	Width [min]	Area [mAU*s]	Height [mAU]	Area %
1	29.940	MM	1.0660	2.85475e4	446.33585	50.7935
2	32.515	MM	1.1365	2.76555e4	405.57602	49.2065

Asymmetric sample of **3e**

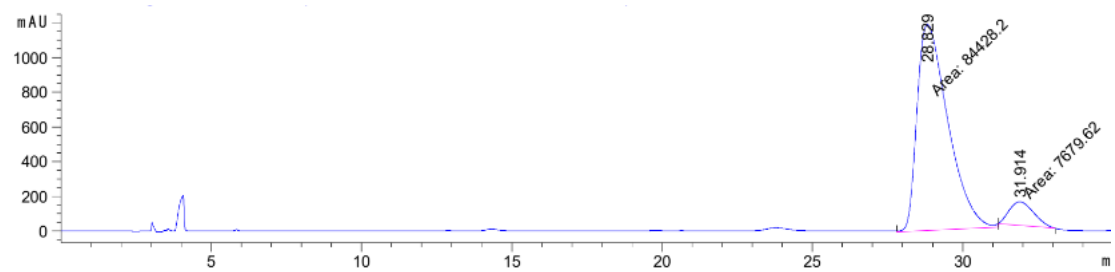

Signal 1: DAD1 A, Sig=254,4 Ref=360,100

Peak #	RetTime [min]	Type	Width [min]	Area [mAU*s]	Height [mAU]	Area %
1	28.829	MM	1.1866	8.44282e4	1185.87756	91.6624
2	31.914	MM	0.9434	7679.62061	135.67398	8.3376

Racemic sample of **3f**

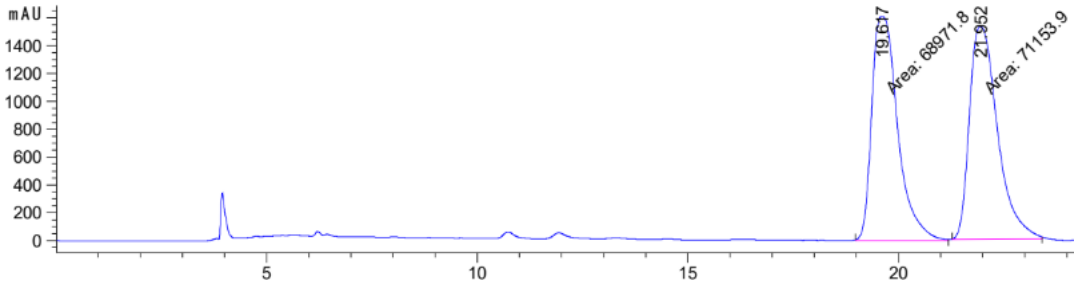

Signal 1: DAD1 A, Sig=254,4 Ref=360,100

Peak #	RetTime [min]	Type	Width [min]	Area [mAU*s]	Height [mAU]	Area %
1	19.617	MM	0.7146	6.89718e4	1608.73792	49.2214
2	21.952	MM	0.7728	7.11539e4	1534.60779	50.7786

Asymmetric sample of **3f**

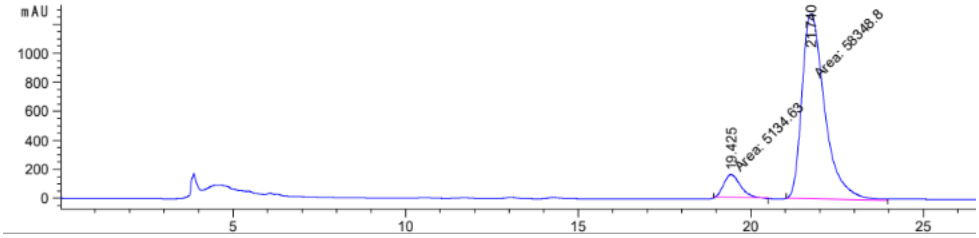

Signal 1: DAD1 A, Sig=254,4 Ref=360,100

Peak #	RetTime [min]	Type	Width [min]	Area [mAU*s]	Height [mAU]	Area %
1	19.425	MM	0.5495	5134.63232	155.73788	8.0881
2	21.740	MM	0.7630	5.83488e4	1274.47681	91.9119

Racemic sample of **3g**

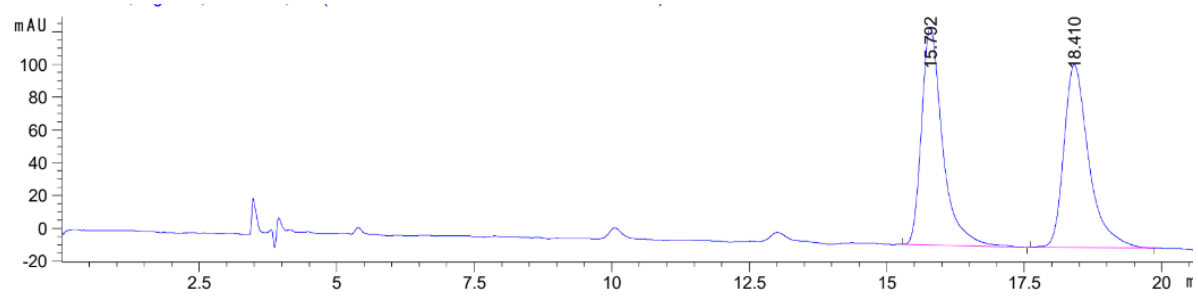

Signal 1: DAD1 A, Sig=254,4 Ref=360,100

Peak #	RetTime [min]	Type	Width [min]	Area [mAU*s]	Height [mAU]	Area %
1	15.792	BB	0.3992	3542.21460	132.79080	50.0887
2	18.410	BB	0.4683	3529.66772	111.79710	49.9113

Asymmetric sample of **3g**

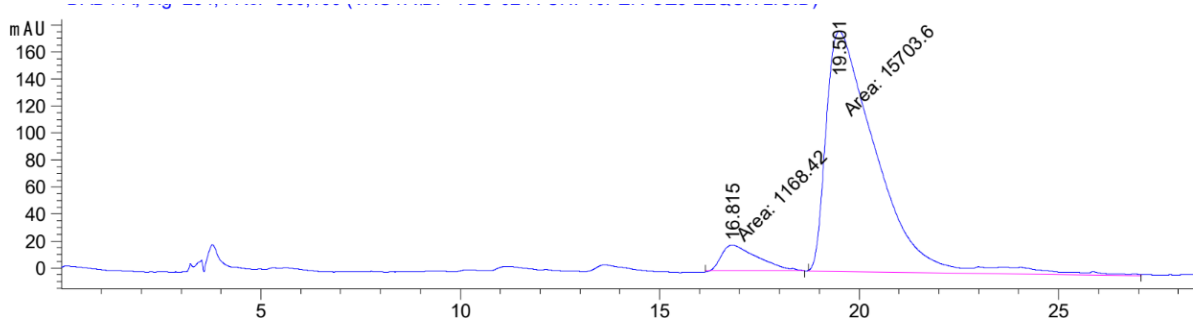

Signal 1: DAD1 A, Sig=254,4 Ref=360,100

Peak #	RetTime [min]	Type	Width [min]	Area [mAU*s]	Height [mAU]	Area %
1	16.815	MM	1.0339	1168.41846	18.83574	6.9252
2	19.501	MM	1.4725	1.57036e4	177.73994	93.0748

Racemic sample of **3h**

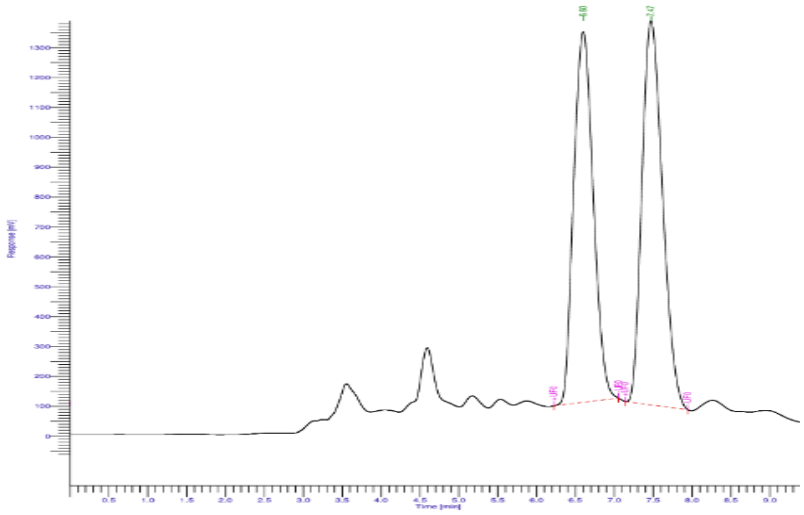

Peak #	Time [min]	Area [µV·s]	Height [µV]	Area [%]	Norm. Area [%]	BL	Area/Height [s]
1	6.600	21641411.77	1.24e+06	47.82	47.82	MM	17.4633
2	7.472	23616896.12	1.28e+06	52.18	52.18	MM	18.3803

Asymmetric sample of **3h**

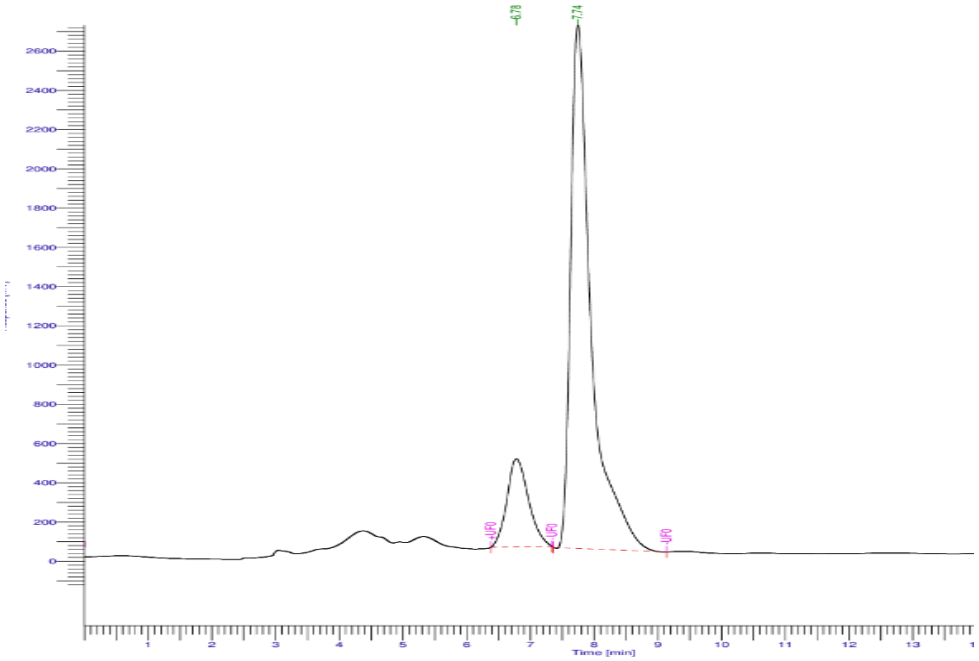

Peak #	Time [min]	Area [µV·s]	Height [µV]	Area [%]	Norm. Area [%]	BL	Area/Height [s]
1	6.777	10631117.70	448279.63	15.02	15.02	MM	23.7154
2	7.743	60147770.74	2.67e+06	84.98	84.98	MM	22.5487

Racemic sample of **3n**

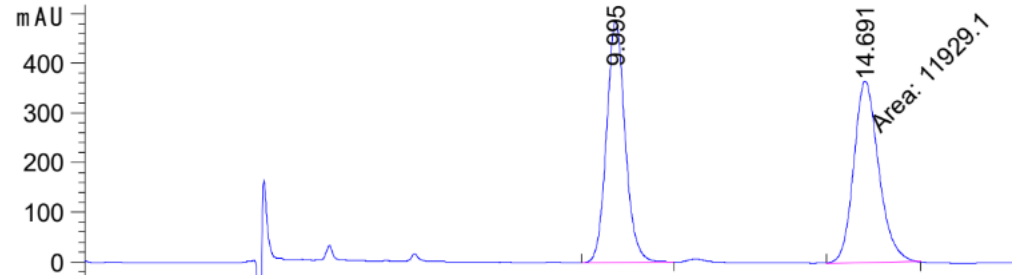

Signal 1: DAD1 A, Sig=254,4 Ref=360,100

Peak #	RetTime [min]	Type	Width [min]	Area [mAU*s]	Height [mAU]	Area %
1	9.995	BB	0.3737	1.18431e4	487.10690	49.8190
2	14.691	MM	0.5435	1.19291e4	365.79245	50.1810

Asymmetric sample of **3n**

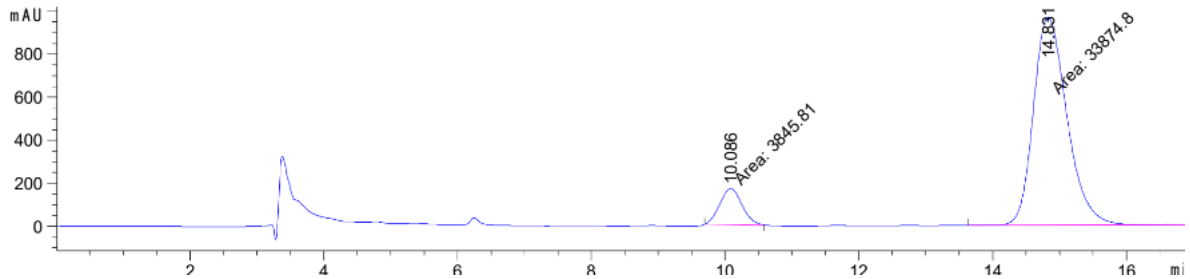

Signal 1: DAD1 A, Sig=254,4 Ref=360,100

Peak #	RetTime [min]	Type	Width [min]	Area [mAU*s]	Height [mAU]	Area %
1	10.086	MM	0.3832	3845.80908	167.27295	10.1955
2	14.831	MM	0.5848	3.38748e4	965.49963	89.8045

Racemic sample of **3o**

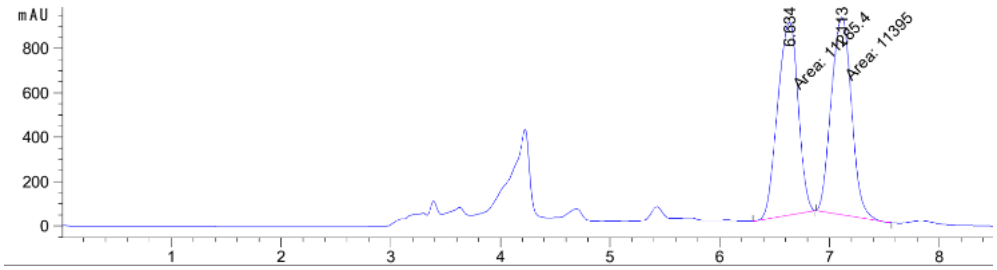

Signal 1: DAD1 A, Sig=254,4 Ref=360,100

Peak #	RetTime [min]	Type	Width [min]	Area [mAU*s]	Height [mAU]	Area %
1	6.634	MM	0.2158	1.12854e4	871.73309	49.7584
2	7.113	MM	0.2134	1.13950e4	890.00079	50.2416

Asymmetric sample of **3o**

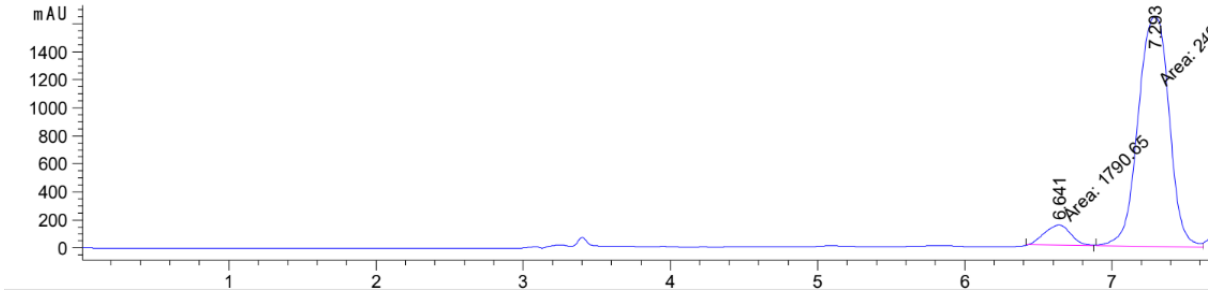

Signal 1: DAD1 A, Sig=254,4 Ref=360,100

Peak #	RetTime [min]	Type	Width [min]	Area [mAU*s]	Height [mAU]	Area %
1	6.641	MM	0.2087	1790.64868	142.98529	6.9395
2	7.293	MM	0.2438	2.40130e4	1641.29297	93.0605

Racemic sample of **3r**

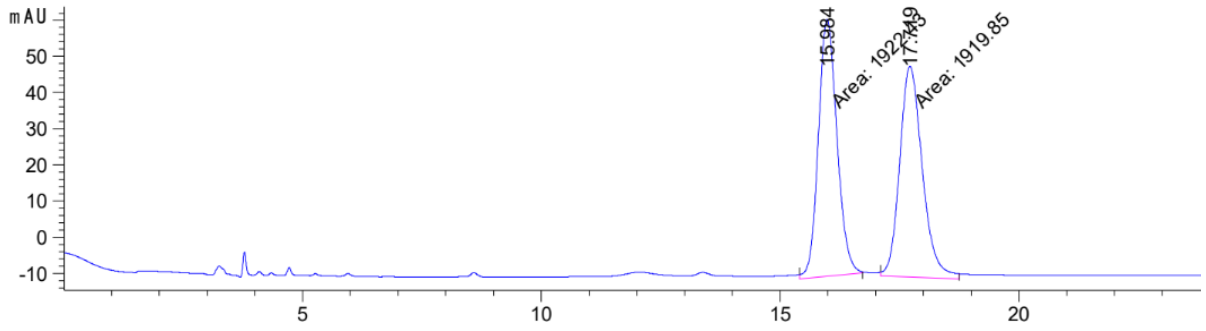

Signal 1: DAD1 A, Sig=254,4 Ref=360,100

Peak #	RetTime [min]	Type	Width [min]	Area [mAU*s]	Height [mAU]	Area %
1	15.984	MM	0.4513	1922.43127	71.00182	50.0336
2	17.719	MM	0.5501	1919.85034	58.16713	49.9664

Asymmetric sample of **3r**

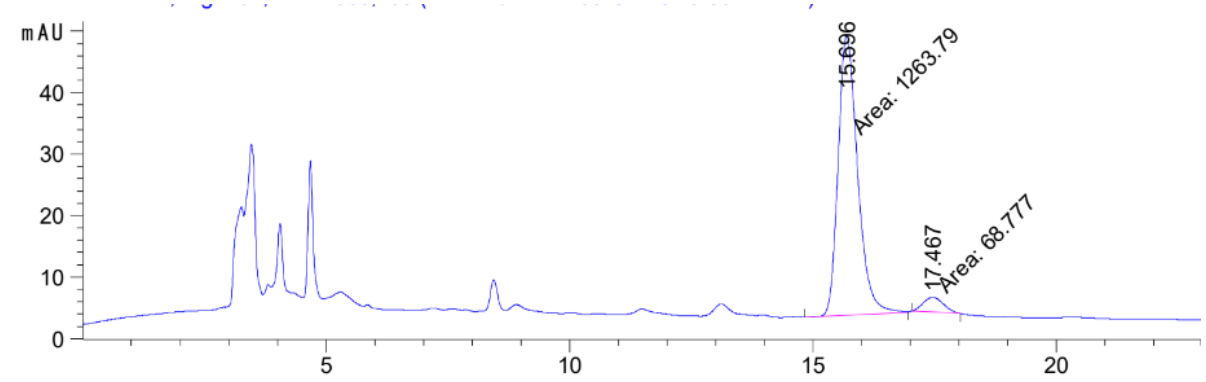

Signal 1: DAD1 A, Sig=254,4 Ref=360,100

Peak #	RetTime [min]	Type	Width [min]	Area [mAU*s]	Height [mAU]	Area %
1	15.696	MM	0.4630	1263.79260	45.48854	94.8388
2	17.467	MM	0.4760	68.77698	2.40837	5.1612

Racemic sample of **3s**

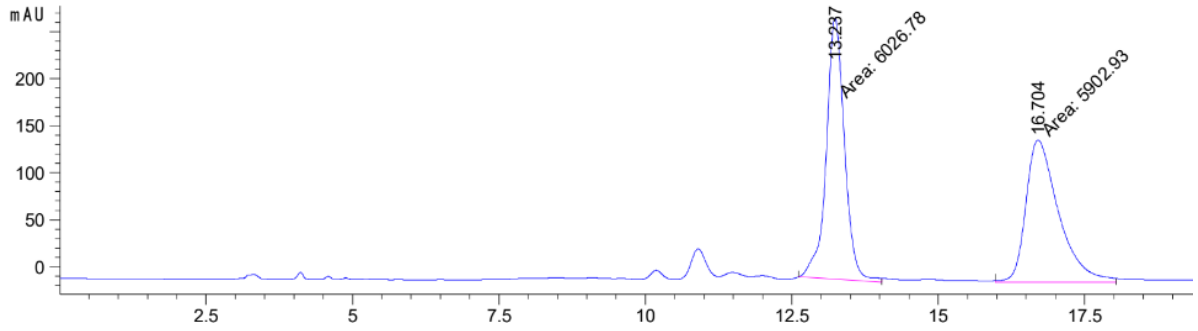

Signal 1: DAD1 A, Sig=254,4 Ref=360,100

Peak #	RetTime [min]	Type	Width [min]	Area [mAU*s]	Height [mAU]	Area %
1	13.237	MM	0.3630	6026.77881	276.72525	50.5191
2	16.704	MM	0.6511	5902.93408	151.09926	49.4809

Asymmetric sample of **3s**

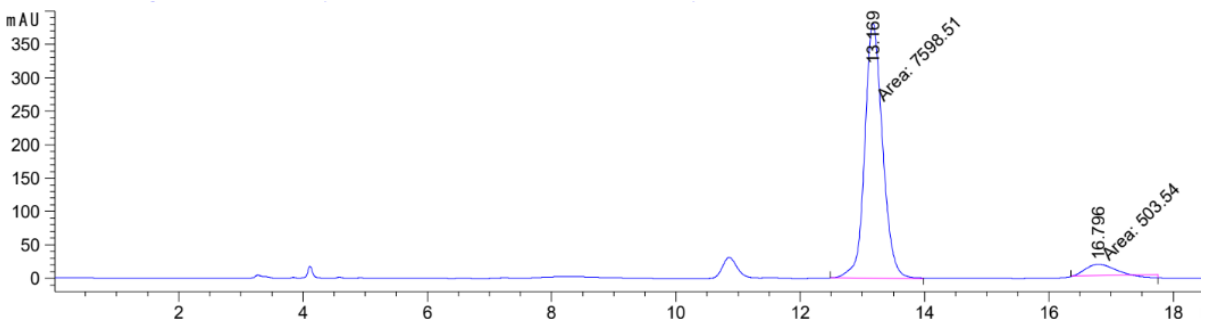

Signal 1: DAD1 A, Sig=254,4 Ref=360,100

Peak #	RetTime [min]	Type	Width [min]	Area [mAU*s]	Height [mAU]	Area %
1	13.169	MM	0.3324	7598.51318	380.94470	93.7850
2	16.796	MM	0.5051	503.53983	16.61453	6.2150

Racemic sample of **3t**

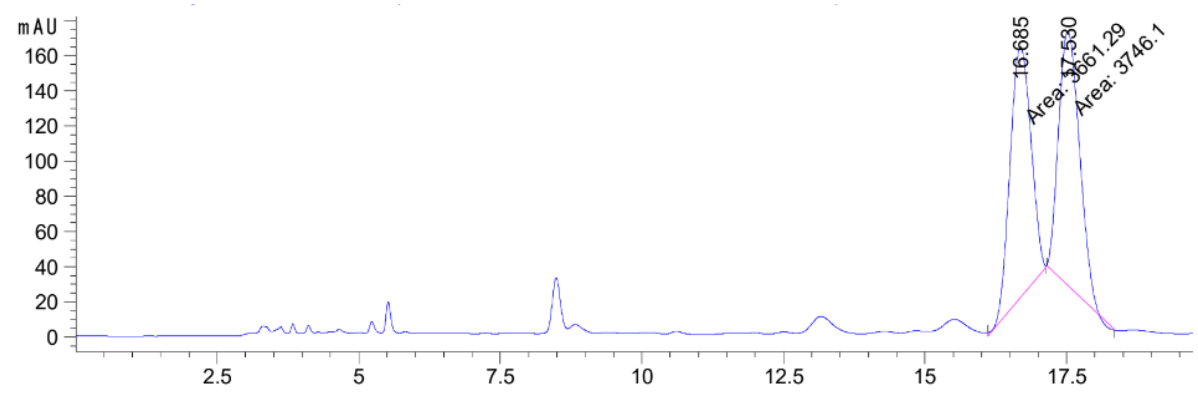

Signal 1: DAD1 A, Sig=254,4 Ref=360,100

Peak #	RetTime [min]	Type	Width [min]	Area [mAU*s]	Height [mAU]	Area %
1	16.685	MM	0.4274	3661.29272	142.77187	49.4275
2	17.530	MM	0.4311	3746.10327	144.81517	50.5725

Asymmetric sample of **3t**

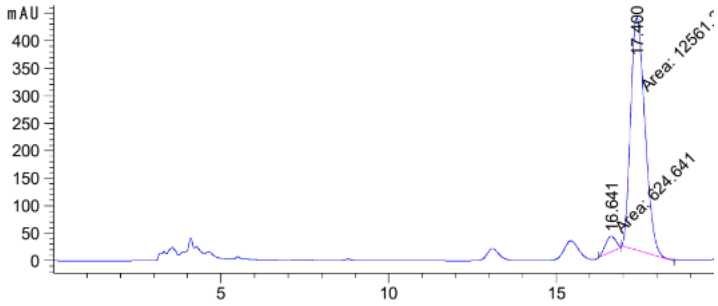

Signal 1: DAD1 A, Sig=254,4 Ref=360,100

Peak #	RetTime [min]	Type	Width [min]	Area [mAU*s]	Height [mAU]	Area %
1	16.641	MM	0.3687	624.64081	28.23552	4.7372
2	17.400	MM	0.4945	1.25612e4	423.32162	95.2628

Racemic sample of **3u**

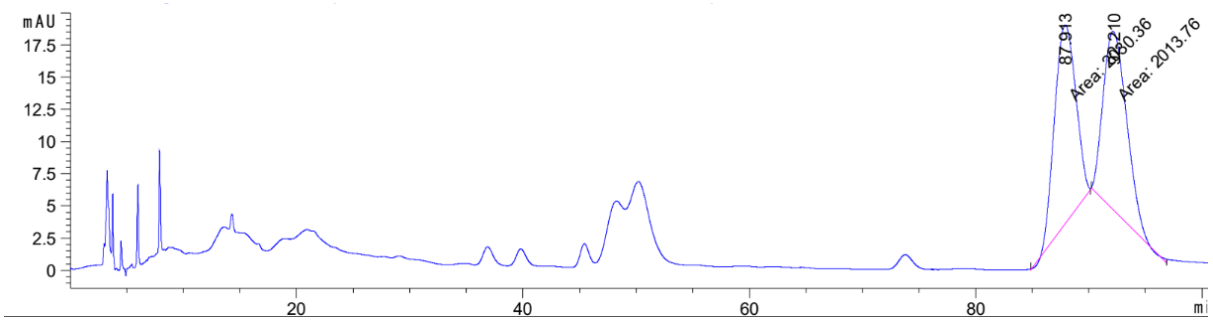

Signal 1: DAD1 A, Sig=254,4 Ref=360,100

Peak #	RetTime [min]	Type	Width [min]	Area [mAU*s]	Height [mAU]	Area %
1	87.913	MM	2.1932	2030.36206	15.42928	50.2053
2	92.210	MM	2.4230	2013.75610	13.85192	49.7947

Asymmetric sample of **3u**

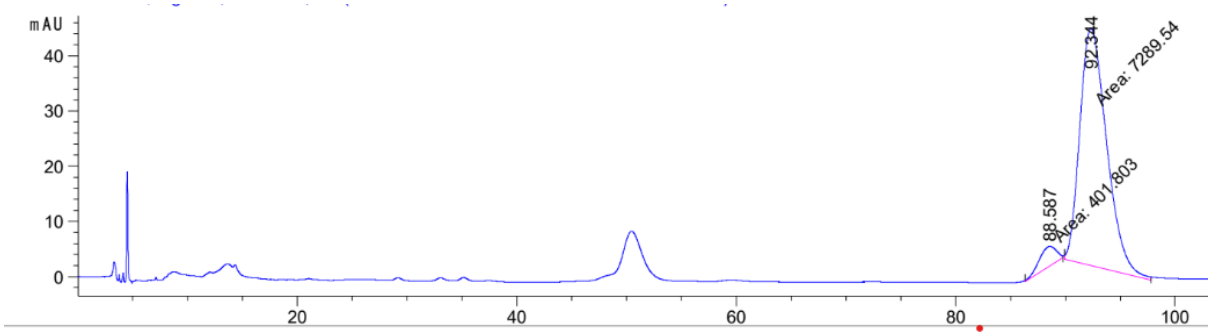

Signal 1: DAD1 A, Sig=254,4 Ref=360,100

Peak #	RetTime [min]	Type	Width [min]	Area [mAU*s]	Height [mAU]	Area %
1	88.587	MM	1.3428	401.80289	3.53212	5.2241
2	92.344	MM	2.8272	7289.54004	42.97228	94.7759

Racemic sample of **3v**

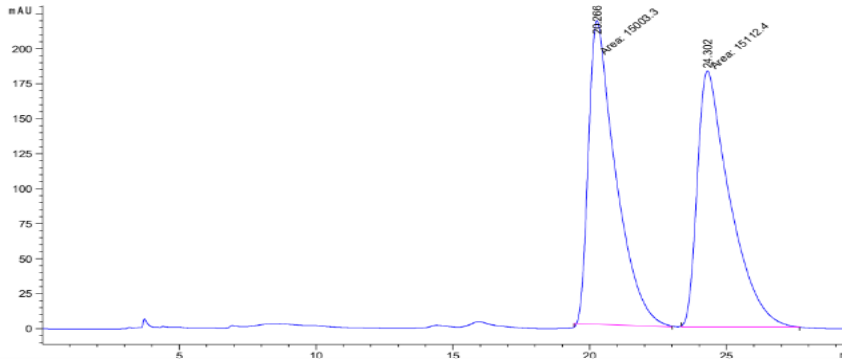

Signal 1: DAD1 A, Sig=254,4 Ref=off

Peak #	RetTime [min]	Type	Width [min]	Area [mAU*s]	Height [mAU]	Area %
1	20.266	MM	1.1534	1.50033e4	216.79150	49.8189
2	24.302	MM	1.3769	1.51124e4	182.92453	50.1811

Asymmetric sample of **3v**

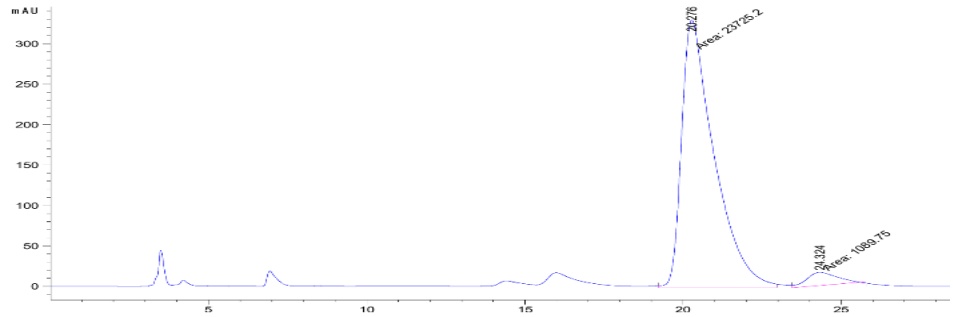

Signal 1: DAD1 A, Sig=254,4 Ref=off

Peak #	RetTime [min]	Type	Width [min]	Area [mAU*s]	Height [mAU]	Area %
1	20.276	MM	1.1937	2.37252e4	331.26447	95.6085
2	24.324	MM	1.1133	1089.75183	16.31369	4.3915

Racemic sample of **4**

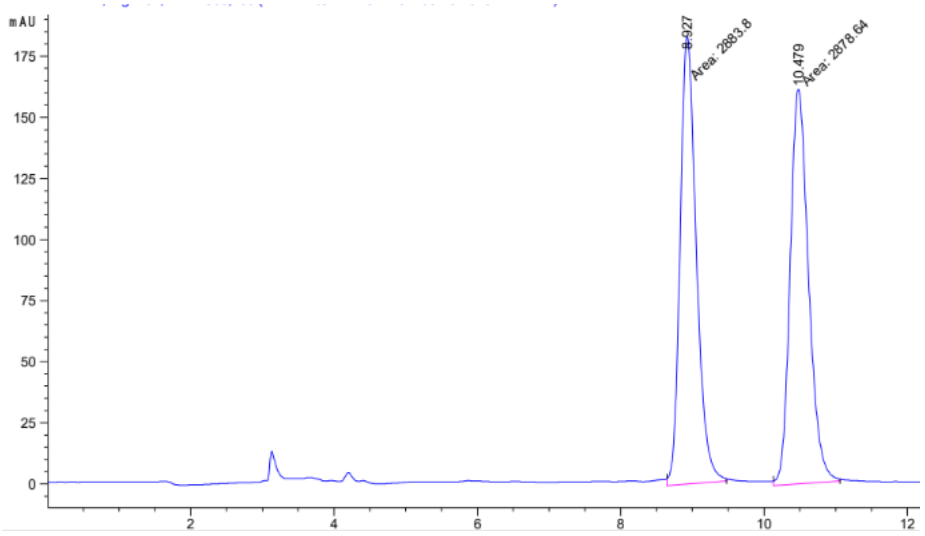

Signal 1: DAD1 A, Sig=254,4 Ref=360,100

Peak #	RetTime [min]	Type	Width [min]	Area [mAU*s]	Height [mAU]	Area %
1	8.927	MM	0.2625	2883.80469	183.07259	50.0449
2	10.479	MM	0.2973	2878.63574	161.39877	49.9551

Asymmetric sample of **4**

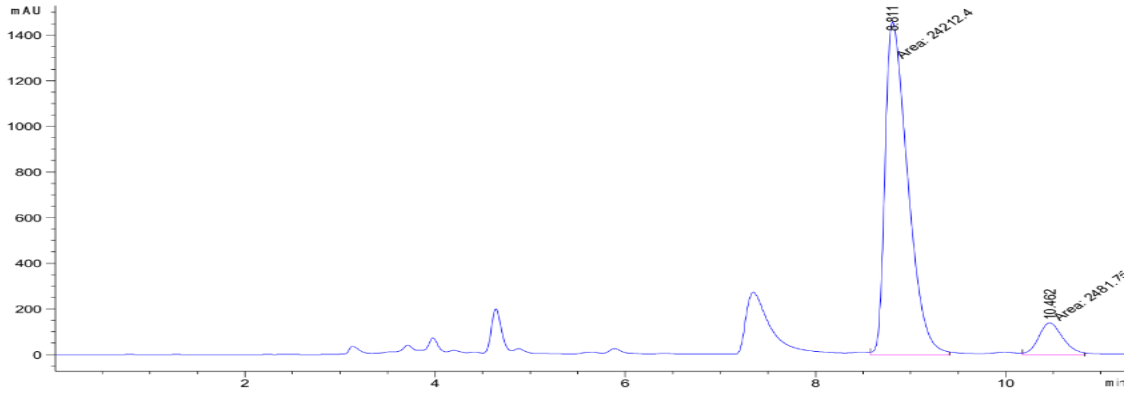

Signal 1: DAD1 A, Sig=254,4 Ref=360,100

Peak #	RetTime [min]	Type	Width [min]	Area [mAU*s]	Height [mAU]	Area %
1	8.811	MM	0.2766	2.42124e4	1459.03650	90.7030
2	10.462	MM	0.2966	2481.75464	139.46638	9.2970

Crystallographic details of compound 3d

The structures of ferrocene fused tetrahydropyridine (*Sp*)-**3d** (CCDC: 2498520), were confirmed by X-ray structure analysis. We isolated the suitable single crystal by the slow evaporation method in a 1:4 ratio of solvents of Hexane in Dichloromethane

Table S4 : Crystal data and structure refinement for **3d**.

Identification code	**3d**
CCDC No	**2498520**
Empirical formula	$C_{28}H_{22}FeO_2$
Formula weight	446.30
Temperature/K	140.00
Crystal system	orthorhombic
Space group	$P2_12_12_1$
a/Å	8.2412(6)
b/Å	11.3911(8)
c/Å	21.8790(15)
α/°	90
β/°	90
γ/°	90
Volume/Å^3	2053.9(3)
Z	4
ρ_{calc}g/cm^3	1.443
μ/mm^{-1}	0.758
F(000)	928.0
Crystal size/mm^3	0.07 × 0.03 × 0.03
Radiation	MoKα (λ = 0.71073)
2Θ range for data collection/°	4.032 to 49.424
Index ranges	$-9 \le h \le 9$, $-13 \le k \le 13$, $-25 \le l \le 25$
Reflections collected	33287
Independent reflections	3508 [R_{int} = 0.1151, R_{sigma} = 0.0725]
Data/restraints/parameters	3508/114/287
Goodness-of-fit on F^2	1.030
Final R indexes [I>=2σ (I)]	R_1 = 0.0535, wR_2 = 0.1138
Final R indexes [all data]	R_1 = 0.0789, wR_2 = 0.1270
Largest diff. peak/hole / e Å^{-3}	0.53/-0.38
Flack parameter	-0.02(2)

Table S5 Fractional Atomic Coordinates ($\times 10^4$) and Equivalent Isotropic Displacement Parameters ($Å^2 \times 10^3$) for 3d. U_{eq} is defined as 1/3 of of the trace of the orthogonalised U_{IJ} tensor.

Atom	***x***	***y***	***z***	**U(eq)**
Fe01	8047.7(11)	2442.4(10)	7388.9(4)	35.6(3)
O002	3964(6)	3606(5)	6881(2)	47.1(13)
O003	3362(6)	1835(5)	7231(2)	55.8(15)
C004	6813(10)	1074(6)	7010(3)	38.8(17)
C005	10016(10)	3239(7)	7762(4)	51(2)
C006	6042(8)	2157(6)	6890(3)	34.8(17)
C007	7141(9)	2891(6)	6553(3)	33.9(17)
C008	8654(10)	4366(6)	5540(3)	39.6(18)
C009	7187(9)	4710(6)	5898(3)	34.6(17)
C00A	8622(10)	3973(7)	7821(4)	52(2)
C00B	4377(8)	2491(8)	7027(3)	40.9(16)
C00C	10184(11)	4395(7)	5792(4)	51(2)
C00D	6611(9)	4061(6)	6365(3)	36.1(17)
C00E	8610(9)	2233(6)	6490(3)	38.7(18)
C00F	8373(9)	1124(6)	6763(3)	42.5(19)
C00G	6472(10)	5844(7)	5699(4)	47.3(19)
C00H	9688(11)	2195(7)	8069(4)	58(2)
C00I	8487(13)	4081(7)	4923(4)	59(2)
C00J	6542(11)	6828(7)	6091(5)	63(2)
C00K	5204(9)	4481(7)	6754(3)	45.2(19)
C00L	7472(10)	3350(8)	8159(4)	55(2)
C00M	11558(14)	4135(8)	5470(5)	71(3)
C00N	5865(12)	5998(10)	5116(4)	72(3)
C00O	8123(11)	2249(8)	8324(3)	62(3)
C00P	9900(18)	3785(9)	4608(5)	87(3)
C00Q	5291(15)	7129(12)	4949(5)	98(4)
C00R	6014(15)	7920(10)	5886(7)	94(3)
C00S	11379(16)	3801(10)	4866(6)	93(3)
C00U	5411(18)	8025(13)	5344(7)	114(4)
C1	6510(30)	4000(16)	4716(9)	51(5)
C3	5860(20)	5271(16)	4630(7)	56(4)
C2	7350(30)	4229(18)	4477(9)	56(4)
C4	5780(30)	4540(20)	4728(10)	51(5)

Table S6 Anisotropic Displacement Parameters ($Å^2×10^3$) for 3d. The Anisotropic displacement factor exponent takes the form: $-2\pi^2[h^2a^{*2}U_{11}+2hka^*b^*U_{12}+\ldots]$.

Atom	U_{11}	U_{22}	U_{33}	U_{23}	U_{13}	U_{12}
Fe01	34.9(5)	40.6(5)	31.3(5)	3.4(5)	-0.4(4)	-0.6(6)
O002	36(3)	62(3)	43(3)	8(3)	9(3)	7(3)
O003	37(3)	76(4)	54(3)	8(3)	6(3)	-7(3)
C004	51(5)	37(4)	29(4)	8(3)	0(4)	-8(4)
C005	39(4)	54(5)	61(6)	-3(4)	-8(4)	-6(4)
C006	41(4)	43(5)	21(3)	-5(3)	-2(3)	2(3)
C007	38(4)	39(4)	24(3)	1(3)	6(3)	6(3)
C008	61(5)	25(3)	33(4)	1(3)	8(3)	2(3)
C009	41(4)	37(4)	26(4)	4(3)	-2(3)	2(4)
C00A	59(5)	48(4)	48(5)	-4(4)	-19(4)	-1(4)
C00B	40(4)	56(4)	27(3)	1(4)	-1(3)	0(5)
C00C	59(5)	36(4)	57(5)	-7(4)	15(4)	-2(4)
C00D	42(5)	42(4)	25(3)	-2(3)	1(3)	11(3)
C00E	39(4)	38(5)	40(4)	2(3)	10(3)	3(3)
C00F	45(5)	39(4)	43(4)	4(3)	0(4)	10(4)
C00G	49(5)	45(4)	47(4)	15(4)	3(4)	5(4)
C00H	56(6)	53(6)	64(6)	2(4)	-25(5)	-2(4)
C00I	99(7)	39(4)	40(4)	-5(3)	8(4)	7(5)
C00J	54(5)	43(4)	91(6)	0(4)	-1(5)	9(4)
C00K	46(5)	50(5)	39(4)	4(4)	10(4)	14(4)
C00L	42(5)	80(7)	43(5)	-23(5)	-6(4)	-1(4)
C00M	68(6)	50(4)	96(6)	-9(4)	23(5)	-11(4)
C00N	61(5)	98(6)	58(5)	30(5)	1(4)	22(5)
C00O	66(6)	90(8)	29(4)	14(4)	-16(4)	-31(6)
C00P	134(7)	70(5)	56(5)	-14(4)	31(5)	8(6)
C00Q	94(6)	125(7)	74(6)	64(5)	-3(5)	30(6)
C00R	85(6)	65(5)	133(7)	6(5)	12(6)	13(5)
C00S	104(7)	77(6)	97(6)	1(5)	60(6)	-2(6)
C00U	104(7)	103(7)	134(8)	47(6)	20(7)	29(6)
C1	90(17)	32(10)	31(6)	-6(8)	0(9)	-13(8)
C3	83(11)	52(9)	33(7)	0(6)	-3(7)	-11(7)
C2	83(11)	52(9)	33(7)	0(6)	-3(7)	-11(7)
C4	90(17)	32(10)	31(6)	-6(8)	0(9)	-13(8)

Table S7 Bond Lengths for **3d**.

Atom	Atom	Length/Å	Atom	Atom	Length/Å
Fe01	C004	2.038(7)	C009	C00D	1.347(9)

Fe01	C005	2.030(8)	C009	C00G	1.485(10)
Fe01	C006	2.007(7)	C00A	C00L	1.396(11)
Fe01	C007	2.040(6)	C00C	C00M	1.367(13)
Fe01	C00A	2.039(8)	C00D	C00K	1.516(10)
Fe01	C00E	2.035(7)	C00E	C00F	1.411(10)
Fe01	C00F	2.051(7)	C00G	C00J	1.413(11)
Fe01	C00H	2.030(8)	C00G	C00N	1.380(11)
Fe01	C00L	2.033(8)	C00H	C00O	1.406(12)
Fe01	C00O	2.058(7)	C00I	C00P	1.394(14)
O002	C00B	1.354(10)	C00I	C1	1.69(2)
O002	C00K	1.454(9)	C00I	C2	1.36(2)
O003	C00B	1.207(9)	C00J	C00R	1.393(13)
C004	C006	1.412(9)	C00L	C00O	1.412(12)
C004	C00F	1.396(10)	C00M	C00S	1.382(15)
C005	C00A	1.426(11)	C00N	C00Q	1.420(15)
C005	C00H	1.392(11)	C00N	C3	1.348(18)
C006	C007	1.436(9)	C00N	C4	1.87(2)
C006	C00B	1.455(9)	C00P	C00S	1.343(16)
C007	C00D	1.462(9)	C00Q	C00U	1.341(17)
C007	C00E	1.431(9)	C00R	C00U	1.290(17)
C008	C009	1.494(11)	C1	C3	1.56(2)
C008	C00C	1.377(11)	C2	C4	1.45(4)
C008	C00I	1.394(10)			

Table S8 Bond Angles for **3d**.

Atom	**Atom**	**Atom**	**Angle/°**	**Atom**	**Atom**	**Atom**	**Angle/°**
C004	Fe01	C007	69.2(3)	C00D	C007	Fe01	126.2(5)
C004	Fe01	C00A	163.5(3)	C00E	C007	Fe01	69.3(4)
C004	Fe01	C00F	39.9(3)	C00E	C007	C006	106.1(5)
C004	Fe01	C00O	109.7(3)	C00E	C007	C00D	134.7(6)
C005	Fe01	C004	154.8(3)	C00C	C008	C009	121.6(6)
C005	Fe01	C007	122.7(3)	C00C	C008	C00I	119.0(8)
C005	Fe01	C00A	41.0(3)	C00I	C008	C009	119.3(8)
C005	Fe01	C00E	105.0(3)	C00D	C009	C008	122.6(6)
C005	Fe01	C00F	119.5(3)	C00D	C009	C00G	124.0(7)
C005	Fe01	C00L	68.0(3)	C00G	C009	C008	113.3(6)
C005	Fe01	C00O	67.9(3)	C005	C00A	Fe01	69.2(4)
C006	Fe01	C004	40.9(3)	C00L	C00A	Fe01	69.7(5)
C006	Fe01	C005	161.6(3)	C00L	C00A	C005	107.3(7)

C006	Fe01	C007	41.6(3)	O002	C00B	C006	115.7(7)
C006	Fe01	C00A	125.6(3)	O003	C00B	O002	119.6(7)
C006	Fe01	C00E	69.1(3)	O003	C00B	C006	124.6(8)
C006	Fe01	C00F	68.0(3)	C00M	C00C	C008	123.1(8)
C006	Fe01	C00H	157.6(3)	C007	C00D	C00K	111.0(6)
C006	Fe01	C00L	110.0(3)	C009	C00D	C007	127.5(6)
C006	Fe01	C00O	123.2(3)	C009	C00D	C00K	121.5(6)
C007	Fe01	C00F	68.5(3)	C007	C00E	Fe01	69.6(4)
C007	Fe01	C00O	158.2(3)	C00F	C00E	Fe01	70.4(4)
C00A	Fe01	C007	106.6(3)	C00F	C00E	C007	108.1(6)
C00A	Fe01	C00F	154.9(3)	C004	C00F	Fe01	69.5(4)
C00A	Fe01	C00O	67.9(3)	C004	C00F	C00E	109.1(6)
C00E	Fe01	C004	68.3(3)	C00E	C00F	Fe01	69.2(4)
C00E	Fe01	C007	41.1(3)	C00J	C00G	C009	119.7(7)
C00E	Fe01	C00A	119.7(3)	C00N	C00G	C009	121.7(8)
C00E	Fe01	C00F	40.4(3)	C00N	C00G	C00J	118.4(8)
C00E	Fe01	C00O	160.2(3)	C005	C00H	Fe01	70.0(5)
C00F	Fe01	C00O	125.5(3)	C005	C00H	C00O	109.4(8)
C00H	Fe01	C004	121.6(3)	C00O	C00H	Fe01	71.0(4)
C00H	Fe01	C005	40.1(3)	C008	C00I	C1	111.5(10)
C00H	Fe01	C007	159.3(3)	C00P	C00I	C008	116.9(10)
C00H	Fe01	C00A	67.9(3)	C00P	C00I	C1	131.1(10)
C00H	Fe01	C00E	122.7(3)	C2	C00I	C008	137.1(13)
C00H	Fe01	C00F	107.5(3)	C2	C00I	C00P	104.5(12)
C00H	Fe01	C00L	67.6(3)	C00R	C00J	C00G	119.9(10)
C00H	Fe01	C00O	40.2(3)	O002	C00K	C00D	115.4(6)
C00L	Fe01	C004	127.6(3)	C00A	C00L	Fe01	70.2(5)
C00L	Fe01	C007	122.0(3)	C00A	C00L	C00O	109.2(7)
C00L	Fe01	C00A	40.1(3)	C00O	C00L	Fe01	70.8(4)
C00L	Fe01	C00E	156.0(3)	C00C	C00M	C00S	117.7(11)
C00L	Fe01	C00F	163.1(3)	C00G	C00N	C00Q	118.2(11)
C00L	Fe01	C00O	40.4(3)	C00G	C00N	C4	108.7(10)
C00B	O002	C00K	120.8(6)	C00Q	C00N	C4	132.7(12)
C006	C004	Fe01	68.4(4)	C3	C00N	C00G	130.7(12)
C00F	C004	Fe01	70.5(4)	C3	C00N	C00Q	110.7(11)
C00F	C004	C006	107.8(6)	C00H	C00O	Fe01	68.8(4)
C00A	C005	Fe01	69.8(4)	C00H	C00O	C00L	106.6(7)
C00H	C005	Fe01	69.9(5)	C00L	C00O	Fe01	68.9(4)
C00H	C005	C00A	107.5(8)	C00S	C00P	C00I	123.2(10)
C004	C006	Fe01	70.7(4)	C00U	C00Q	C00N	120.1(11)
C004	C006	C007	108.7(6)	C00U	C00R	C00J	120.0(12)

C004	C006	C00B	127.9(7)	C00P	C00S	C00M	120.1(11)
C007	C006	Fe01	70.4(4)	C00R	C00U	C00Q	123.3(13)
C007	C006	C00B	123.2(6)	C3	C1	C00I	108.3(14)
C00B	C006	Fe01	128.4(5)	C00N	C3	C1	118.4(14)
C006	C007	Fe01	68.0(4)	C00I	C2	C4	111.9(18)
C006	C007	C00D	119.2(6)	C2	C4	C00N	110.7(17)

Table S9 Torsion Angles for **3d**.

A	**B**	**C**	**D**	**Angle/°**	**A**	**B**	**C**	**D**	**Angle/°**
Fe01	C004	C006	C007	60.5(5)	C00A	C005	C00H	Fe01	60.0(5)
Fe01	C004	C006	C00B	-124.2(7)	C00A	C005	C00H	C00O	-0.3(9)
Fe01	C004	C00F	C00E	-58.0(5)	C00A	C00L	C00O	Fe01	-59.9(5)
Fe01	C005	C00A	C00L	59.6(5)	C00A	C00L	C00O	C00H	-1.2(9)
Fe01	C005	C00H	C00O	-60.2(5)	C00B	O002	C00K	C00D	42.2(9)
Fe01	C006	C007	C00D	-120.3(6)	C00B	C006	C007	Fe01	123.7(6)
Fe01	C006	C007	C00E	59.1(5)	C00B	C006	C007	C00D	3.5(10)
Fe01	C006	C00B	O002	83.0(7)	C00B	C006	C007	C00E	-177.2(6)
Fe01	C006	C00B	O003	-100.5(8)	C00C	C008	C009	C00D	-69.5(10)
Fe01	C007	C00D	C009	120.9(7)	C00C	C008	C009	C00G	108.9(8)
Fe01	C007	C00D	C00K	-61.8(8)	C00C	C008	C00I	C00P	3.1(12)
Fe01	C007	C00E	C00F	60.1(5)	C00C	C008	C00I	C1	176.0(9)
Fe01	C00A	C00L	C00O	60.3(5)	C00C	C008	C00I	C2	-159.6(17)
Fe01	C00E	C00F	C004	58.1(5)	C00C	C00M	C00S	C00P	2.5(16)
Fe01	C00H	C00O	C00L	-58.7(5)	C00D	C007	C00E	Fe01	120.9(8)
Fe01	C00L	C00O	C00H	58.7(5)	C00D	C007	C00E	C00F	-179.0(7)
C004	C006	C007	Fe01	-60.6(5)	C00D	C009	C00G	C00J	66.4(11)
C004	C006	C007	C00D	179.1(6)	C00D	C009	C00G	C00N	-119.6(9)
C004	C006	C007	C00E	-1.6(7)	C00E	C007	C00D	C009	24.7(13)
C004	C006	C00B	O002	177.8(6)	C00E	C007	C00D	C00K	-158.0(7)
C004	C006	C00B	O003	-5.7(11)	C00F	C004	C006	Fe01	-59.8(5)
C005	C00A	C00L	Fe01	-59.2(5)	C00F	C004	C006	C007	0.7(8)
C005	C00A	C00L	C00O	1.0(9)	C00F	C004	C006	C00B	176.1(7)
C005	C00H	C00O	Fe01	59.6(6)	C00G	C009	C00D	C007	173.7(7)
C005	C00H	C00O	C00L	0.9(9)	C00G	C009	C00D	C00K	-3.3(11)
C006	C004	C00F	Fe01	58.4(5)	C00G	C00J	C00R	C00U	2.3(19)
C006	C004	C00F	C00E	0.5(8)	C00G	C00N	C00Q	C00U	2.8(18)
C006	C007	C00D	C009	-156.2(7)	C00G	C00N	C3	C1	5(3)
C006	C007	C00D	C00K	21.1(9)	C00G	C00N	C4	C2	-82.3(19)
C006	C007	C00E	Fe01	-58.2(4)	C00H	C005	C00A	Fe01	-60.0(5)

C006	C007	C00E	C00F	1.9(8)	C00H	C005	C00A	C00L	-0.5(9)
C007	C006	C00B	O002	-7.5(9)	C00I	C008	C009	C00D	114.7(8)
C007	C006	C00B	O003	169.0(6)	C00I	C008	C009	C00G	-66.9(9)
C007	C00D	C00K	O002	-42.5(9)	C00I	C008	C00C	C00M	-1.3(12)
C007	C00E	C00F	Fe01	-59.6(5)	C00I	C00P	C00S	C00M	-0.7(18)
C007	C00E	C00F	C004	-1.5(8)	C00I	C1	C3	C00N	-62(2)
C008	C009	C00D	C007	-8.1(12)	C00I	C2	C4	C00N	65(2)
C008	C009	C00D	C00K	174.9(7)	C00J	C00G	C00N	C00Q	-2.1(14)
C008	C009	C00G	C00J	-112.0(8)	C00J	C00G	C00N	C3	169.9(15)
C008	C009	C00G	C00N	62.1(11)	C00J	C00G	C00N	C4	-175.9(11)
C008	C00C	C00M	C00S	-1.6(14)	C00J	C00R	C00U	C00Q	-2(2)
C008	C00I	C00P	C00S	-2.2(16)	C00K	O002	C00B	O003	167.4(6)
C008	C00I	C1	C3	78.2(15)	C00K	O002	C00B	C006	-15.9(9)
C008	C00I	C2	C4	-16(3)	C00N	C00G	C00J	C00R	-0.3(15)
C009	C008	C00C	C00M	-177.1(7)	C00N	C00Q	C00U	C00R	-1(2)
C009	C008	C00I	C00P	179.0(8)	C00P	C00I	C1	C3	-110.3(15)
C009	C008	C00I	C1	-8.2(12)	C00P	C00I	C2	C4	179.6(16)
C009	C008	C00I	C2	16(2)	C00Q	C00N	C3	C1	177.7(16)
C009	C00D	C00K	O002	135.0(7)	C00Q	C00N	C4	C2	105(2)
C009	C00G	C00J	C00R	173.9(9)	C1	C00I	C00P	C00S	-173.3(13)
C009	C00G	C00N	C00Q	-176.2(9)	C3	C00N	C00Q	C00U	-170.7(14)
C009	C00G	C00N	C3	-4(2)	C2	C00I	C00P	C00S	165.8(14)
C009	C00G	C00N	C4	9.9(14)	C4	C00N	C00Q	C00U	174.8(15)

Table S10 Hydrogen Atom Coordinates (Å×10^4) and Isotropic Displacement Parameters (Å^2×10^3) for **3d**.

Atom	***x***	***y***	***z***	**U(eq)**
H004	6352.27	426.74	7221.9	47
H005	10990.15	3428.86	7552.15	61
H00A	8499.7	4742.03	7659.87	62
H00C	10289.5	4606.04	6210.41	61
H00E	9576.99	2496.39	6297.05	46
H00F	9151.29	508.69	6775.93	51
H00H	10409.13	1547.7	8101.3	69
H00J	6949.88	6744.33	6495.32	75
H00B	5639.8	4769.55	7147.74	54
H00D	4685.42	5154.93	6545.29	54
H00L	6418.14	3624.66	8261.61	66
H00M	12599.92	4181.02	5653.88	85
H00O	7605.52	1658.33	8560.23	74

H00P	9811.76	3560.34	4191.59	104
H00Q	4822.86	7250.33	4557.77	117
H00R	6096.98	8587.55	6143.99	113
H00S	12303.73	3583.4	4632.83	111
H00U	5033.3	8775.63	5218.72	137
H1A	6407.64	3554.3	4329.7	61
H1B	5882.67	3589.37	5036.28	61
H3A	6507.2	5647.4	4302.78	67
H3B	4731.07	5214.01	4480.01	67
H2A	7253.21	3493.37	4239.27	67
H2B	7713.73	4856.23	4195.34	67
H4A	5438.89	3929.7	5025.3	61
H4B	4967.36	4561.55	4395.43	61

Table S11 Atomic Occupancy for **3d**.

Atom	***Occupancy***	**Atom**	***Occupancy***	**Atom**	***Occupancy***
C1	0.543(13)	H1A	0.543(13)	H1B	0.543(13)
C3	0.543(13)	H3A	0.543(13)	H3B	0.543(13)
C2	0.457(13)	H2A	0.457(13)	H2B	0.457(13)
C4	0.457(13)	H4A	0.457(13)	H4B	0.457(13)

Computational Studies

Computational studies were performed with the Gaussian 09 Revision A.02 program suite with the DFT method of Becke's three-parameter hybrid Hartree-Fock procedure with the Lee Yang-Parr correlation function (B3LYP). The geometry optimization and energy calculations of the reactants, intermediates, and transition state were fully optimized by the DFT/B3LYP method with LANL2DZ basis set in the solution phase using the CPCM (conductor-like Polarizable Continuum Model) model in tert-amyl alcohol solvent. Energy obtained from computation is listed in Hartree and converted to kcal/mol. The difference between the favorable and unfavorable transition states is 12.94 kcal/mol.

Favorable TS I **Unfavorable TS II**

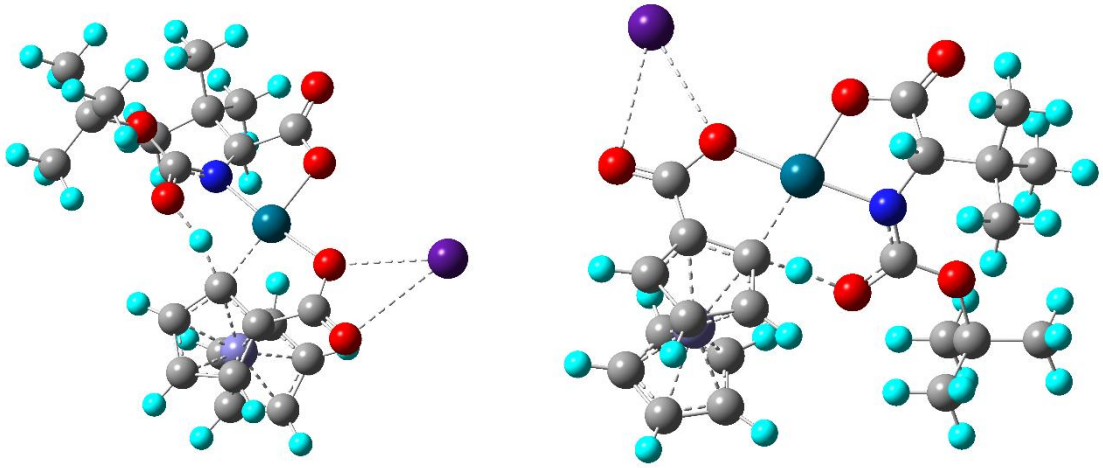

Figure S3. Optimized structure of favorable and unfavorable transition states

Energy Data

Structure	Electronic and Thermal Correction to G_{solv}	ΔG_{solv}
TS I	-1630.857732	0.00 kcal/mol
TS II	-1630.837105	+12.94 kcal/mol

Relative energies were calculated at the level of B3LYP/LANL2DZ/CPCM(THF) at 298K

Co-ordinates of Optimized Structures

Favourable TS I

Zero-point correction 0.462680 (Hartree/Particle)

Thermal correction to Energy 0.497605

Thermal correction to Enthalpy 0.498549

Thermal correction to Gibbs Free Energy 0.392023

Sum of electronic and zero-point energies -1630.892657

Sum of electronic and thermal Energies -1630.857732

Sum of electronic and thermal Enthalpies -1630.856788

Sum of electronic and thermal Free Energies -1630.963314

Imaginary vibration frequency: 1 (associated imaginary frequency i1260.95 cm^{-1})

Atomic	Forces (Hartrees/Bohr)		
Number	X	Y	Z
Fe	0.000020277	-0.000032994	-0.000000830
C	0.000005216	0.000001920	0.000001015
C	-0.000006473	0.000005709	-0.000001764
C	-0.000007548	0.000001770	-0.000008488
C	-0.000006536	0.000004470	-0.000005002
C	-0.000000743	0.000002098	-0.000002763
C	-0.000007196	-0.000000501	-0.000004087
H	0.000000445	-0.000003210	-0.000003803
H	0.000002039	0.000000020	-0.000002670
H	0.000001162	-0.000000279	-0.000002249
H	0.000002503	-0.000001994	-0.000000931
H	-0.000001837	0.000001248	-0.000000668
H	-0.000000658	0.000000541	-0.000001223
C	-0.000007980	-0.000005113	-0.000004452
H	0.000001744	0.000000407	-0.000002688
C	0.000018365	0.000022757	-0.000003133
C	-0.000023529	-0.000002472	0.000012183
C	-0.000012066	-0.000001734	-0.000011891
H	-0.000012944	-0.000026050	0.000003893

C	-0.000001317	-0.000001206	0.000001630
C	0.000013667	0.000003643	0.000000716
Pd	0.000006617	-0.000006054	-0.000005593
O	0.000000466	0.000013415	-0.000000249
O	-0.000000058	0.000002962	0.000004974
Cs	-0.000008230	-0.000003578	0.000000642
C	-0.000000075	0.000011306	0.000012857
H	0.000003046	0.000000134	-0.000004800
O	0.000000360	-0.000000054	0.000002608
O	0.000001055	0.000002600	-0.000001493
C	-0.000000963	0.000000264	0.000000954
C	-0.000001780	0.000000064	0.000000720
H	-0.000001745	-0.000000138	-0.000000236
H	-0.000001966	-0.000000078	0.000001034
H	-0.000001141	-0.000000382	0.000000584
C	-0.000000529	-0.000000093	-0.000000756
H	-0.000000180	-0.000000142	-0.000000564
H	-0.000001188	-0.000000343	-0.000001523
H	-0.000001336	-0.000000413	-0.000001240
C	-0.000001737	-0.000000218	-0.000000884
H	-0.000002390	-0.000001185	-0.000000472
H	-0.000002231	-0.000000785	-0.000000175
H	-0.000002312	-0.000000079	-0.000000564
C	0.000000388	0.000000639	0.000001609
C	0.000001118	-0.000000006	0.000000914
H	0.000001569	0.000000129	0.000001117
H	0.000001259	0.000000379	0.000000924
H	0.000000909	0.000000101	0.000001054
C	0.000002299	0.000000543	0.000002161
H	0.000002524	0.000000378	0.000001975

H	0.000001326	0.000000106	0.000002473
H	0.000001303	0.000000165	0.000001057
C	0.000000802	0.000000661	0.000002504
H	0.000001269	0.000000584	0.000002801
H	0.000000562	0.000000065	0.000002888
H	0.000000278	0.000000483	0.000002839
C	0.000000482	0.000000085	0.000003077
H	0.000000390	0.000000256	0.000001395
N	-0.000006441	0.000002551	0.000002855
O	0.000024774	0.000011052	0.000000360
O	0.000004917	-0.000004408	-0.000000623

Unfavorable TS II

Zero-point correction 0.462721 (Hartree/Particle)

Thermal correction to Energy 0.497534

Thermal correction to Enthalpy 0.498478

Thermal correction to Gibbs Free Energy 0.392986

Sum of electronic and zero-point energies -1630.871918

Sum of electronic and thermal Energies -1630.837105

Sum of electronic and thermal Enthalpies -1630.836161

Sum of electronic and thermal Free Energies -1630.941653

Imaginary vibration frequency: 1 (associated imaginary frequency i1236.41 cm^{-1})

Atomic	Forces (Hartrees/Bohr)		
Number	X	Y	Z
Fe	0.000029699	-0.000015200	0.000018878
C	0.000011904	0.000014730	0.000018015
C	-0.000023525	0.000008034	-0.000008719
C	-0.000004891	-0.000012274	-0.000017858
C	-0.000022952	0.000002262	-0.000023363
C	-0.000018377	0.000020984	-0.000005954

C	-0.000001878	0.000004062	0.000015667
H	-0.000002027	0.000004190	0.000000723
H	0.000000056	-0.000001432	-0.000000692
H	-0.000000118	0.000003649	0.000002428
H	-0.000003664	0.000002256	0.000002207
H	-0.000003284	0.000000777	0.000001773
H	-0.000004937	0.000001977	0.000000407
C	0.000009903	-0.000016233	0.000017160
H	-0.000003852	-0.000000051	0.000000983
C	-0.000015146	0.000015004	-0.000008533
C	-0.000005526	0.000000382	0.000004074
C	0.000027530	0.000002482	0.000001574
H	-0.000018118	-0.000001730	-0.000000678
C	-0.000000586	-0.000001773	-0.000001656
C	-0.000016340	0.000005943	0.000012450
Pd	-0.000011625	-0.000011445	-0.000015853
O	-0.000011616	-0.000001062	0.000009764
O	0.000000642	-0.000005148	-0.000001276
Cs	-0.000009755	0.000001473	0.000008221
C	0.000001098	0.000009499	0.000020874
H	-0.000002781	-0.000000661	-0.000005198
O	0.000001516	-0.000003128	0.000006434
O	-0.000007232	-0.000000399	-0.000005198
C	0.000003038	-0.000001292	-0.000003301
C	0.000001983	0.000002013	-0.000002995
H	0.000002219	0.000004182	-0.000004592
H	0.000003476	0.000001494	-0.000001905
H	0.000003771	0.000000386	-0.000004310
C	-0.000000335	0.000003648	-0.000005549
H	0.000005559	0.000002137	-0.000003556

H	0.000003327	0.000003237	-0.000002301
H	0.000002843	0.000004992	-0.000003059
C	-0.000000726	0.000002054	-0.000000123
H	-0.000003436	0.000008438	-0.000003217
H	-0.000000190	0.000004554	-0.000000131
H	0.000000777	0.000004400	-0.000002860
C	0.000003004	-0.000004224	-0.000001108
C	0.000003050	-0.000002956	-0.000003343
H	0.000005158	-0.000003400	-0.000003504
H	0.000003006	-0.000004453	-0.000001311
H	0.000002752	0.000000946	-0.000000659
C	0.000003385	-0.000005961	0.000000978
H	0.000004536	-0.000005492	0.000000770
H	0.000001698	-0.000006608	-0.000000281
H	0.000002616	-0.000004649	-0.000000139
C	0.000001620	-0.000000736	-0.000001244
H	0.000002729	-0.000002018	-0.000001750
H	0.000002560	-0.000002087	0.000000010
H	0.000001490	-0.000001607	0.000000074
C	0.000001631	-0.000005846	0.000002532
N	0.000035628	-0.000002589	-0.000011195
O	0.000011702	-0.000009040	0.000006759
O	-0.000002552	-0.000002046	0.000004832
H	-0.000000433	-0.000004645	-0.000000177

NMR Spectra of Chiral Ferrocene Fused Isochroman Derivatives 3a-3v and Post-derivatized Compound 4

^{1}H NMR Spectrum of 3a

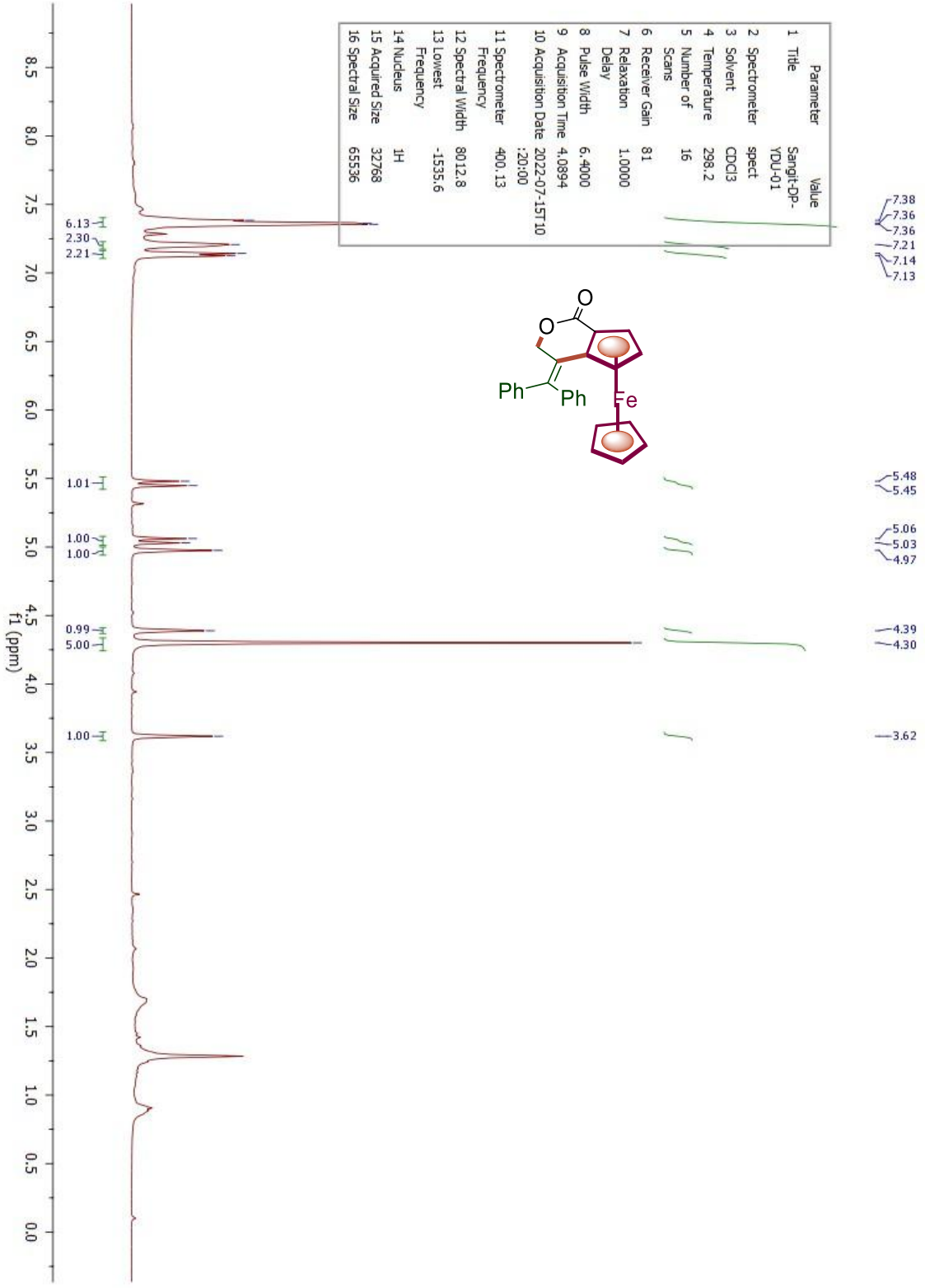

$^{13}C\{^{1}H\}$ NMR Spectrum of 3a

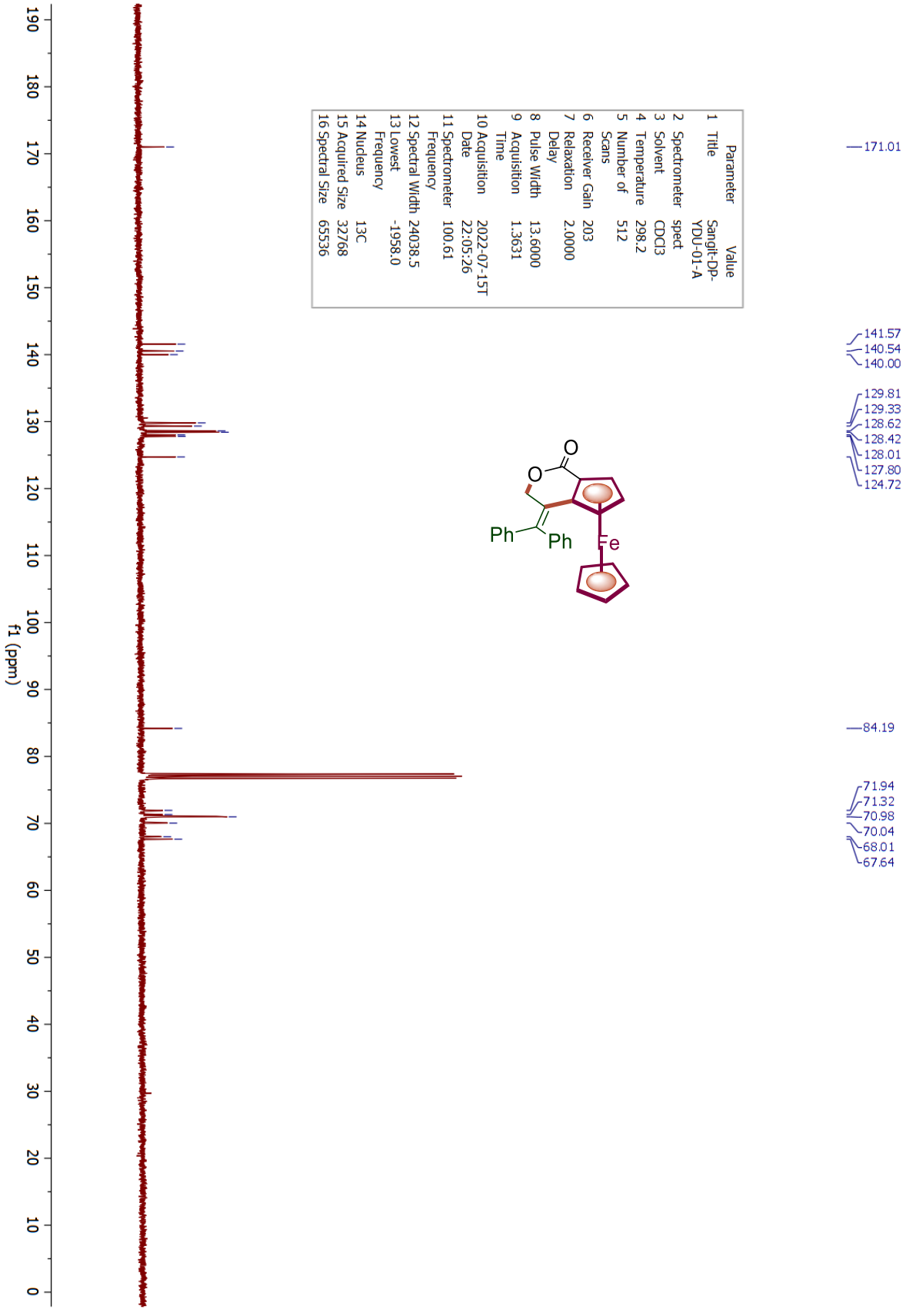

^{1}H NMR Spectrum of 3b

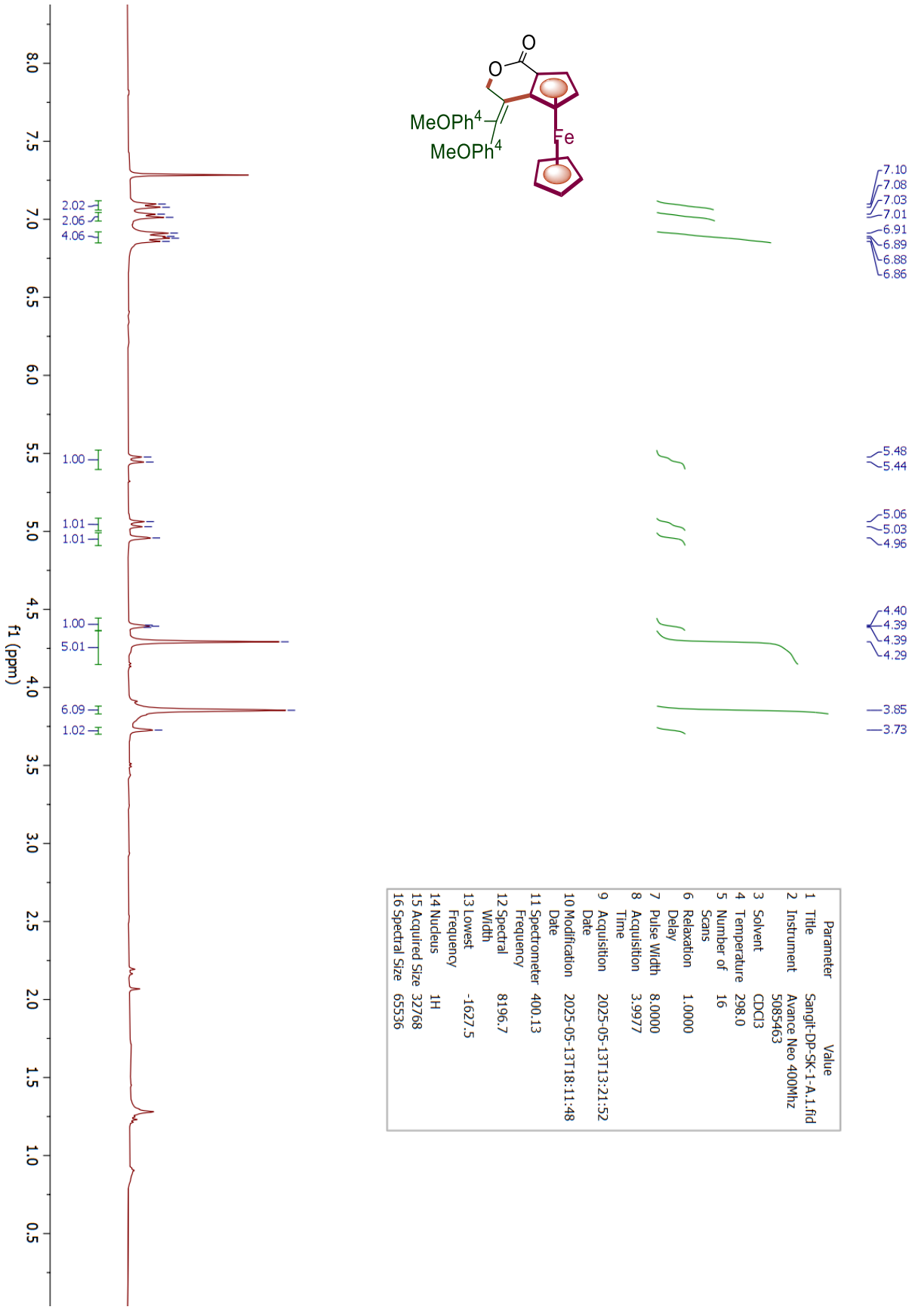

Parameter	Value
1 Title	Sangit-DP-SK-1-A.1.fid
2 Instrument	Avance Neo 400Mhz 5085463
3 Solvent	CDCl3
4 Temperature	298.0
5 Number of Scans	16
6 Relaxation Delay	1.0000
7 Pulse Width	8.0000
8 Acquisition Time	3.9977
9 Acquisition Date	2025-05-13T13:21:52
10 Modification Date	2025-05-13T18:11:48
11 Spectrometer Frequency	400.13
12 Spectral Width	8196.7
13 Lowest Frequency	-1627.5
14 Nucleus	1H
15 Acquired Size	32768
16 Spectral Size	65536

$^{13}C\{^{1}H\}$ NMR Spectrum of 3b

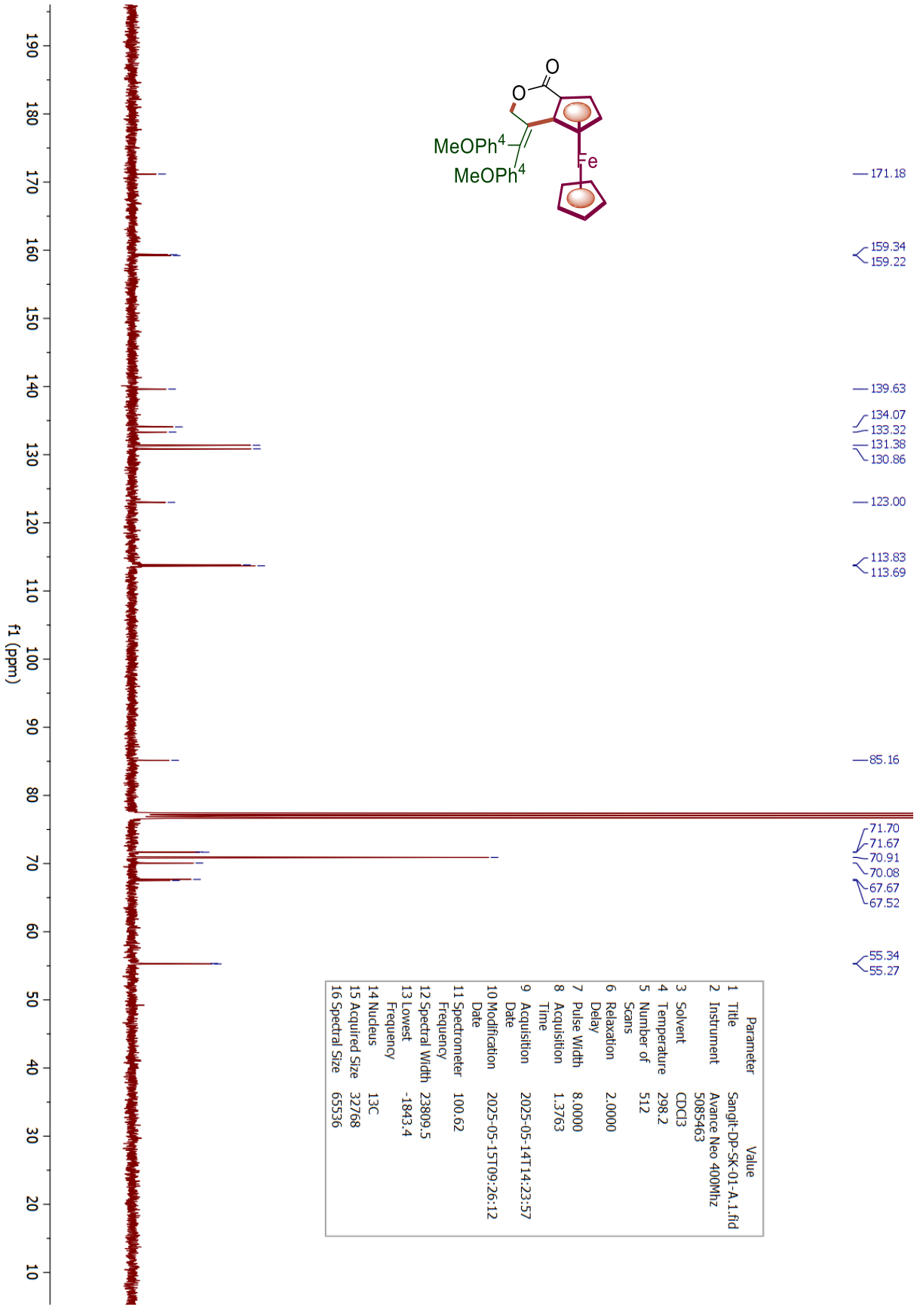

Parameter	Value
1 Title	Sangit-DP-SK-01-A.1.fid
2 Instrument	Avance Neo 400Mhz 5085463
3 Solvent	CDCl3
4 Temperature	298.2
5 Number of Scans	512
6 Relaxation Delay	2.0000
7 Pulse Width	8.0000
8 Acquisition Time	1.3763
9 Acquisition Date	2025-05-14T14:23:57
10 Modification Date	2025-05-15T09:26:12
11 Spectrometer Frequency	100.62
12 Spectral Width	23809.5
13 Lowest Frequency	-1843.4
14 Nucleus	13C
15 Acquired Size	32768
16 Spectral Size	65536

^{1}H NMR Spectrum of 3c

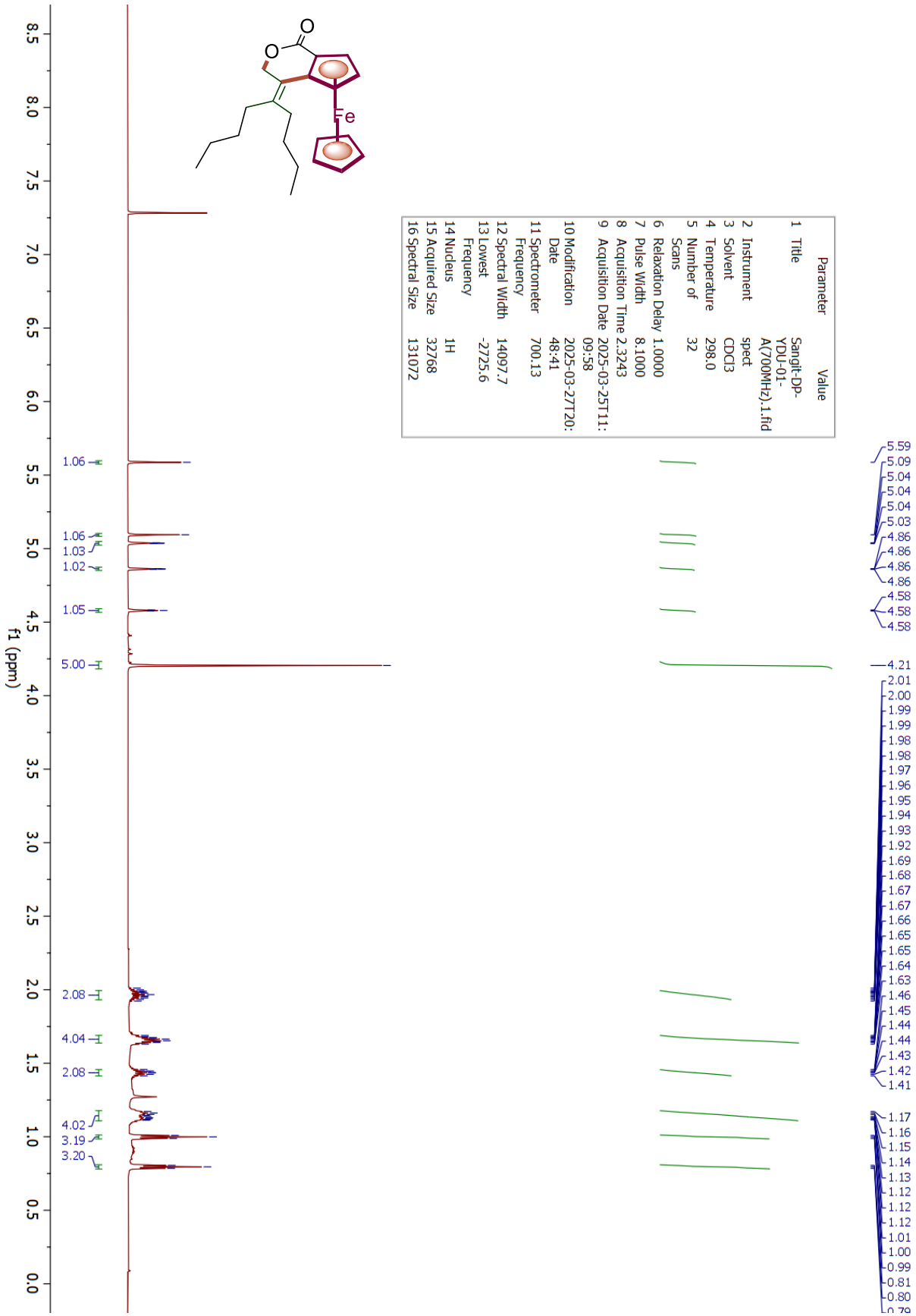

$^{13}C\{^{1}H\}$ NMR Spectrum of 3c

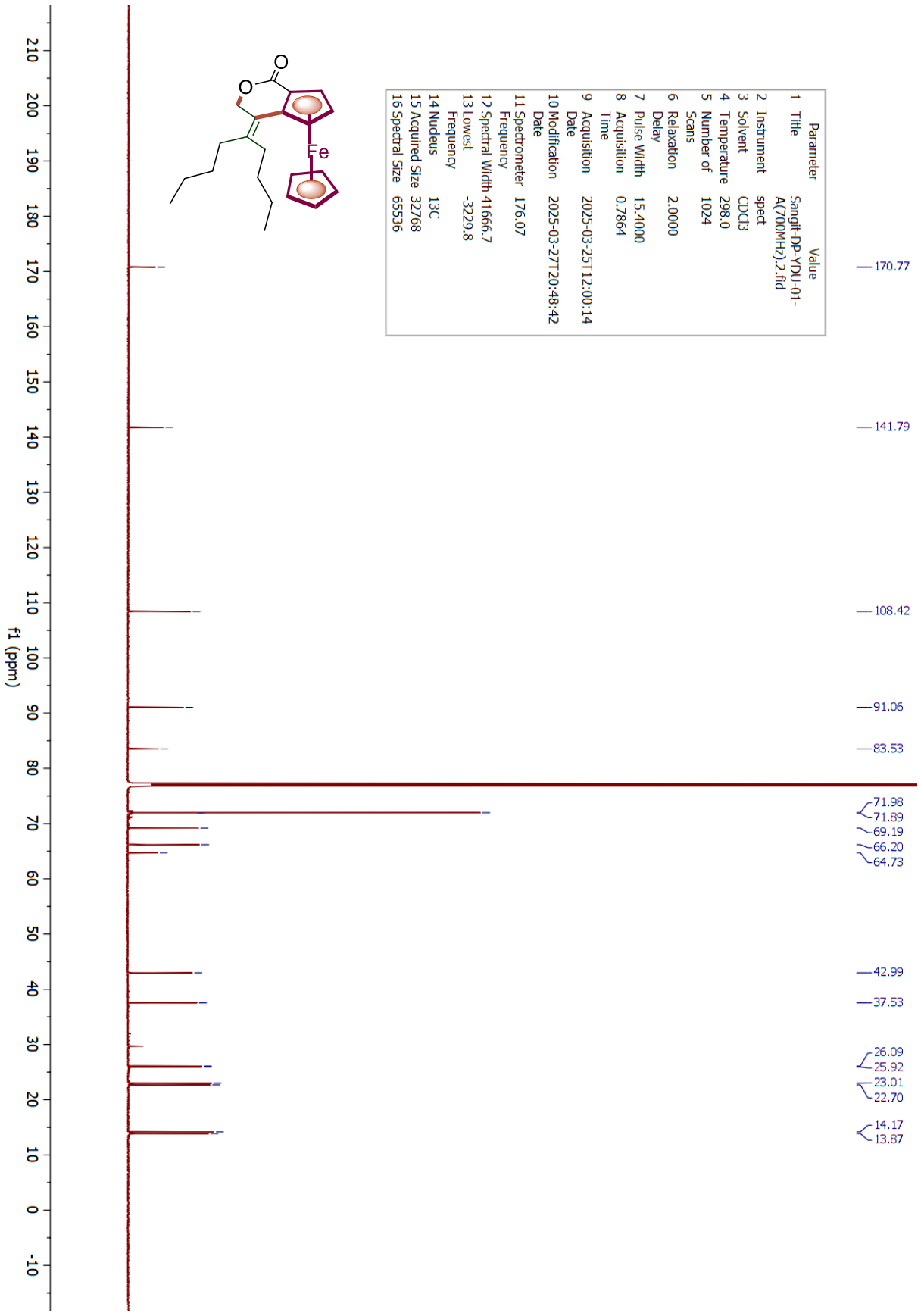

^{1}H NMR Spectrum of 3d

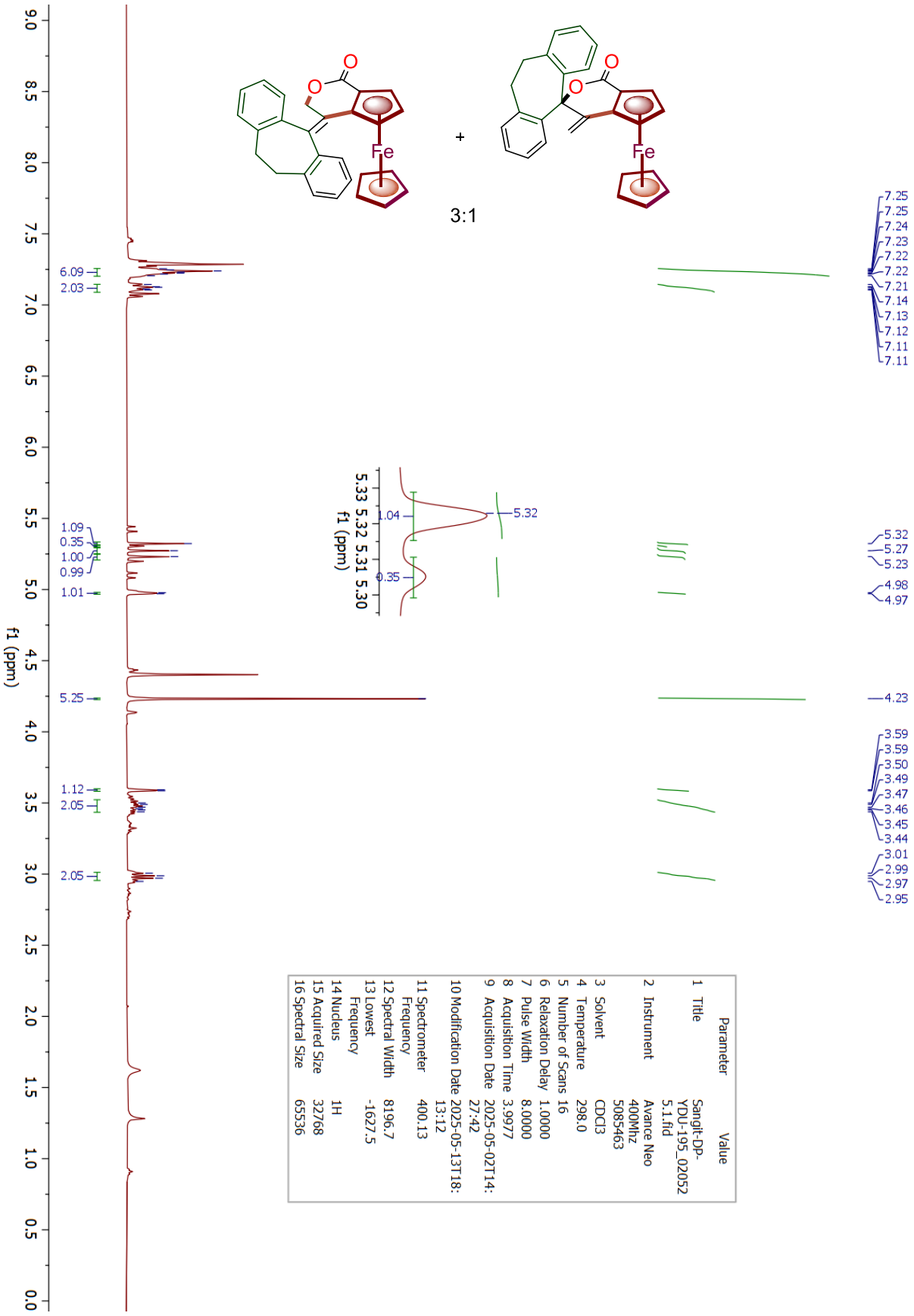

A mixture of regio-isomers were observed as 3:1 in the NMR spectra

$^{13}C\{^{1}H\}$ NMR Spectrum of 3d

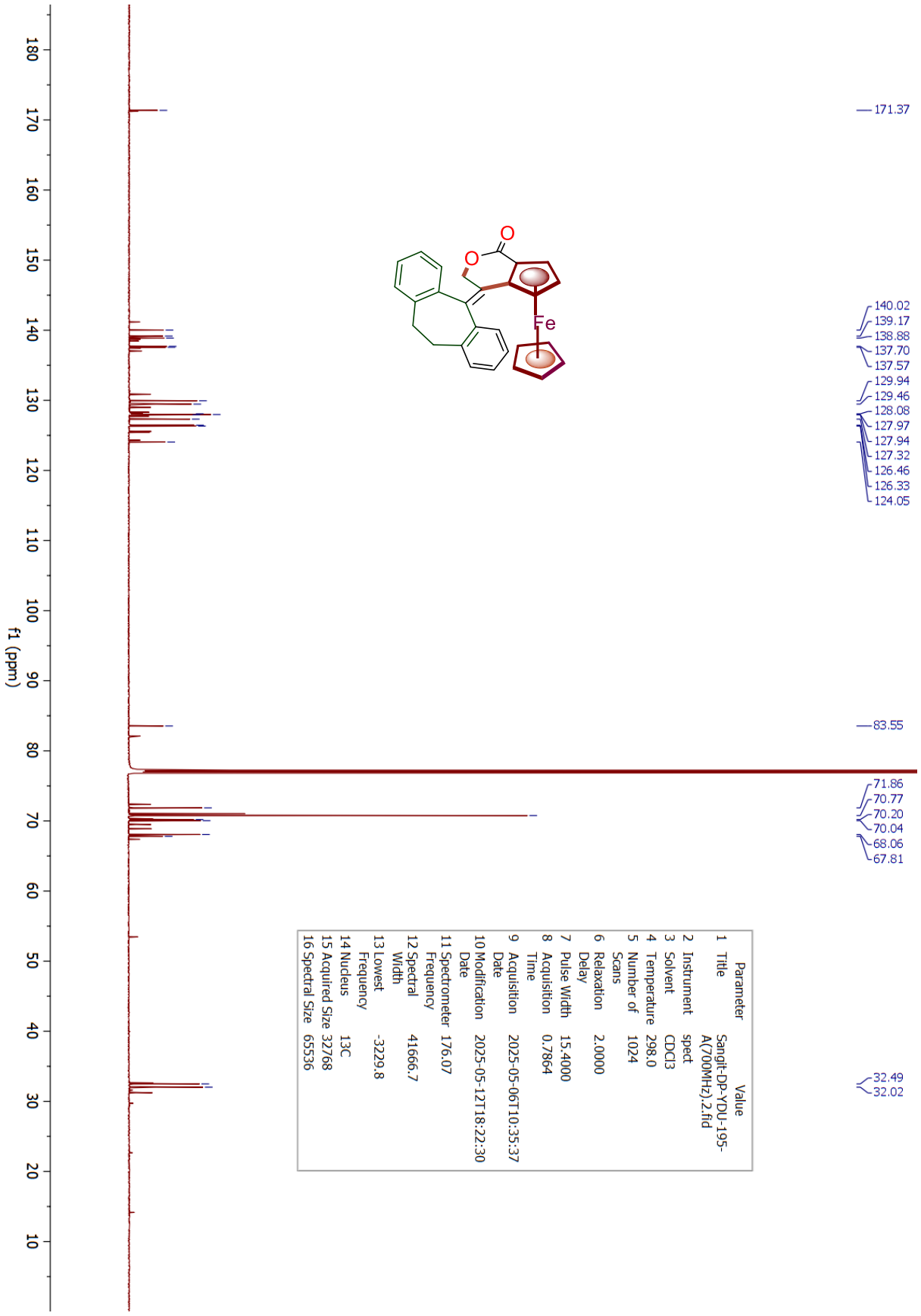

^{1}H NMR Spectrum of 3e

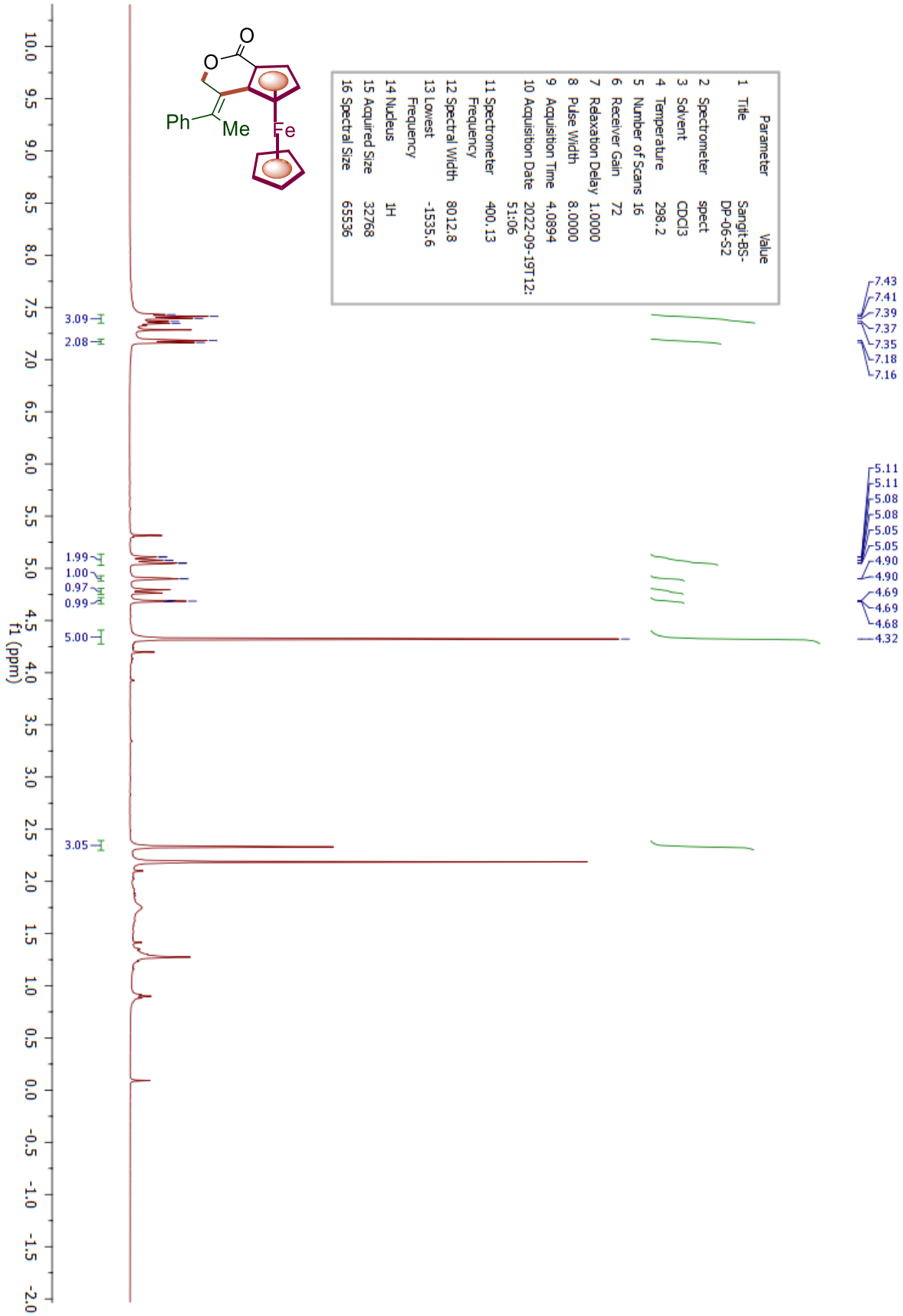

$^{13}C\{^{1}H\}$ NMR Spectrum of 3e

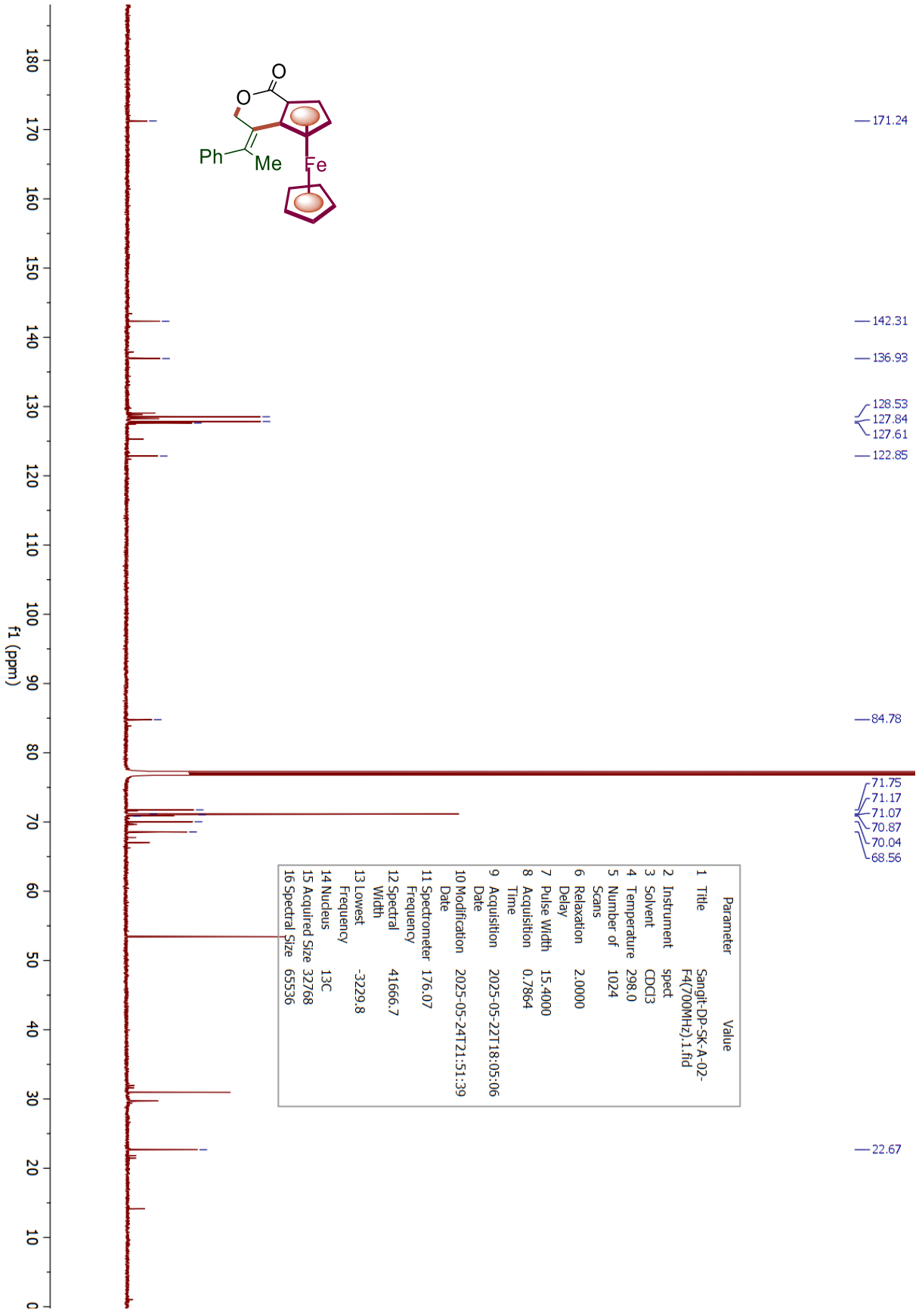

^{1}H NMR Spectrum of 3f

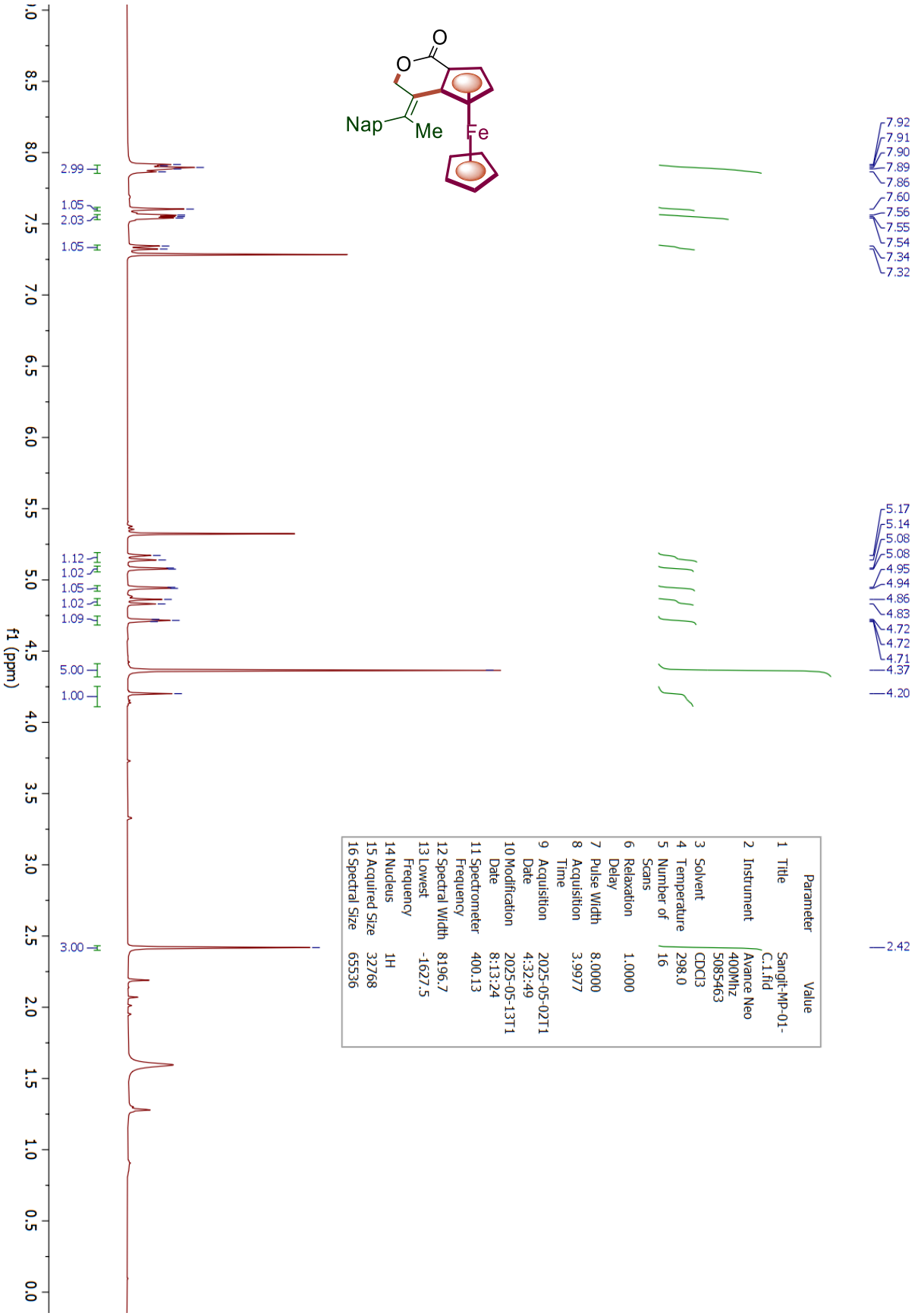

$^{13}C\{^{1}H\}$ NMR Spectrum of 3f

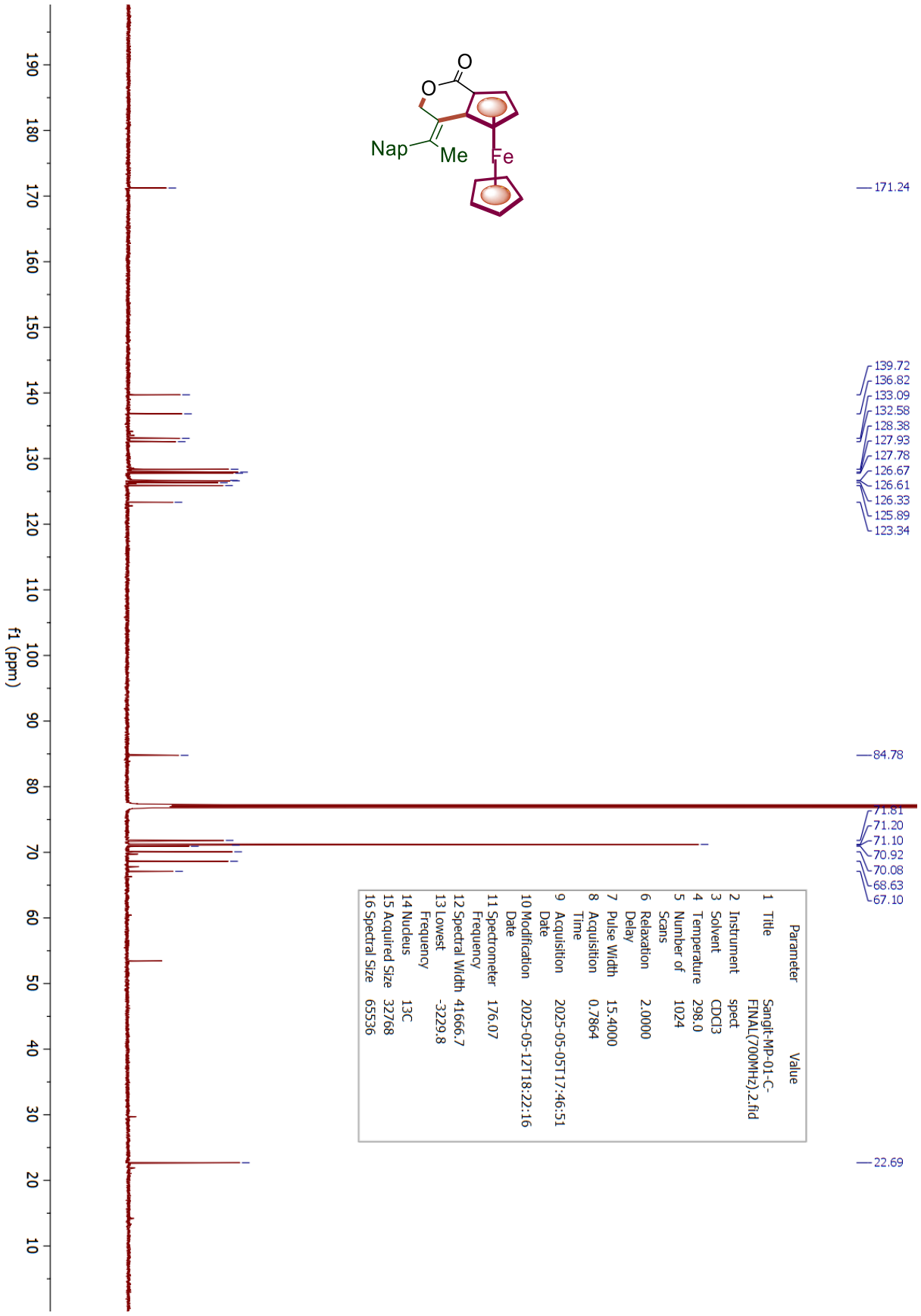

^{1}H NMR Spectrum of 3g

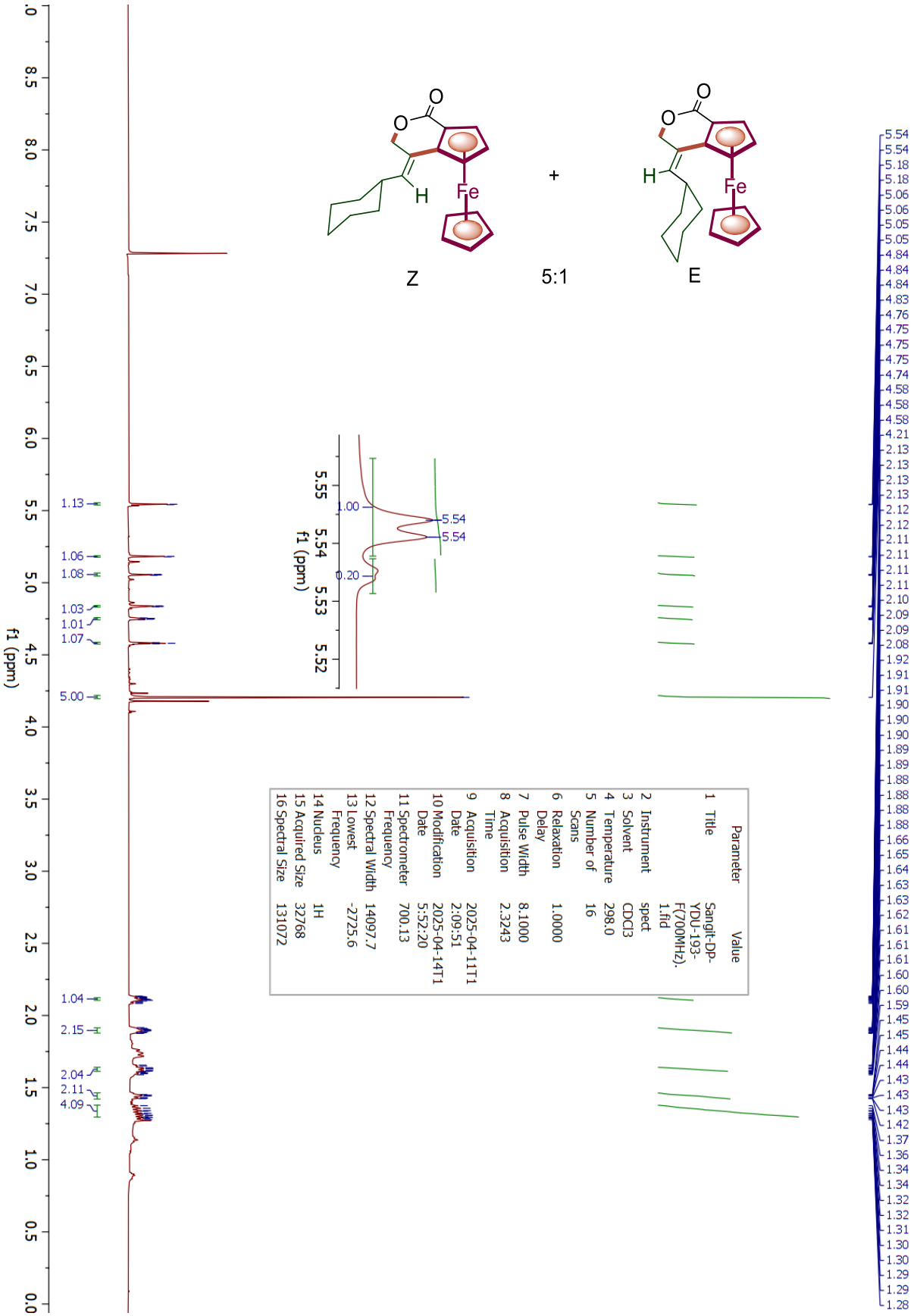

A mixture of E:Z regio-isomer were observed as 5:1 in the NMR spectra

$^{13}C\{^{1}H\}$ NMR Spectrum of 3g

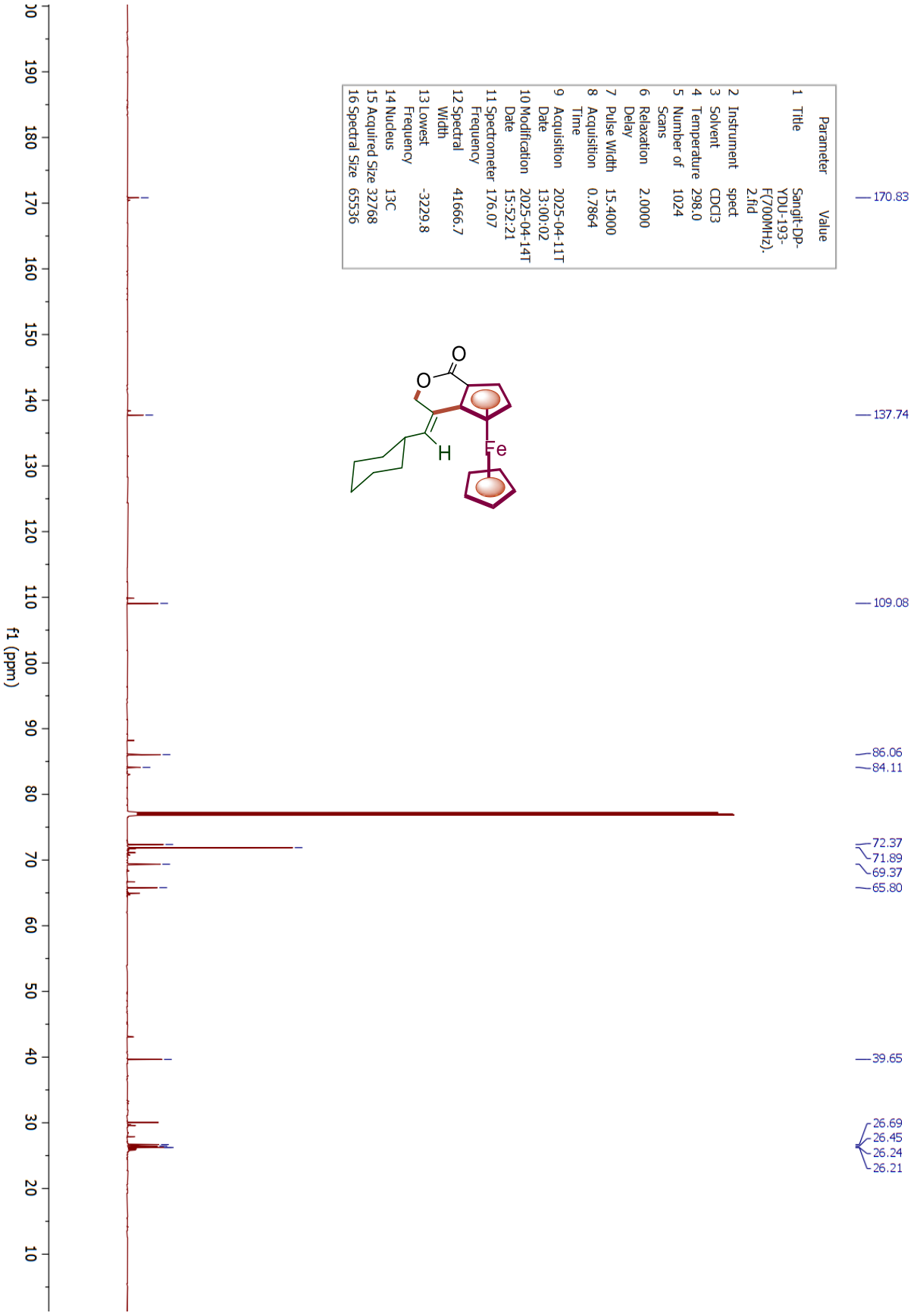

^{1}H NMR Spectrum of 3h

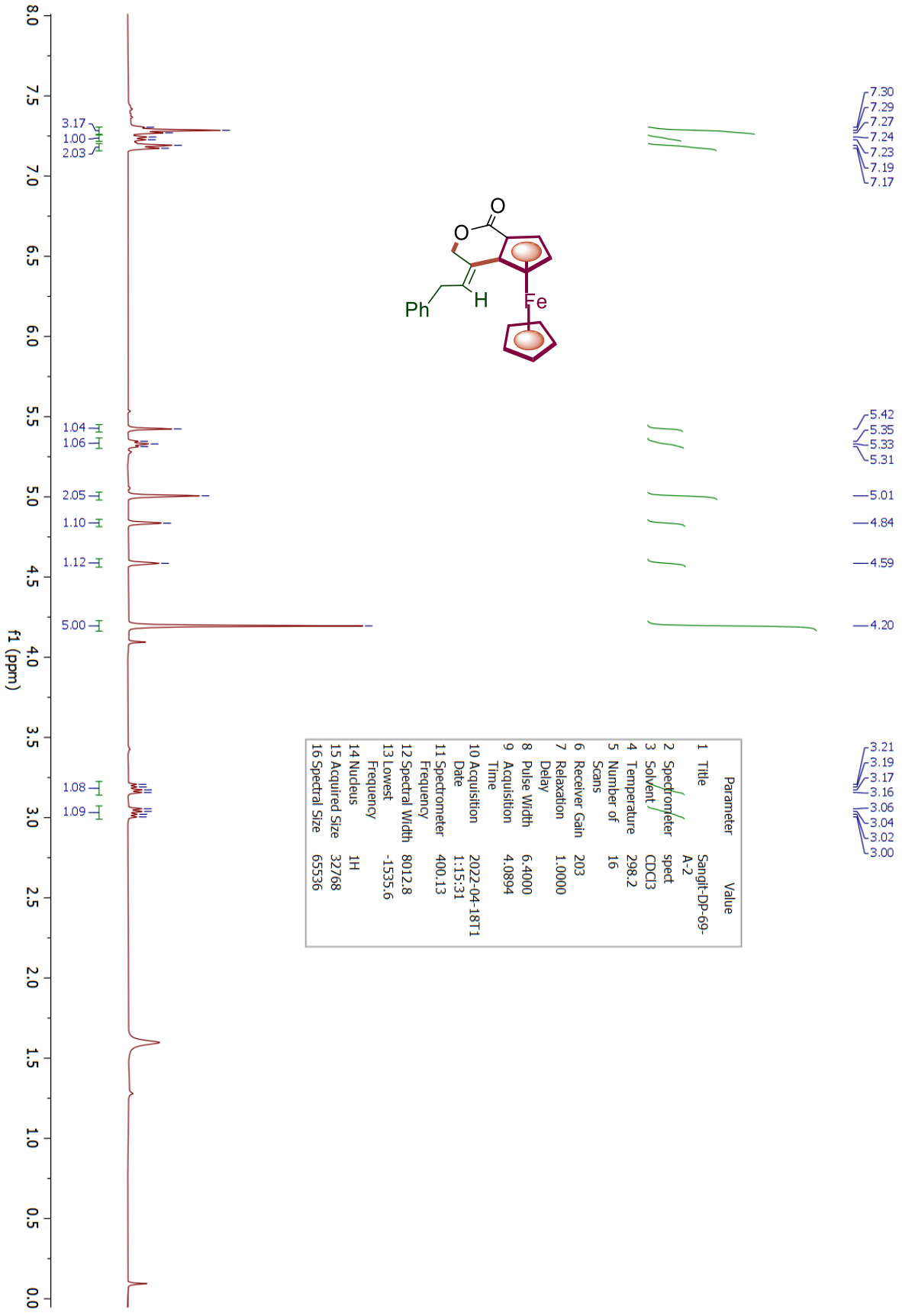

$^{13}C\{^{1}H\}$ NMR Spectrum of 3h

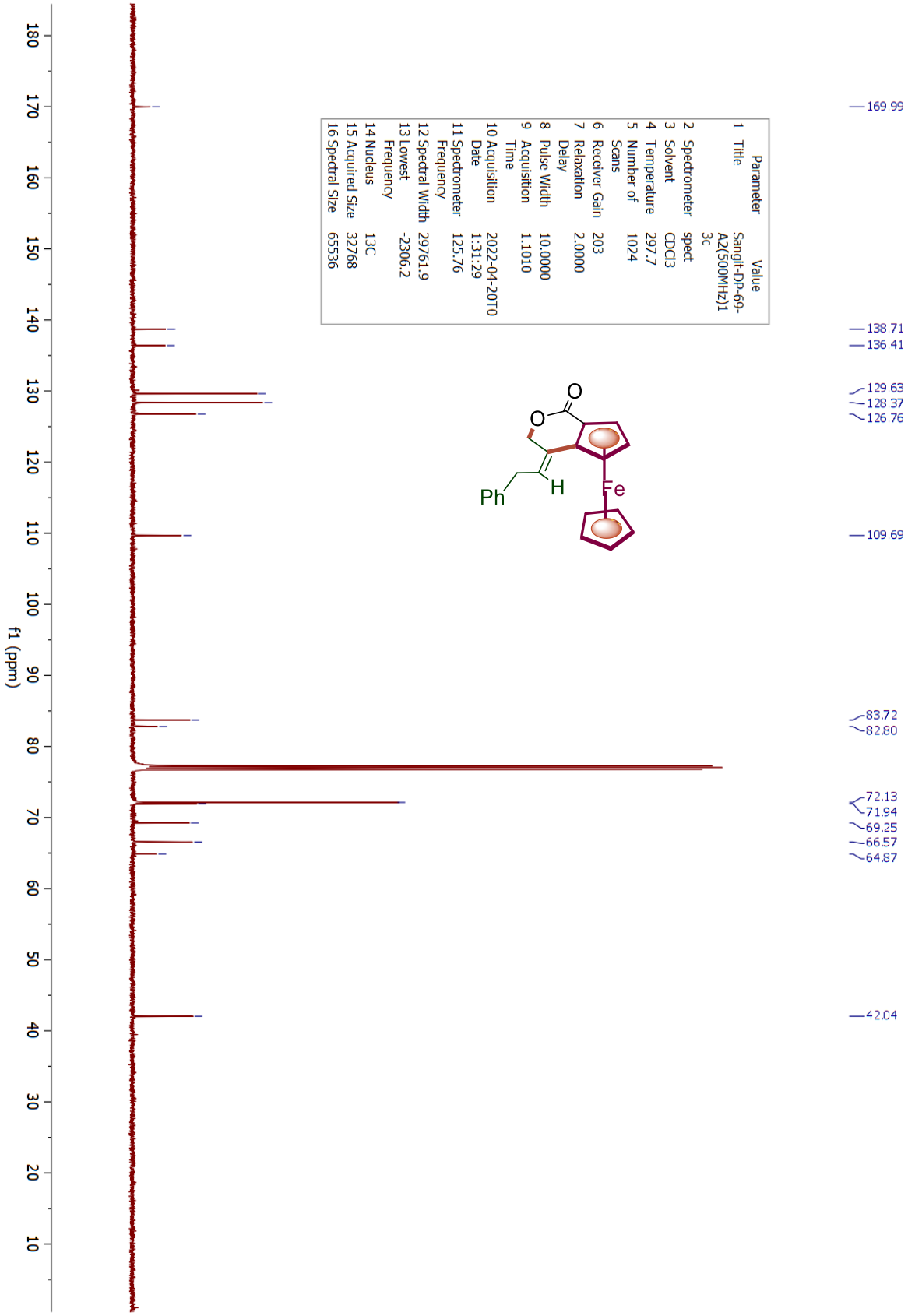

^{1}H NMR Spectrum of 3i

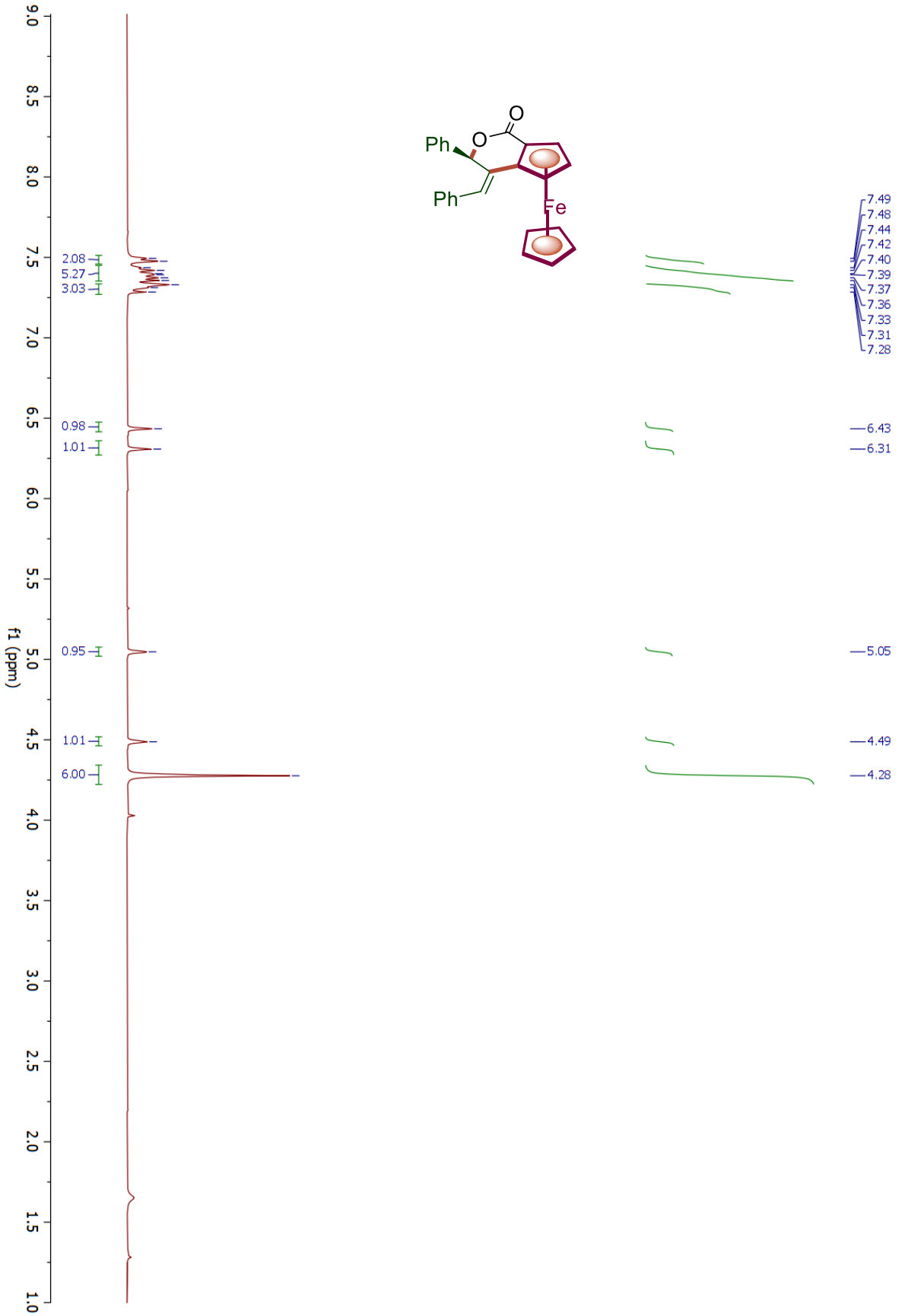

$^{13}C\{^{1}H\}$ NMR Spectrum of 3i

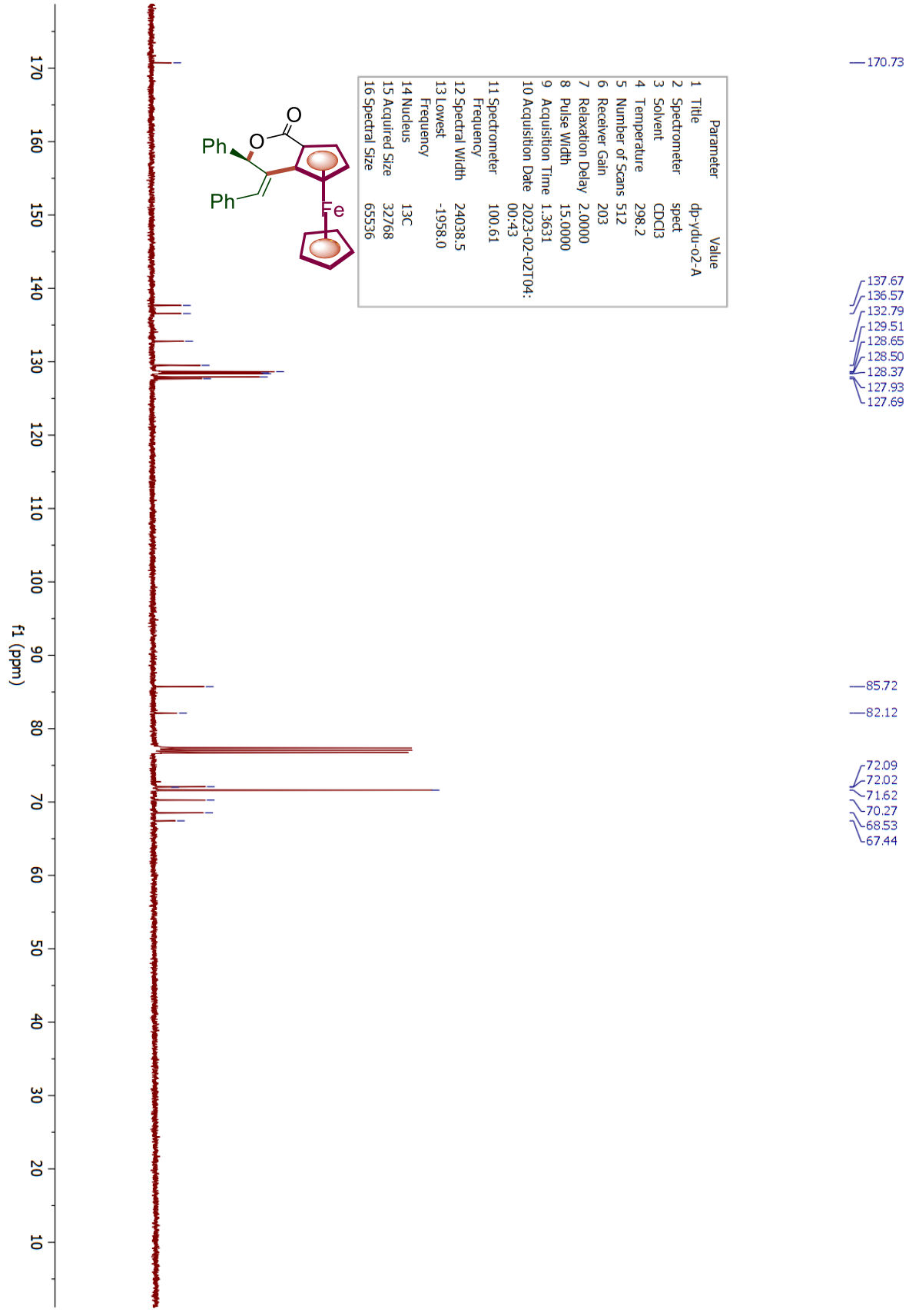

^{1}H NMR Spectrum of 3j

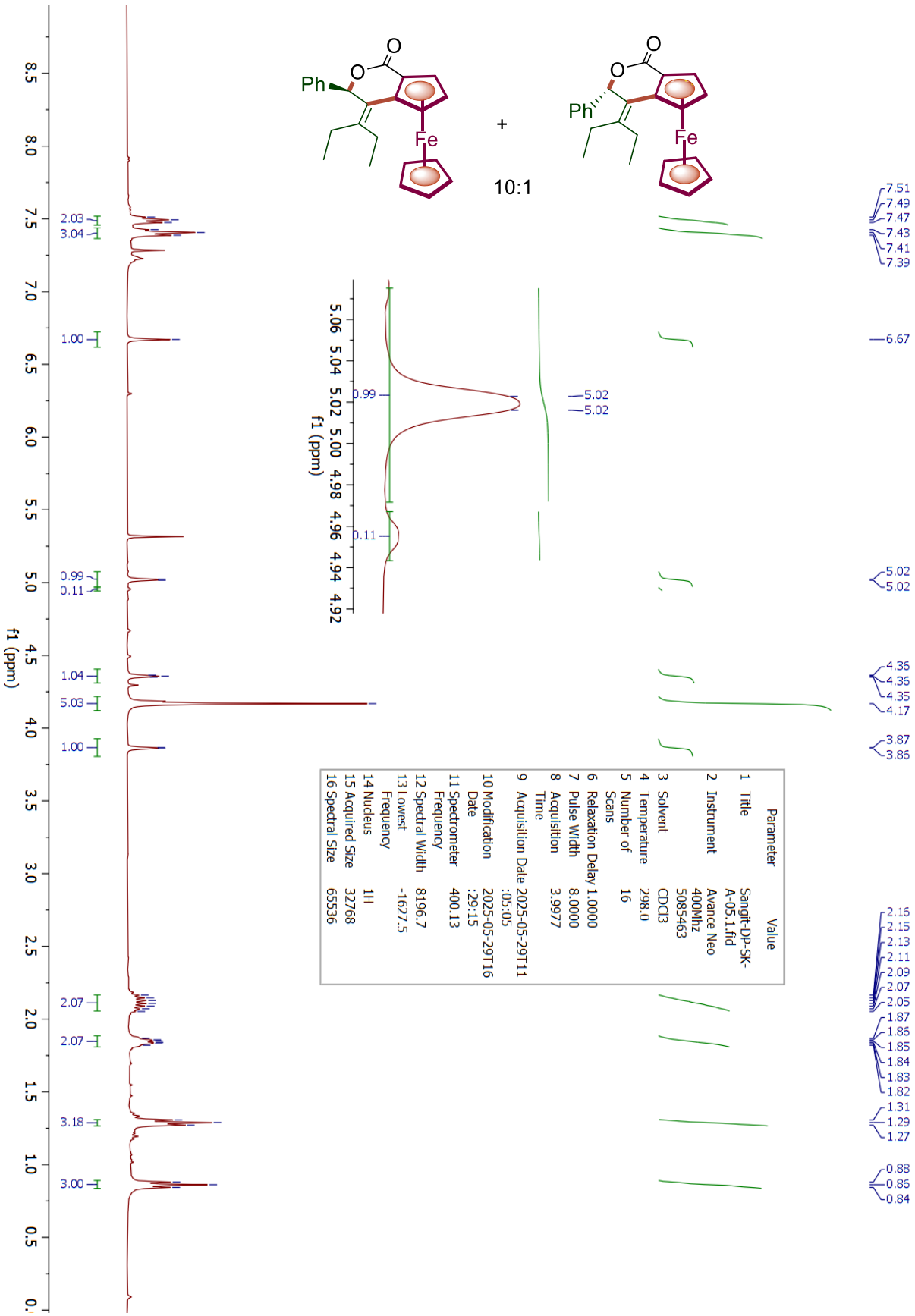

A mixture of diastereomer were observed as 10:1 in the NMR spectra

$^{13}C\{^{1}H\}$ NMR Spectrum of 3j

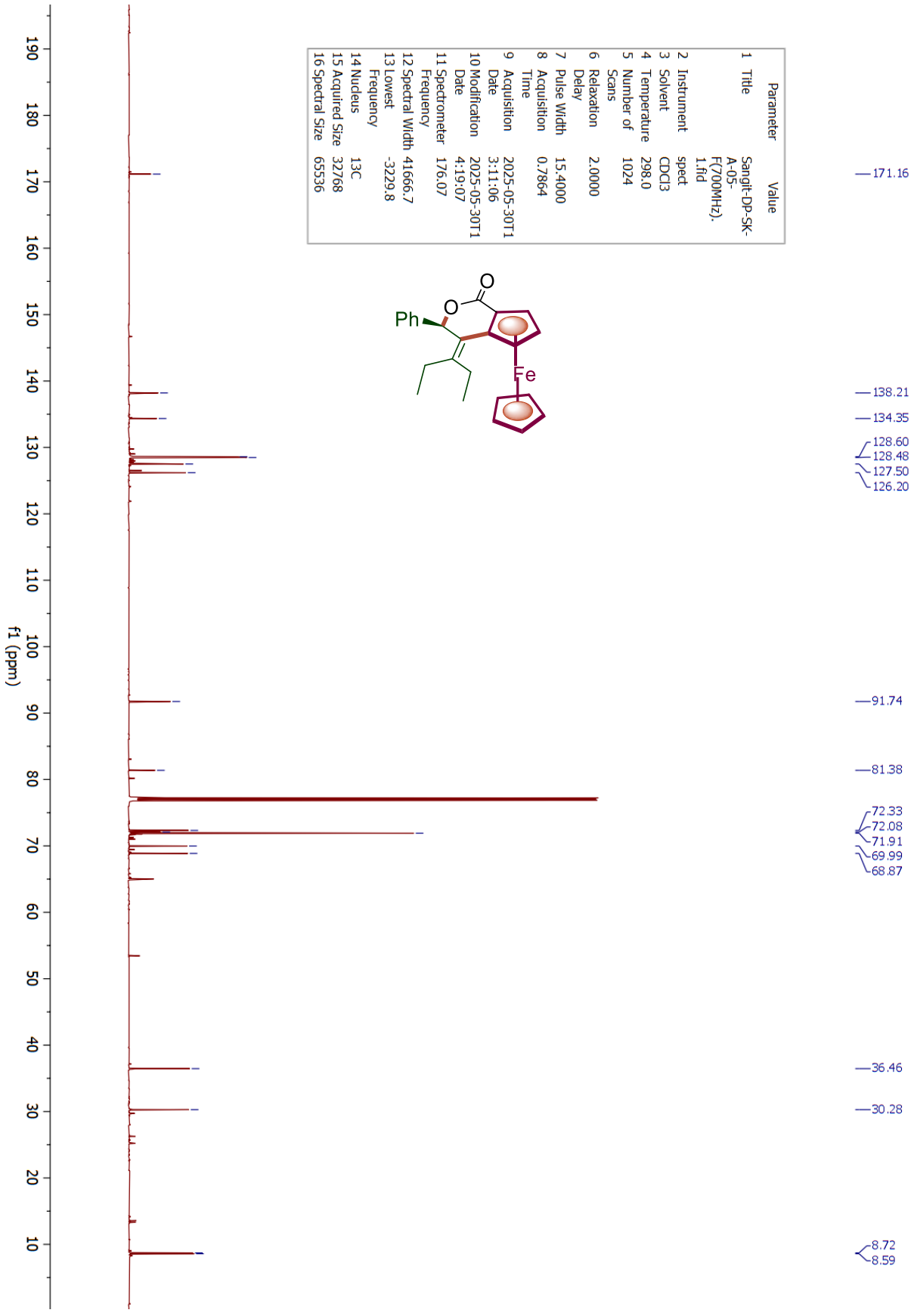

^{1}H NMR Spectrum of 3k

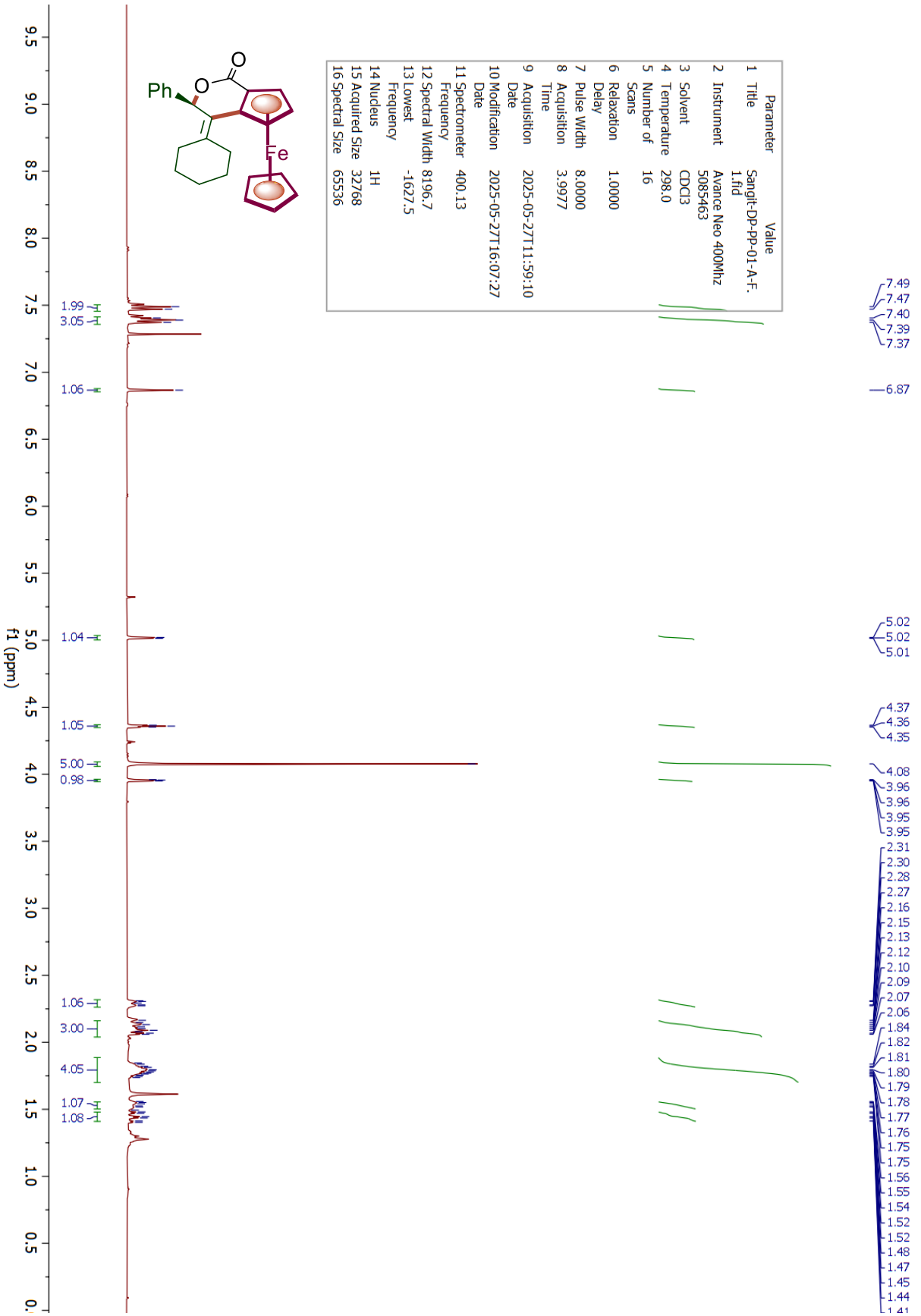

$^{13}C\{^{1}H\}$ NMR Spectrum of 3k

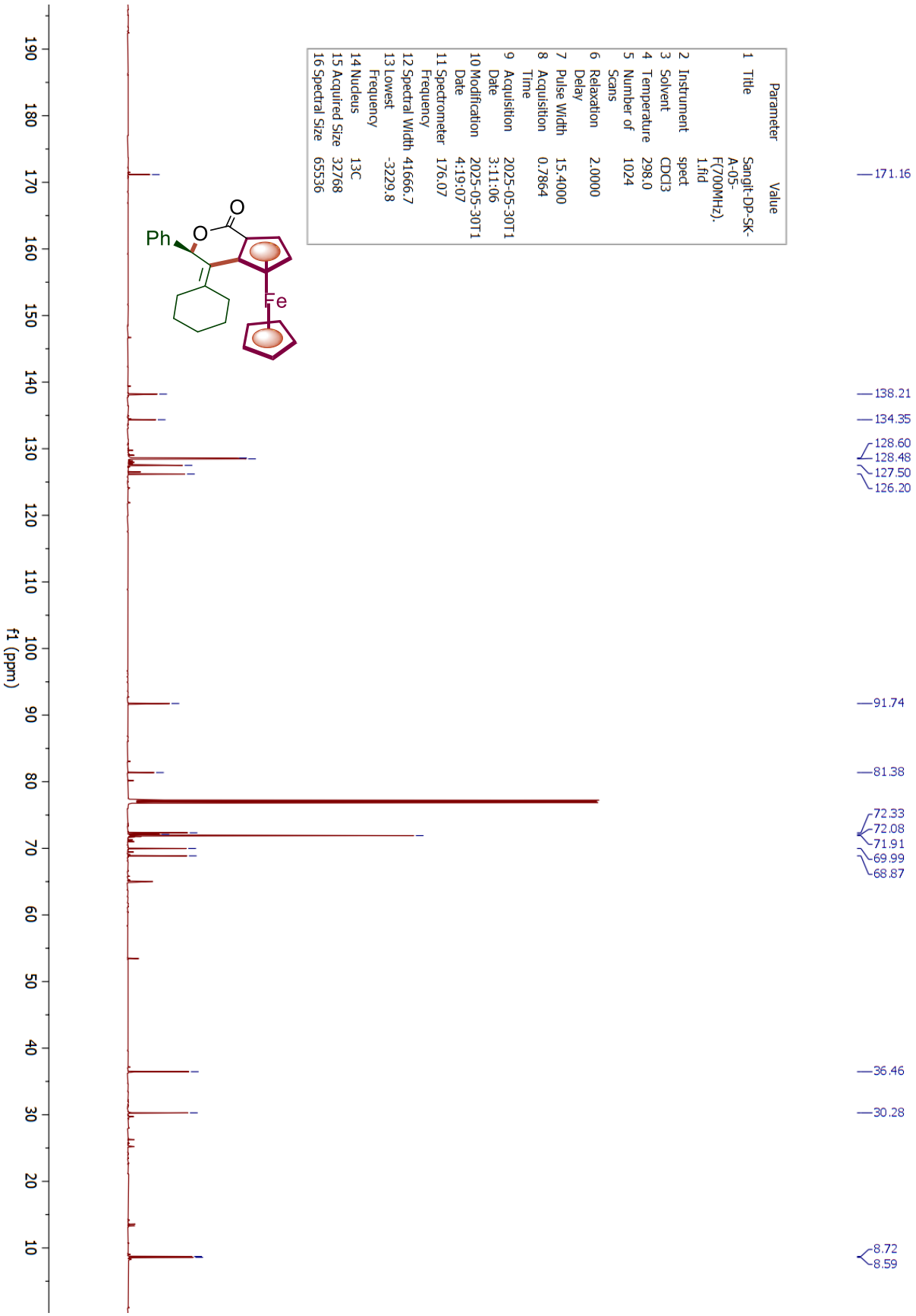

^{1}H NMR Spectrum of 3l

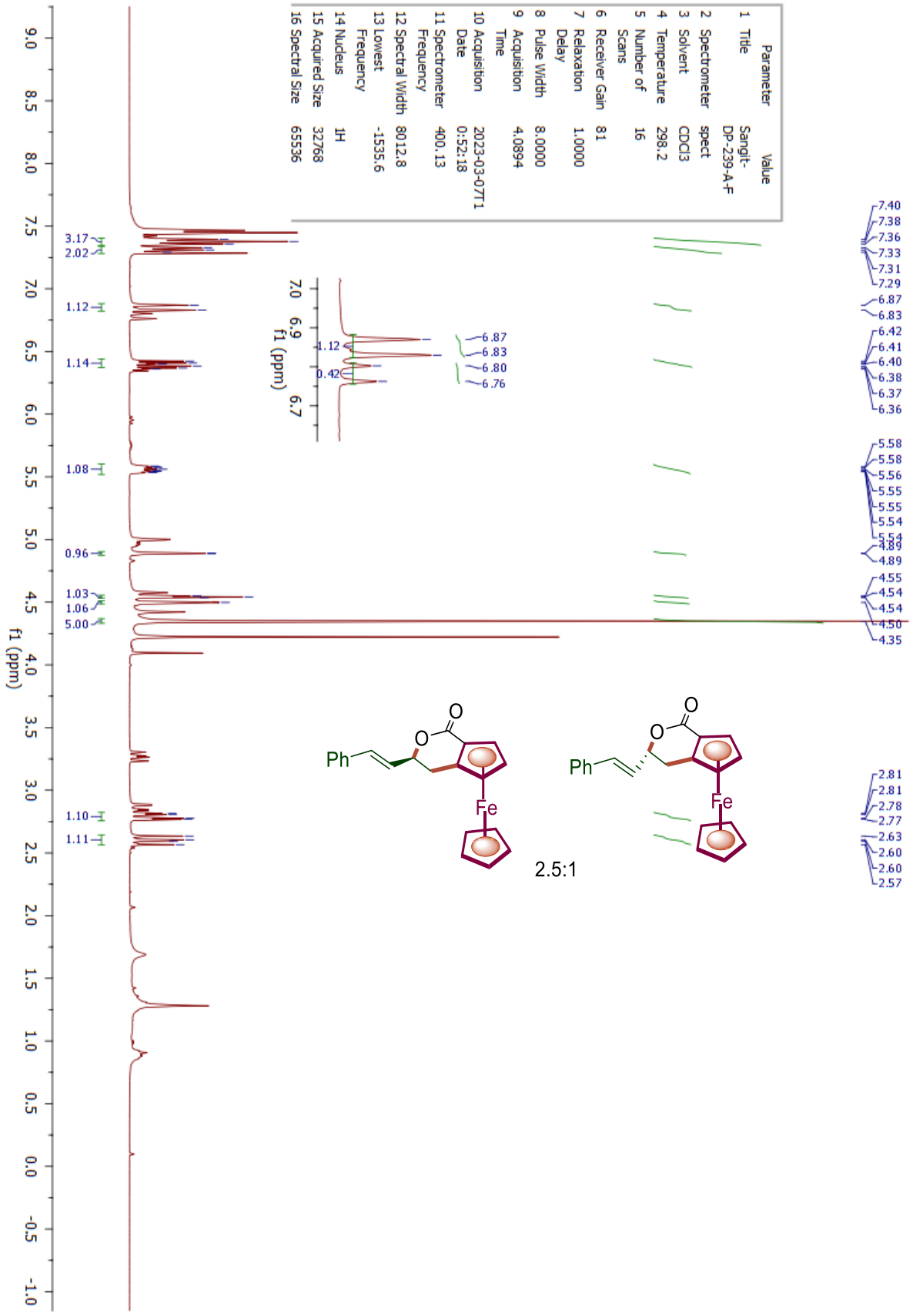

A mixture of diastereomer were observed as 2.5:1 in the NMR spectra

$^{13}C\{^{1}H\}$ NMR Spectrum of 3l

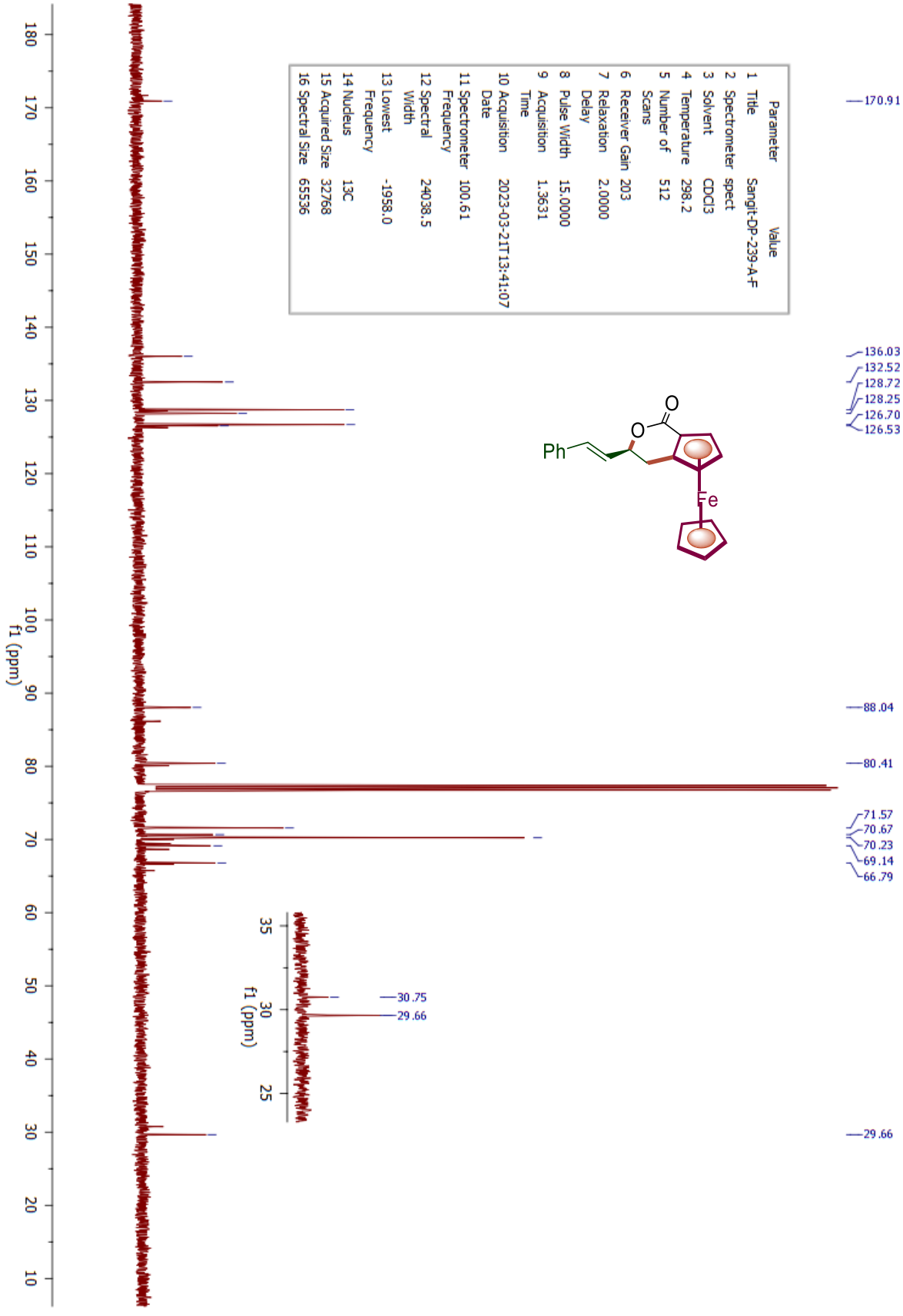

^{1}H NMR Spectrum of 3m

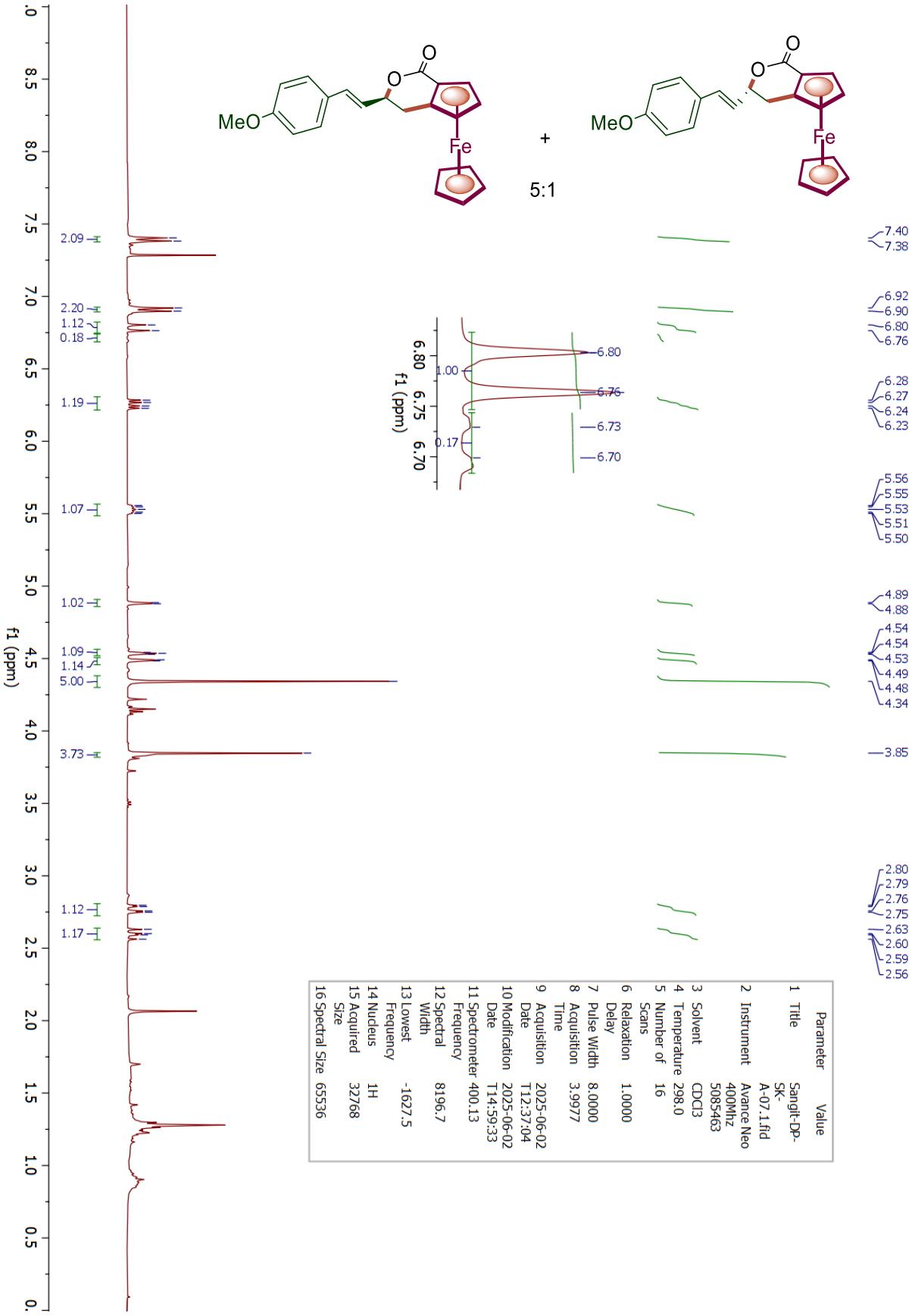

A mixture of diastereomer were observed as 5:1 in the NMR spectra

$^{13}C\{^{1}H\}$ NMR Spectrum of 3m

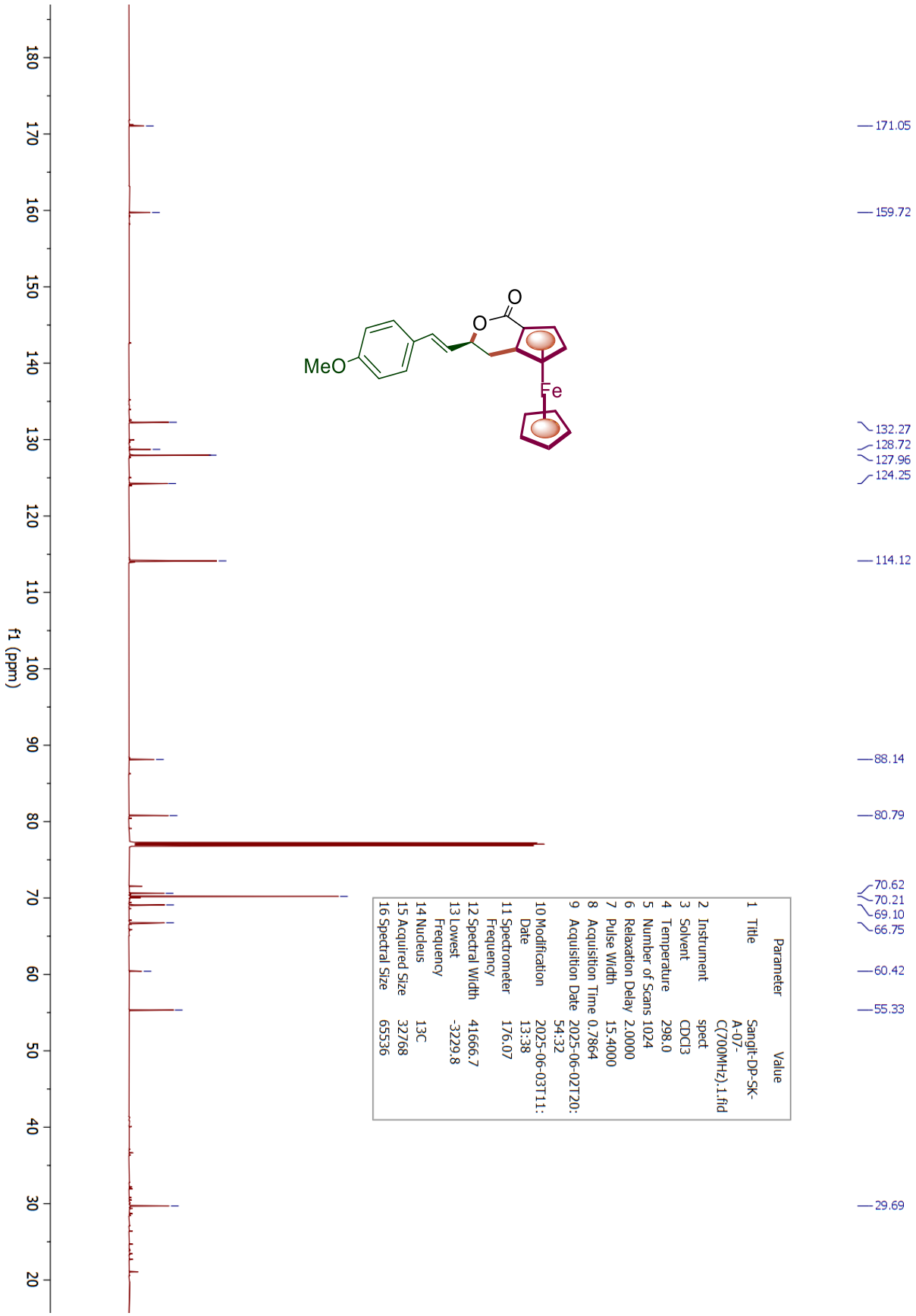

^{1}H NMR Spectrum of 3n

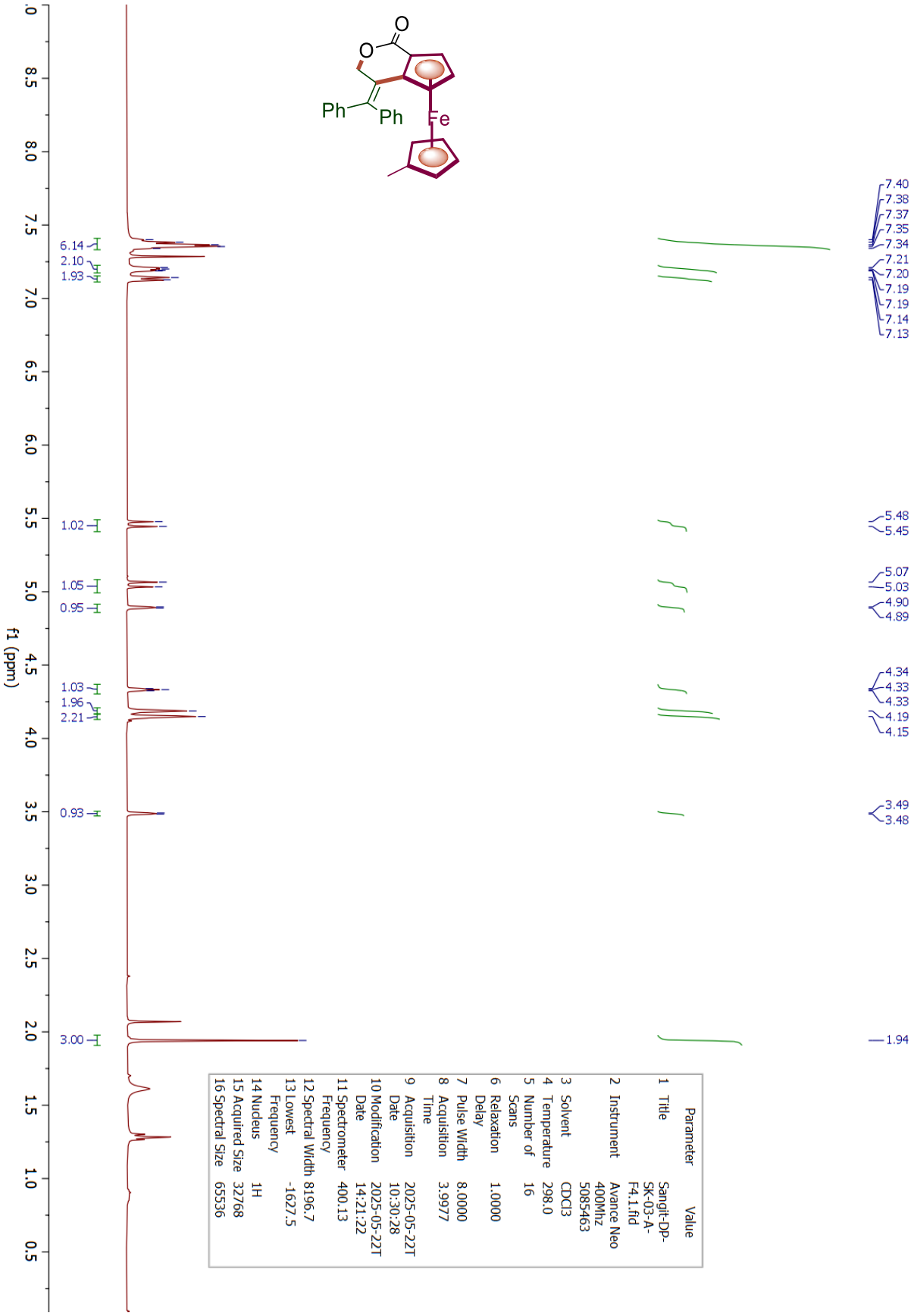

$^{13}C\{^{1}H\}$ NMR Spectrum of 3n

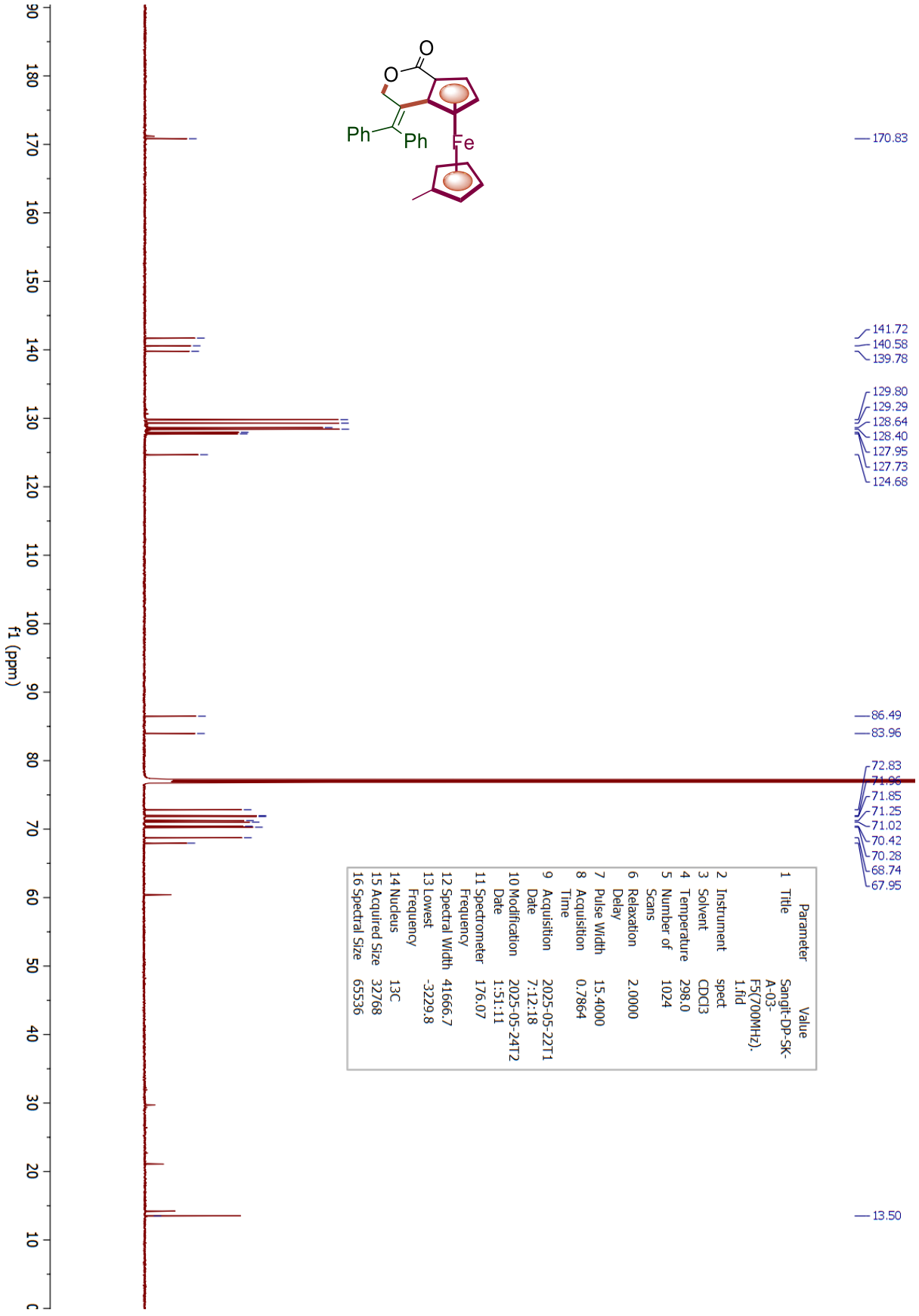

^{1}H NMR Spectrum of 3o

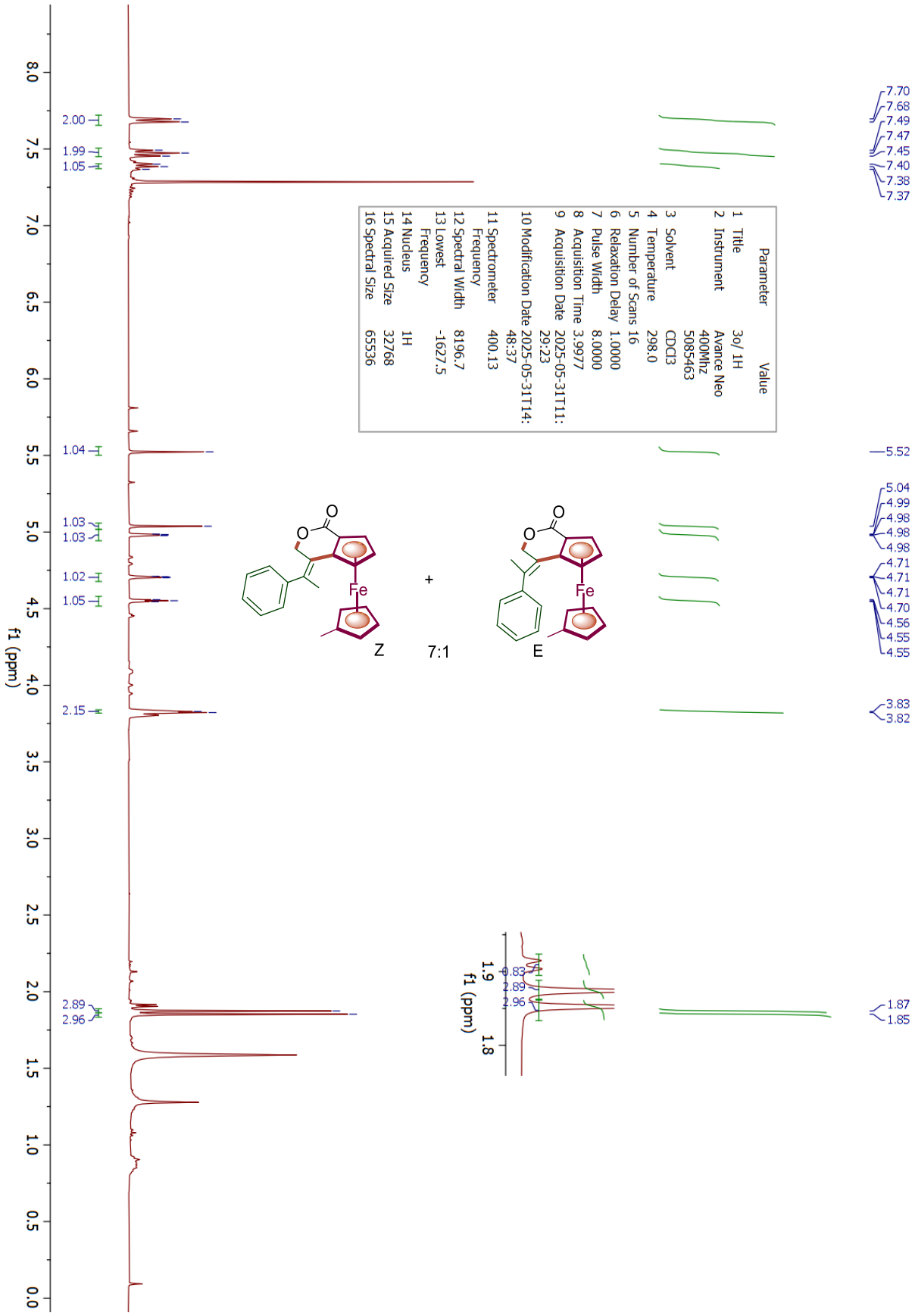

A mixture of E:Z regio-isomer were observed as 1:7 in the NMR spectra

$^{13}C\{^{1}H\}$ NMR Spectrum of 3o

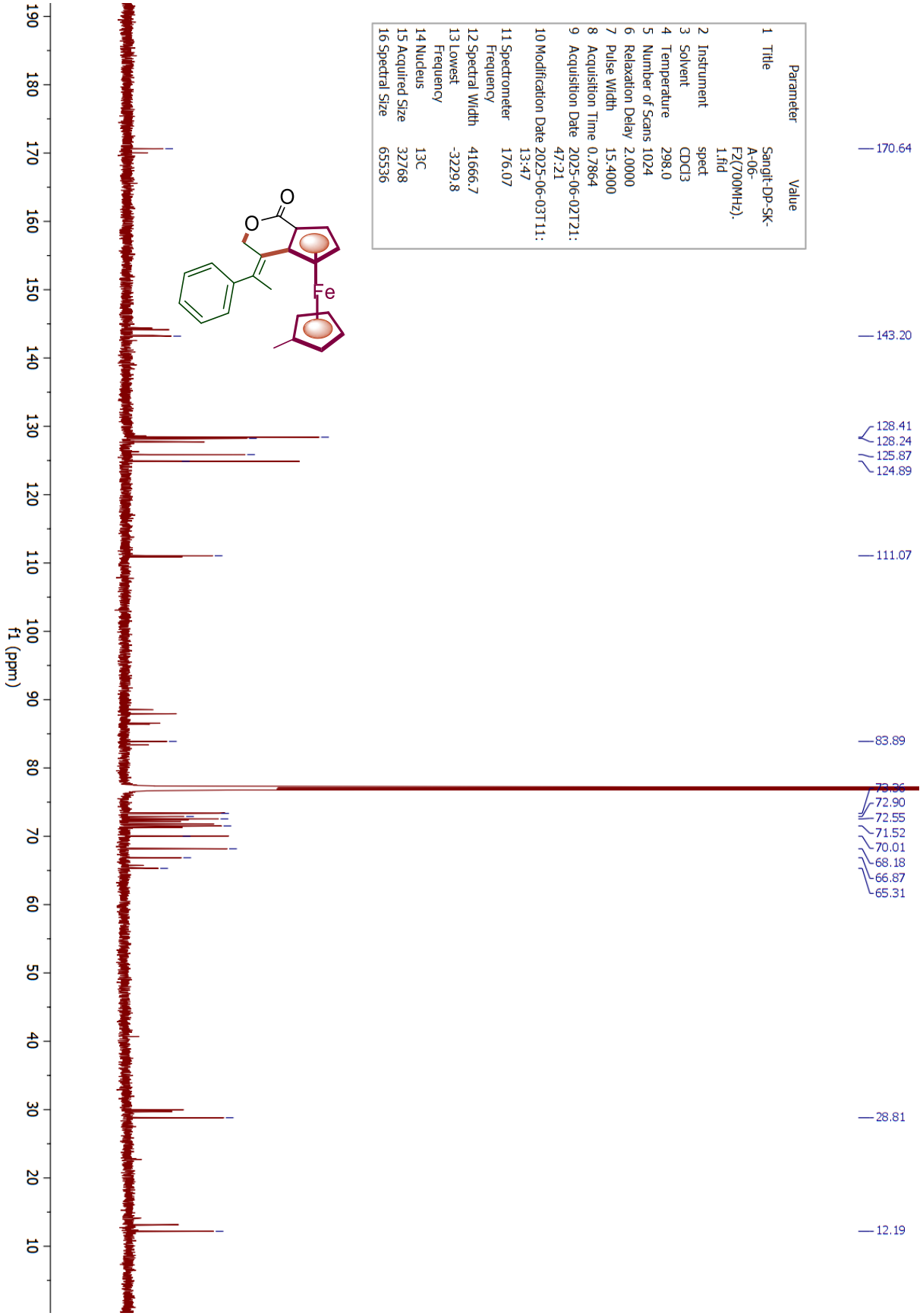

^{1}H NMR Spectrum of 3p

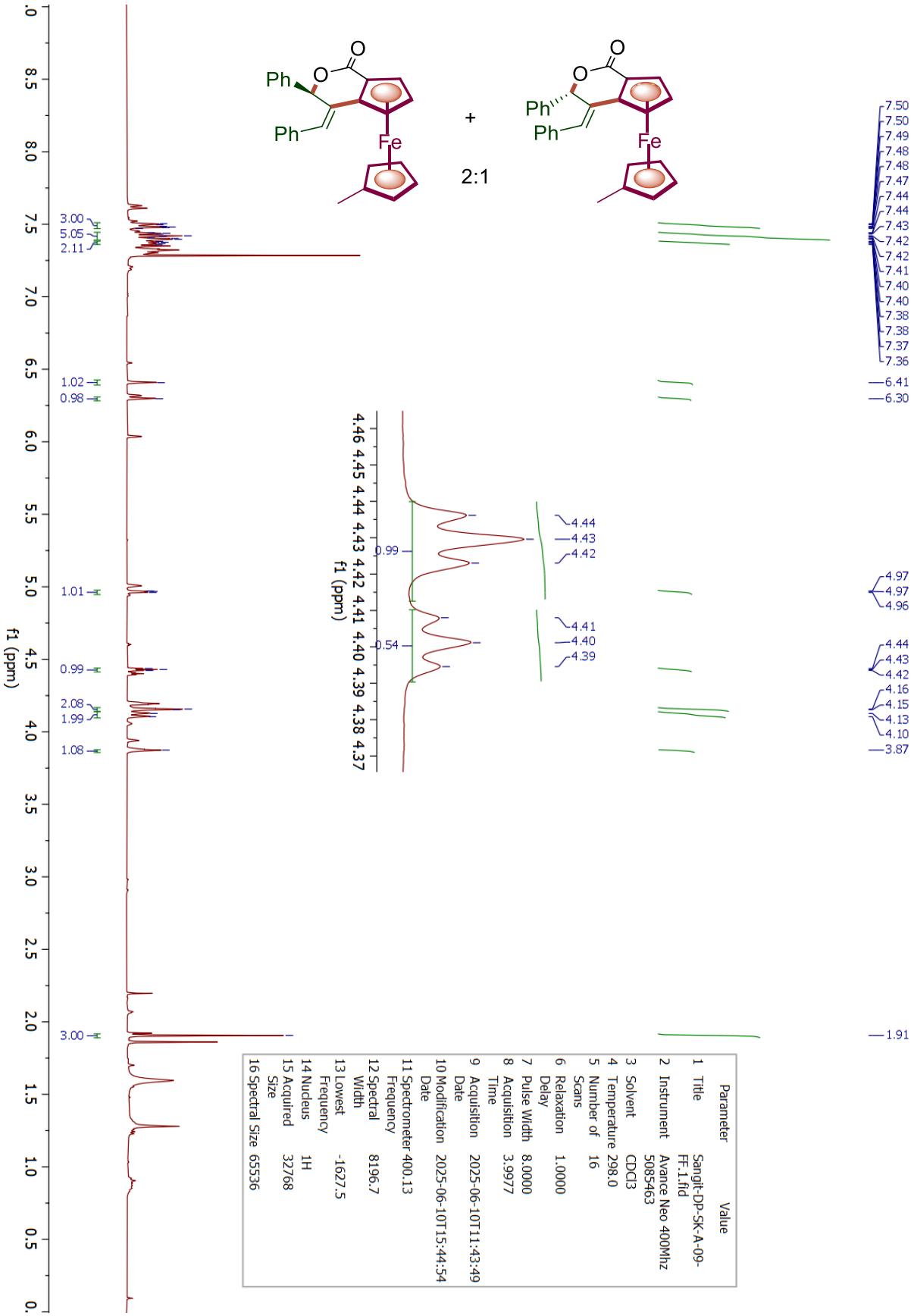

A mixture of diastereomer were observed as 2:1 in the NMR spectra

$^{13}C\{^{1}H\}$ NMR Spectrum of 3p

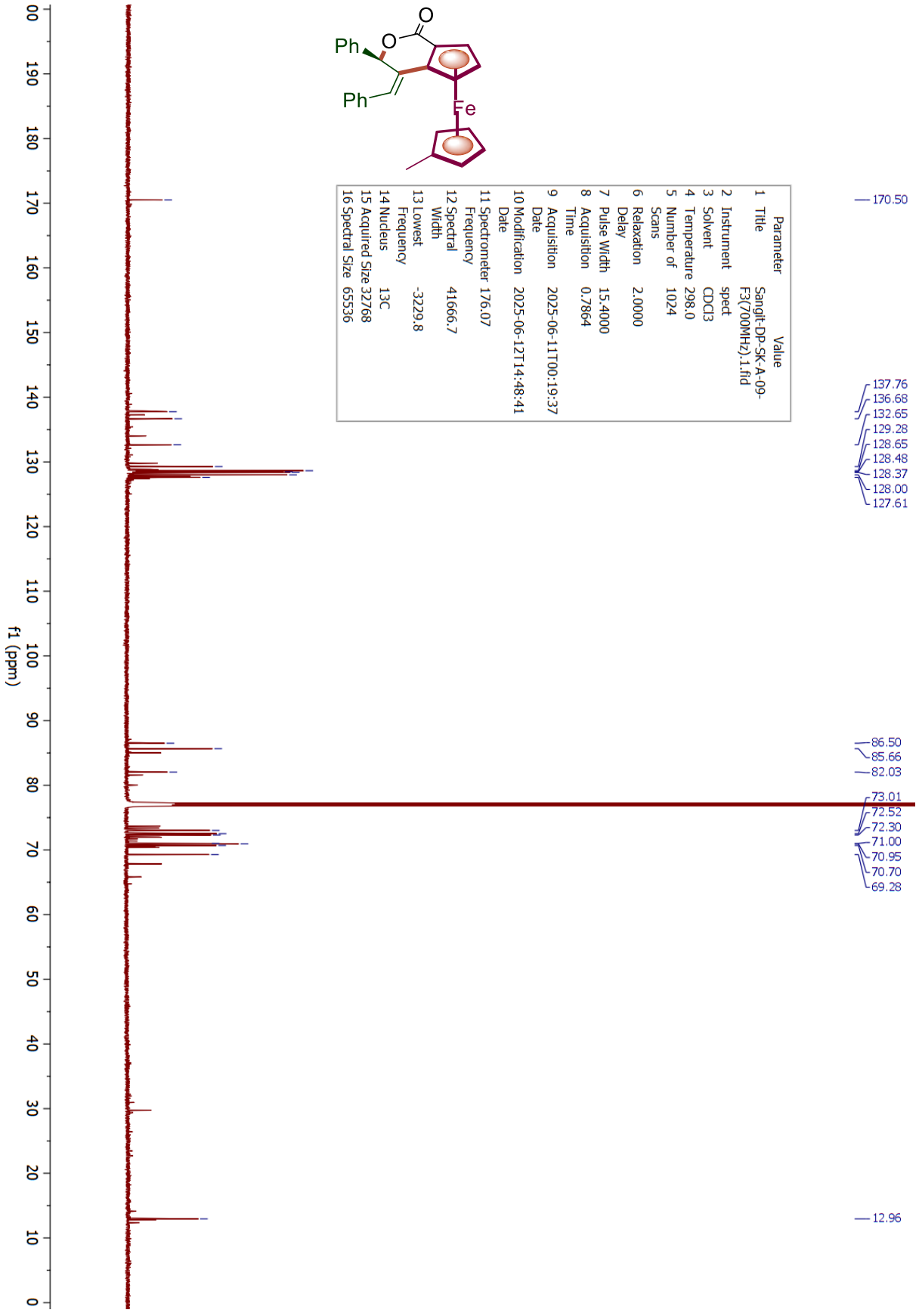

^{1}H NMR Spectrum of 3q

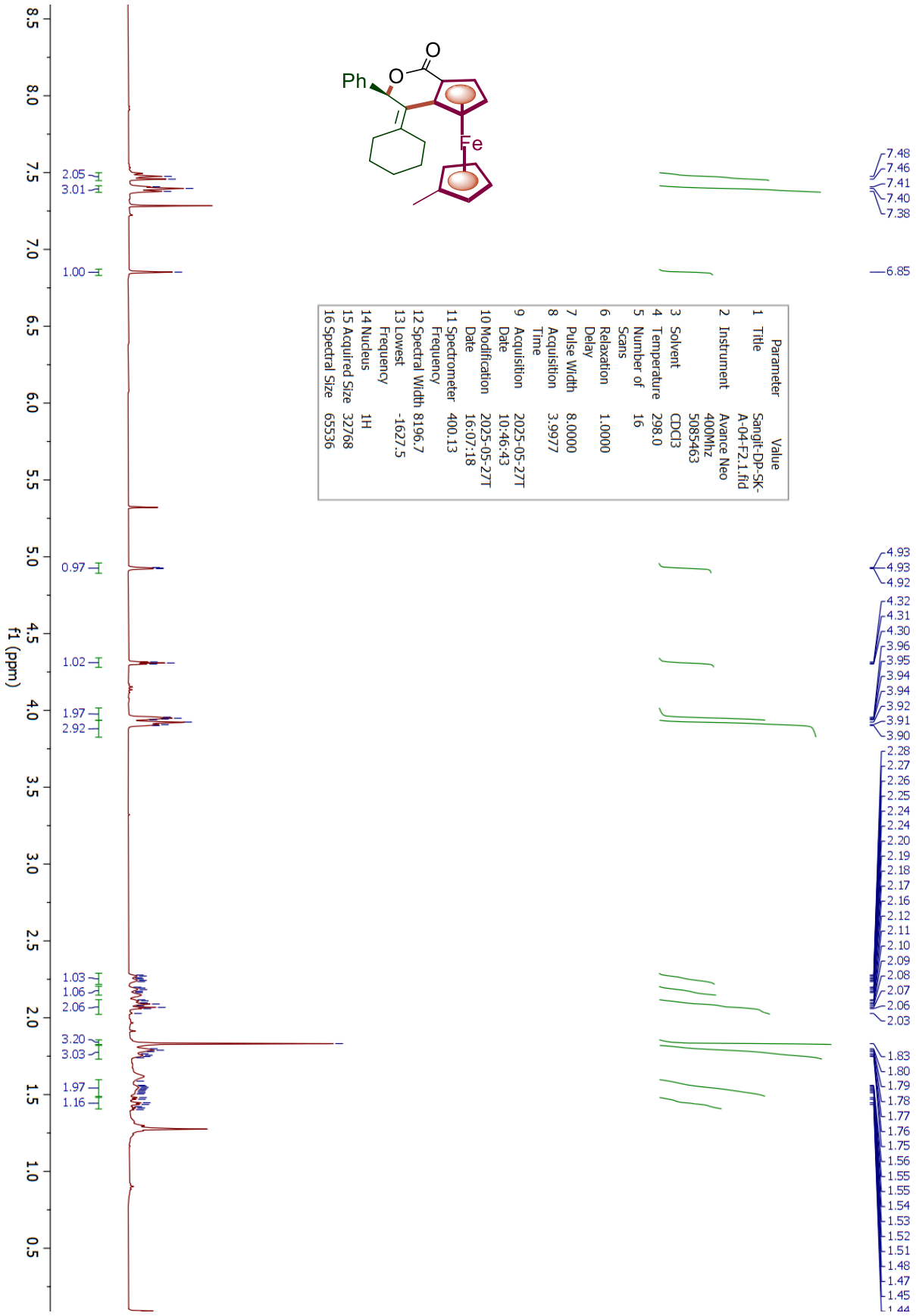

$^{13}C\{^{1}H\}$ NMR Spectrum of 3q

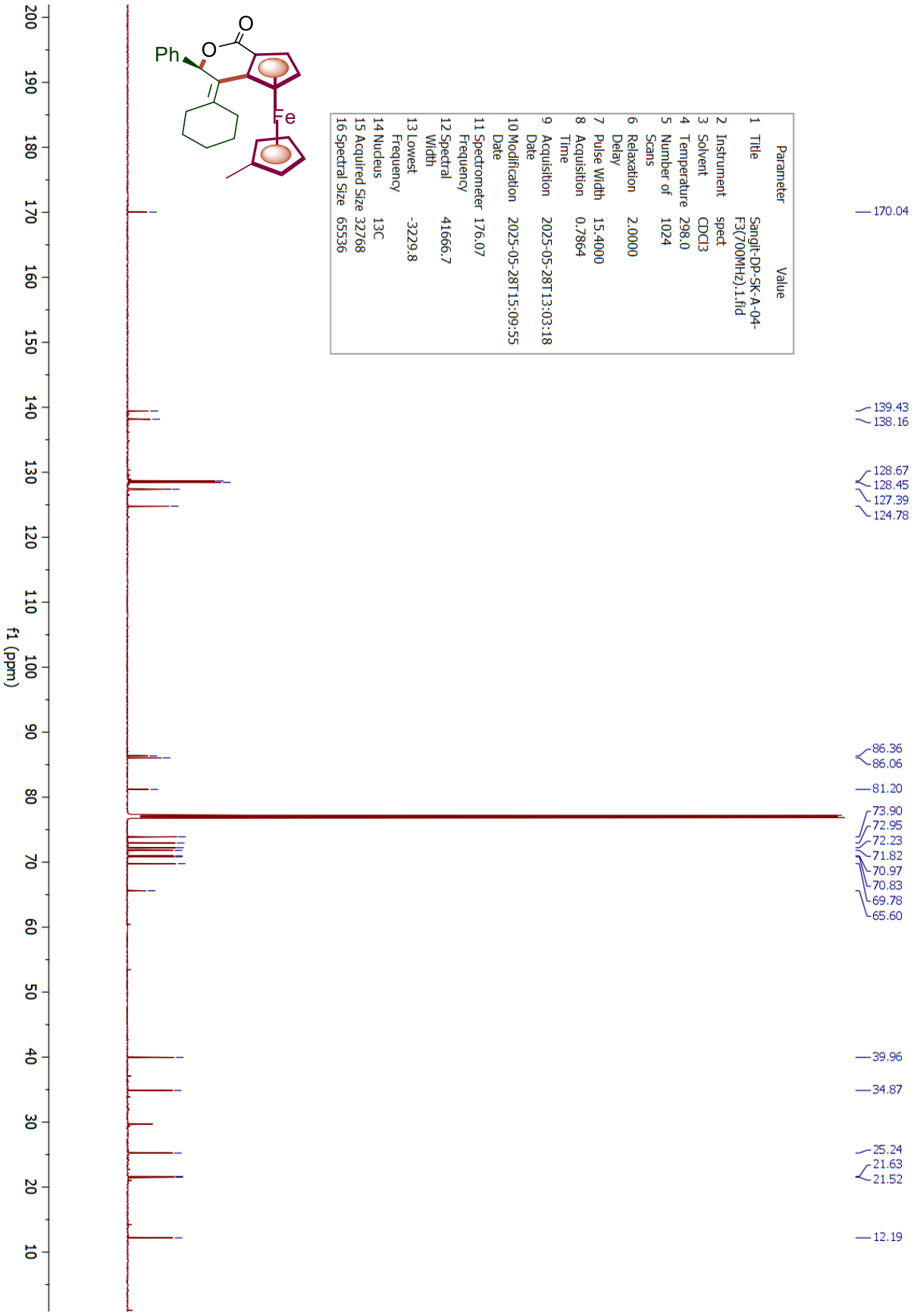

^{1}H NMR Spectrum of 3r

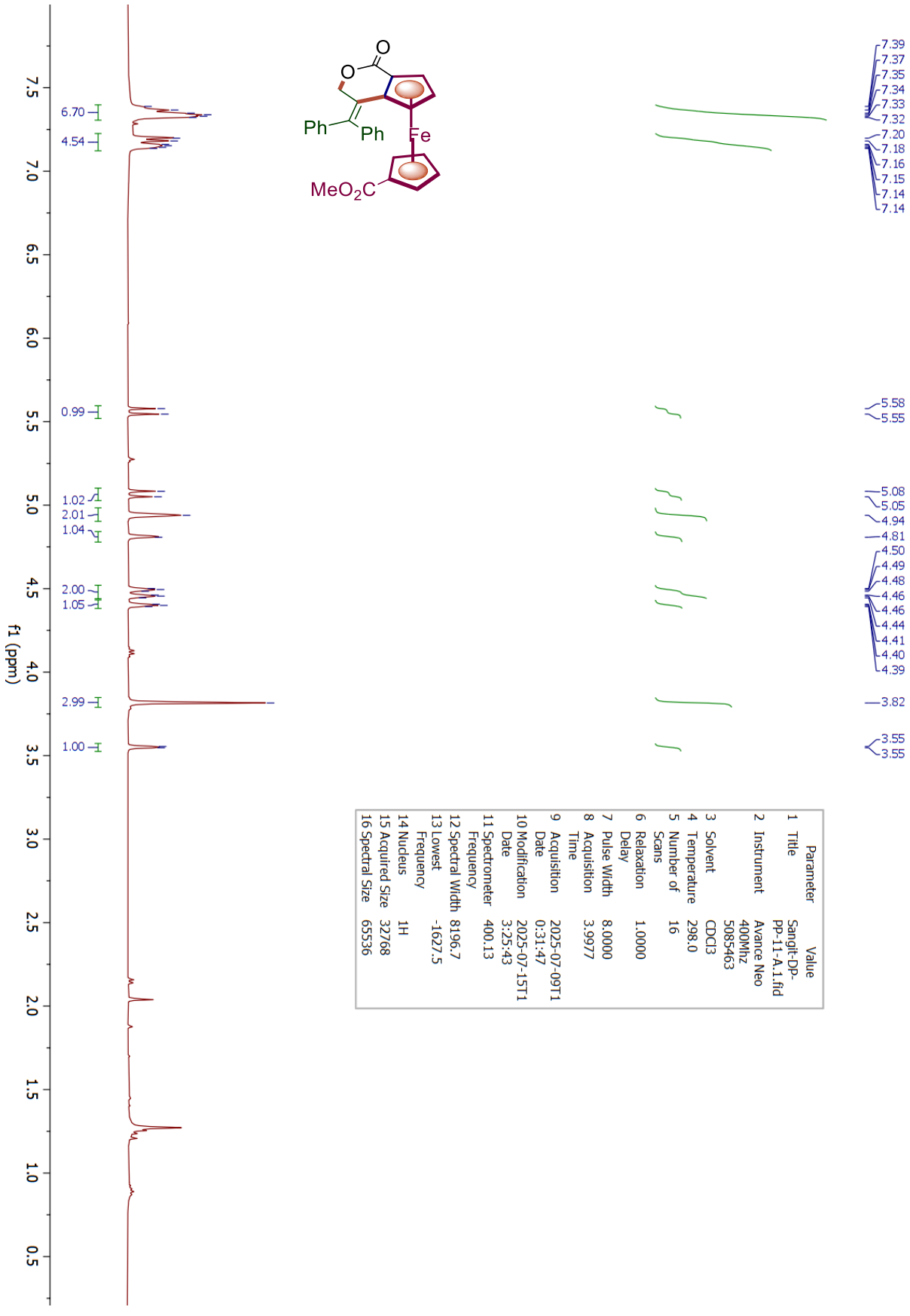

Parameter	Value
1 Title	Sangit-DP-PP-11-A.1.fid
2 Instrument	Avance Neo 400Mhz 5085463
3 Solvent	CDCl3
4 Temperature	298.0
5 Number of Scans	16
6 Relaxation Delay	1.0000
7 Pulse Width	8.0000
8 Acquisition Time	3.9977
9 Acquisition Date	2025-07-09T10:31:47
10 Modification Date	2025-07-15T13:25:43
11 Spectrometer Frequency	400.13
12 Spectral Width	8196.7
13 Lowest Frequency	-1627.5
14 Nucleus	1H
15 Acquired Size	32768
16 Spectral Size	65536

$^{13}C\{^{1}H\}$ NMR Spectrum of 3r

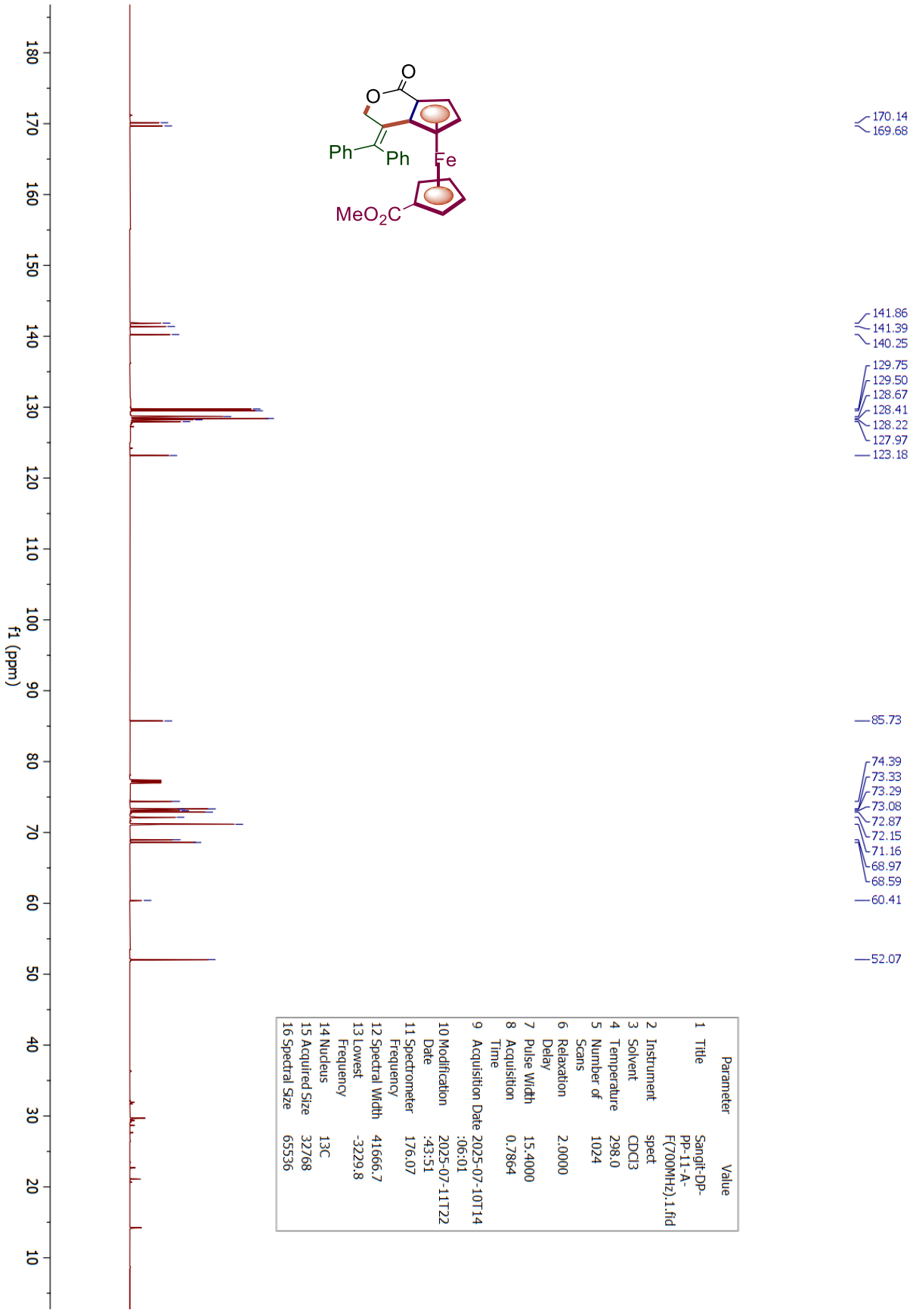

	Parameter	Value
1	Title	Sangit-DP-PP-11-A-F(700MHz).1.fid
2	Instrument	spect
3	Solvent	CDCl3
4	Temperature	298.0
5	Number of Scans	1024
6	Relaxation Delay	2.0000
7	Pulse Width	15.4000
8	Acquisition Time	0.7864
9	Acquisition Date	2025-07-10T14:06:01
10	Modification Date	2025-07-11T22:43:51
11	Spectrometer Frequency	176.07
12	Spectral Width	41666.7
13	Lowest Frequency	-3229.8
14	Nucleus	13C
15	Acquired Size	32768
16	Spectral Size	65536

^{1}H NMR Spectrum of 3s

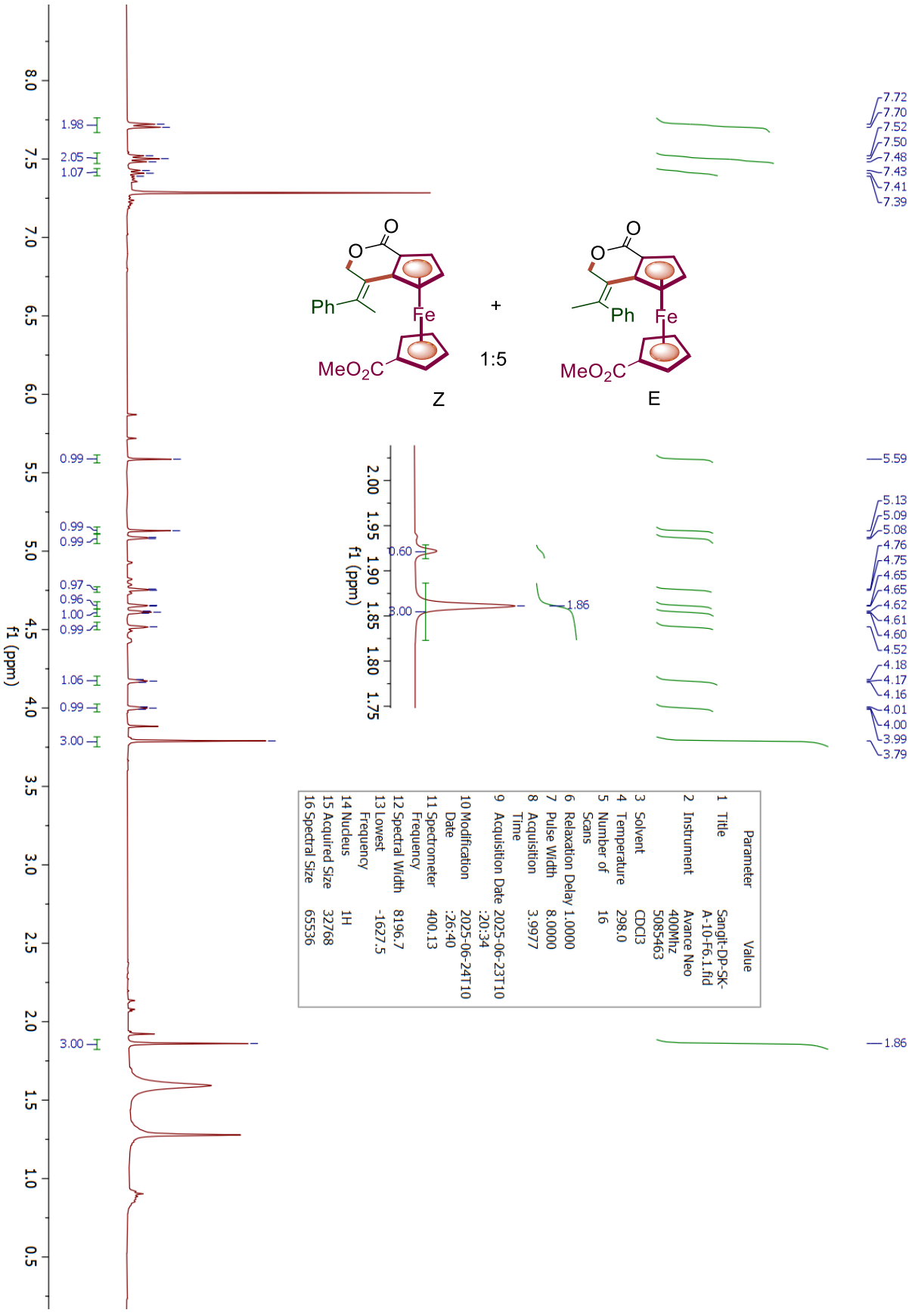

A mixture of E:Z regio-isomer were observed as 1:5 in the NMR spectra

$^{13}C\{^{1}H\}$ NMR Spectrum of 3s

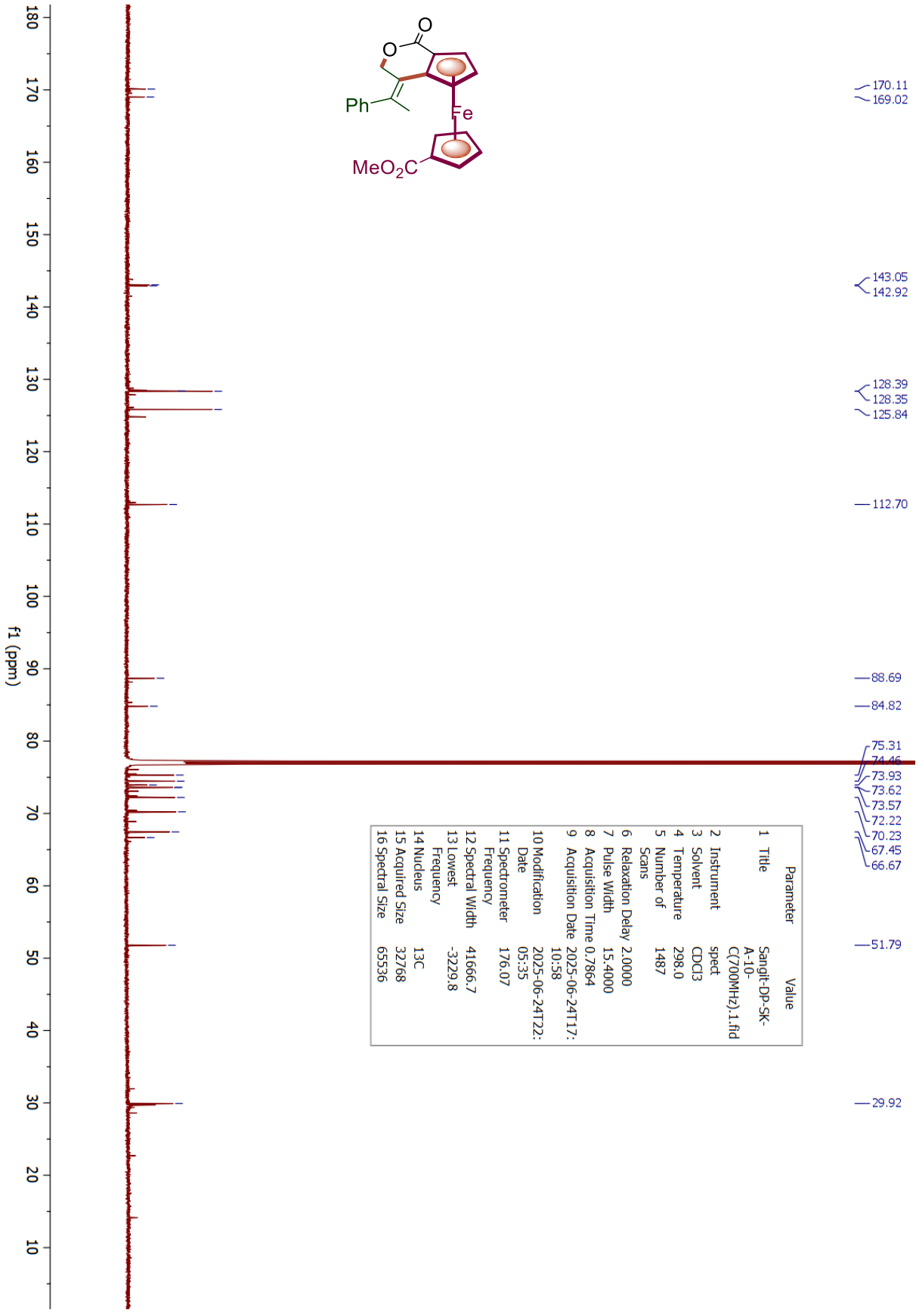

	Parameter	Value
1	Title	Sangit-DP-SK-A-10-C(700MHz).1.fid
2	Instrument	spect
3	Solvent	CDCl3
4	Temperature	298.0
5	Number of Scans	1487
6	Relaxation Delay	2.0000
7	Pulse Width	15.4000
8	Acquisition Time	0.7864
9	Acquisition Date	2025-06-24T17:10:58
10	Modification Date	2025-06-24T22:05:35
11	Spectrometer Frequency	176.07
12	Spectral Width	41666.7
13	Lowest Frequency	-3229.8
14	Nucleus	13C
15	Acquired Size	32768
16	Spectral Size	65536

^{1}H NMR Spectrum of 3t

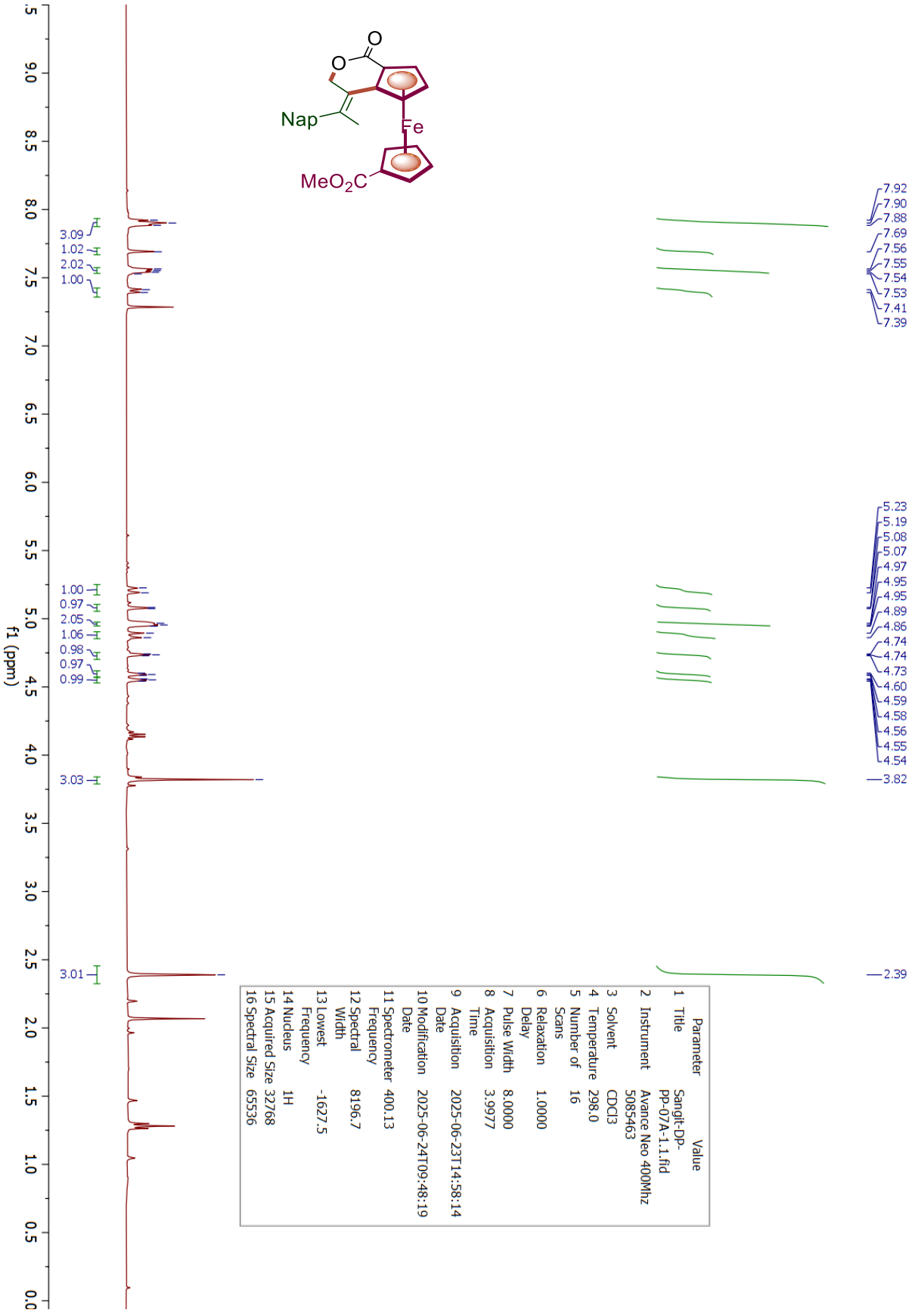

$^{13}C\{^{1}H\}$ NMR Spectrum of 3t

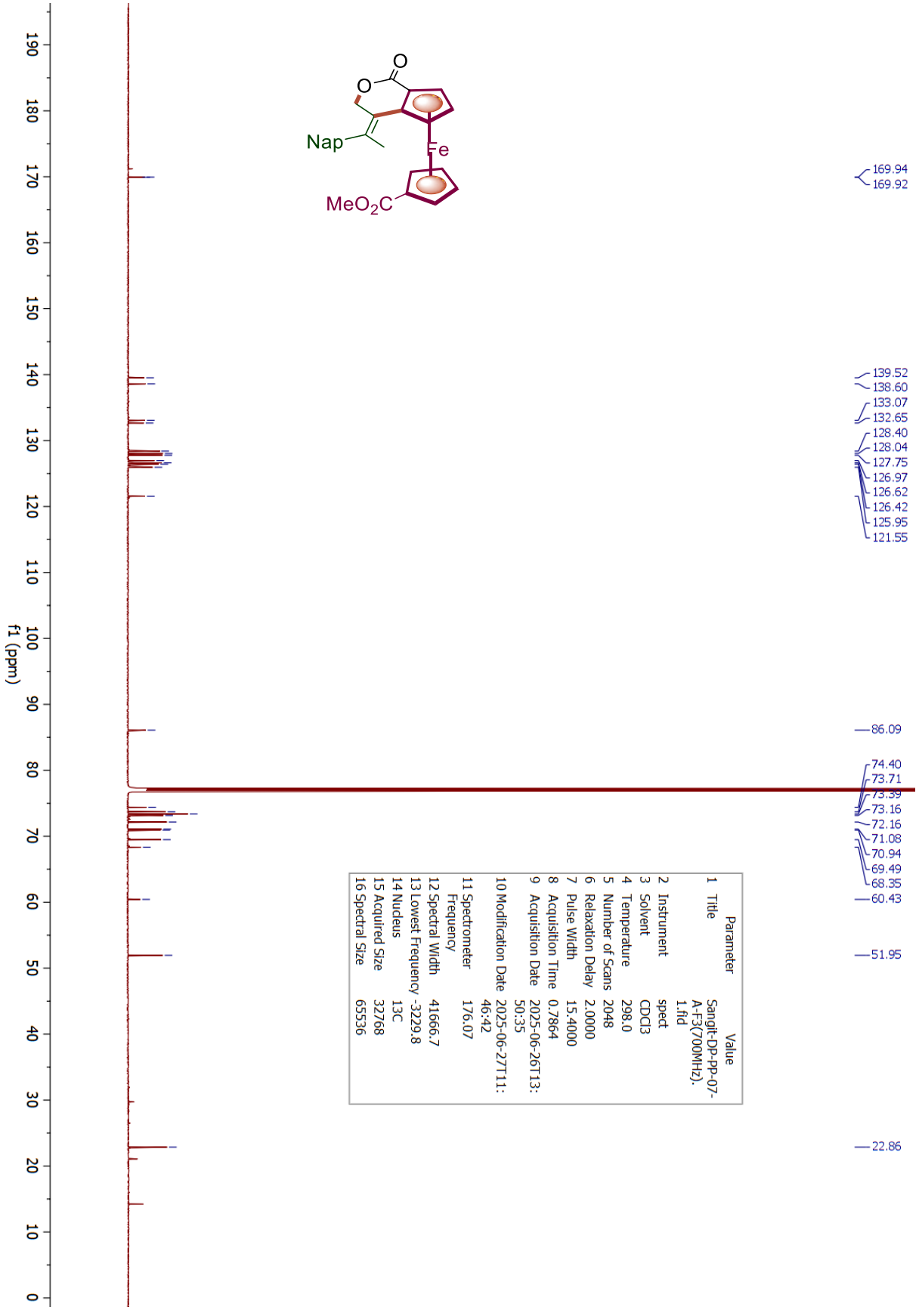

^{1}H NMR Spectrum of 3u

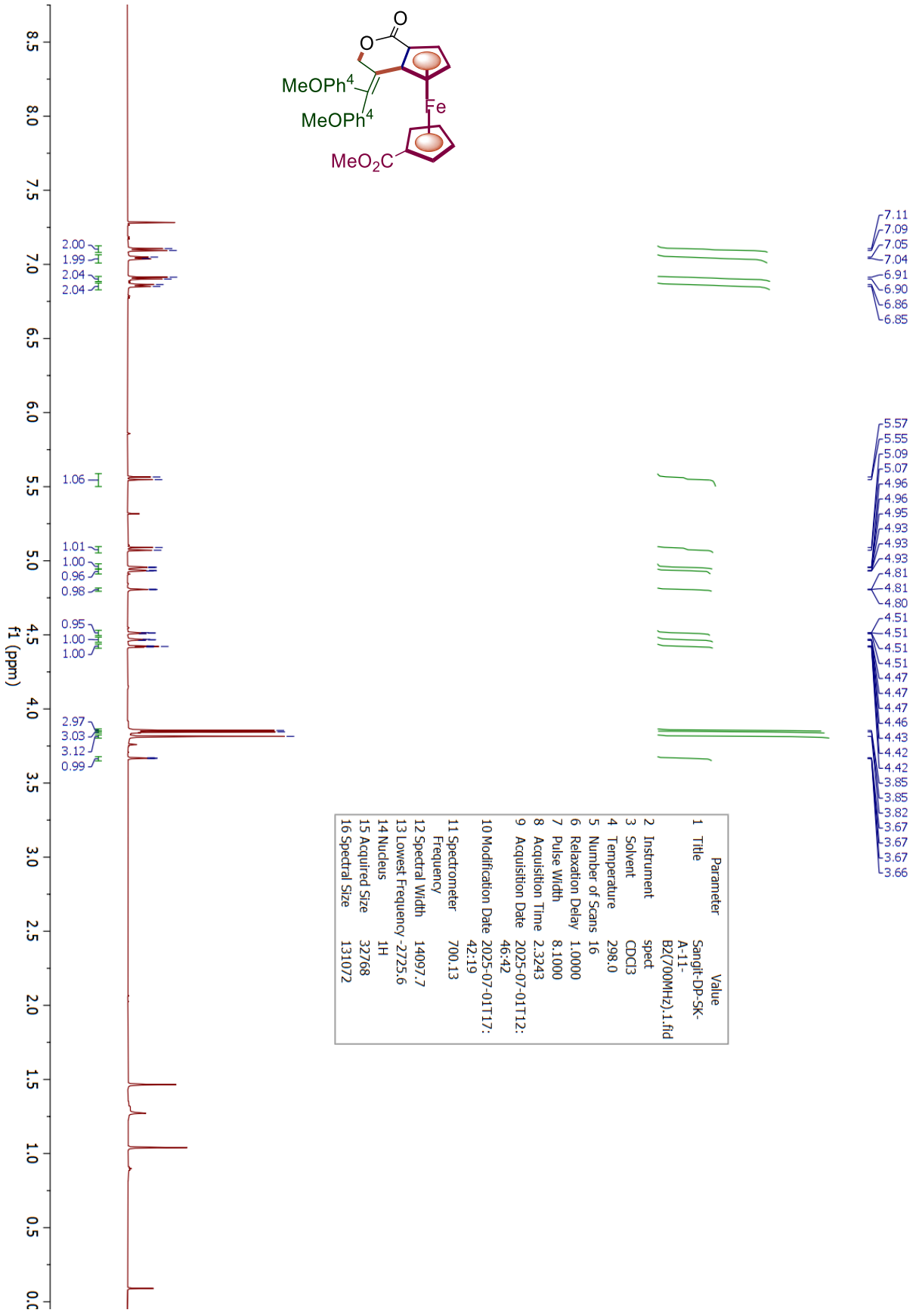

Parameter	Value
1 Title	Sangit-DP-SK-A-11-B2(700MHz).1.fid
2 Instrument	spect
3 Solvent	CDCl3
4 Temperature	298.0
5 Number of Scans	16
6 Relaxation Delay	1.0000
7 Pulse Width	8.1000
8 Acquisition Time	2.3243
9 Acquisition Date	2025-07-01T12:46:42
10 Modification Date	2025-07-01T17:42:19
11 Spectrometer Frequency	700.13
12 Spectral Width	14097.7
13 Lowest Frequency	-2725.6
14 Nucleus	1H
15 Acquired Size	32768
16 Spectral Size	131072

$^{13}C\{^{1}H\}$ NMR Spectrum of 3u

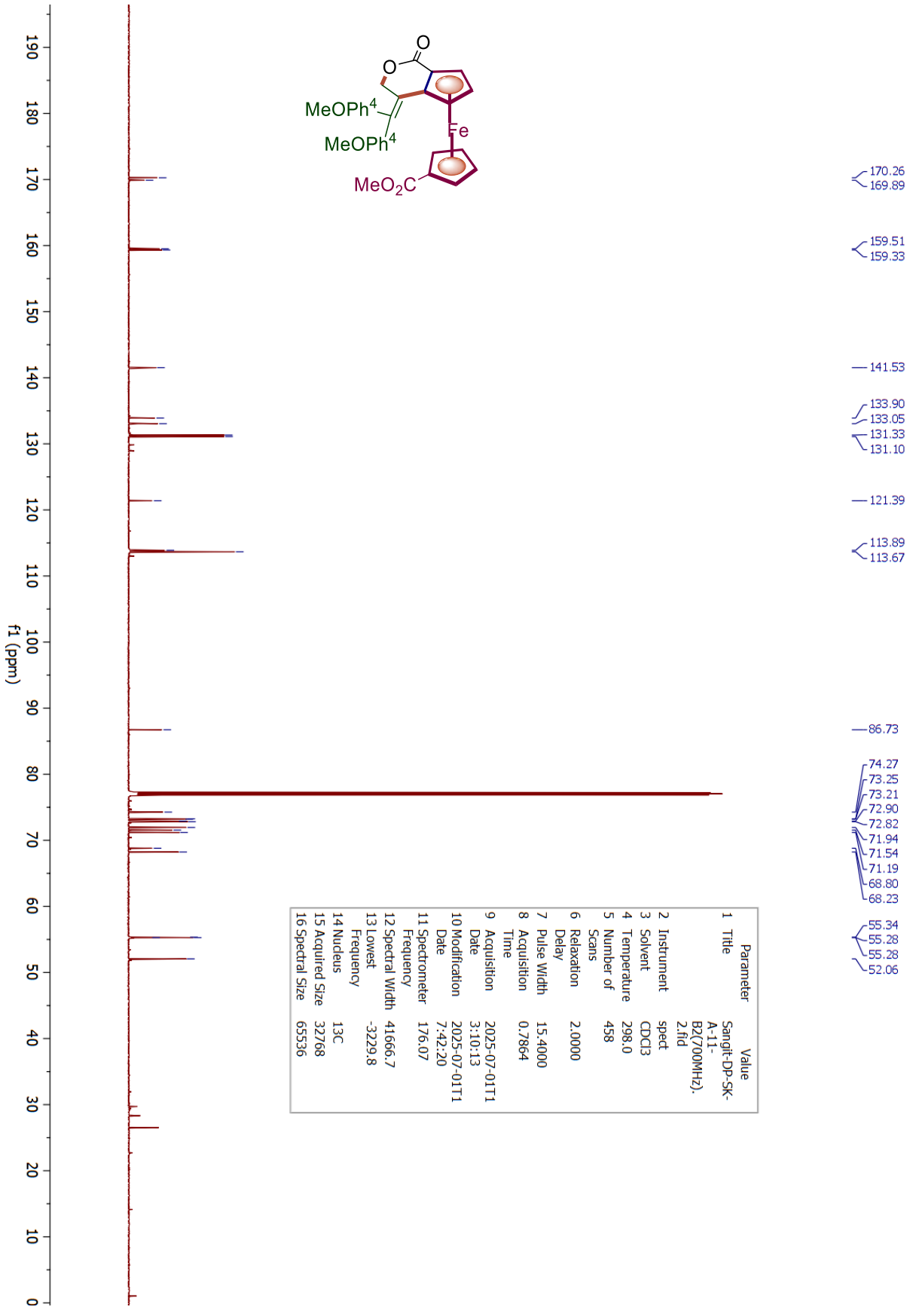

^{1}H NMR Spectrum of 3v

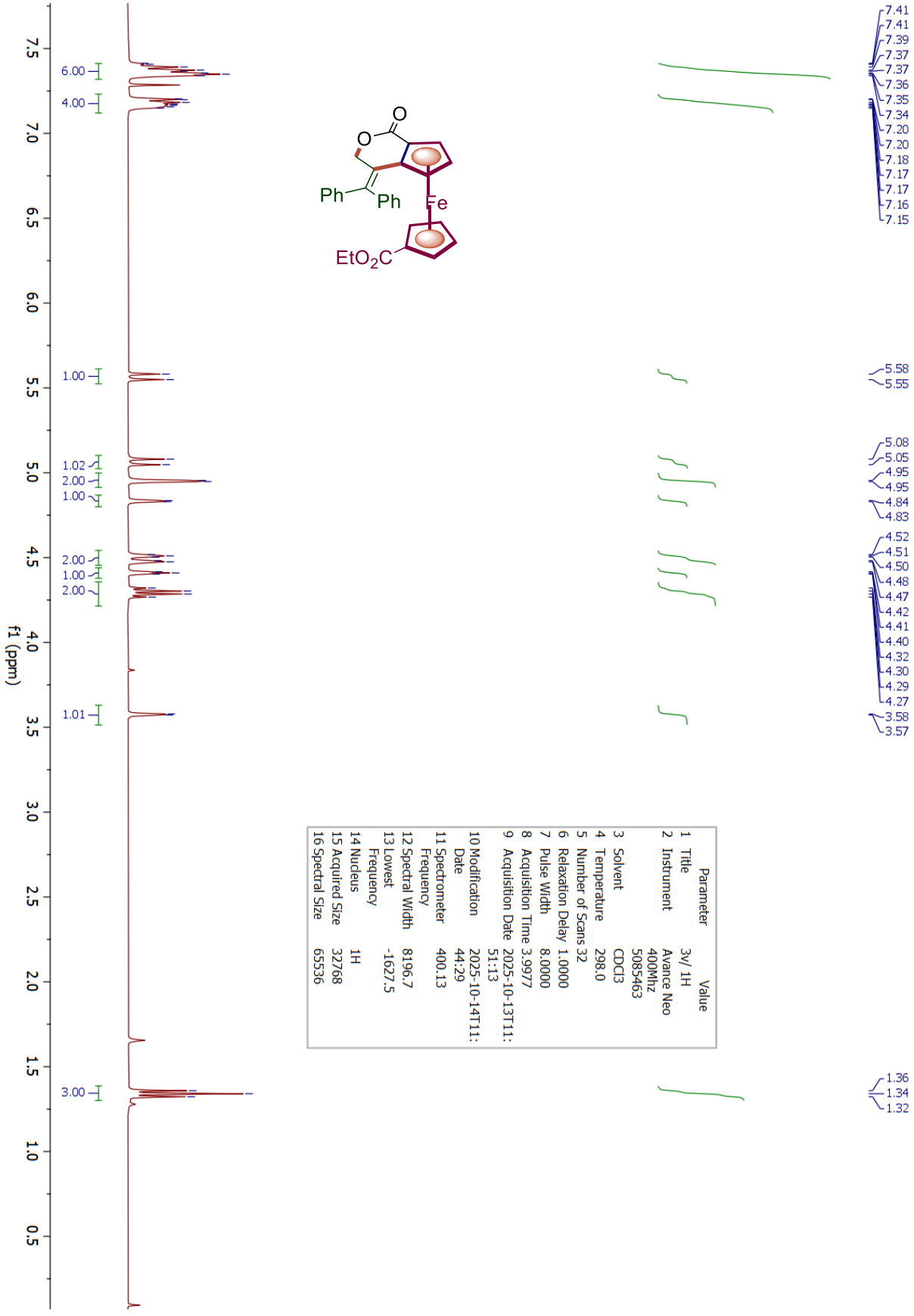

	Parameter	Value
1	Title	3v/ 1H
2	Instrument	Avance Neo 400Mhz 5085463
3	Solvent	CDCl3
4	Temperature	298.0
5	Number of Scans	32
6	Relaxation Delay	1.0000
7	Pulse Width	8.0000
8	Acquisition Time	3.9977
9	Acquisition Date	2025-10-13T11:51:13
10	Modification Date	2025-10-14T11:44:29
11	Spectrometer Frequency	400.13
12	Spectral Width	8196.7
13	Lowest Frequency	-1627.5
14	Nucleus	1H
15	Acquired Size	32768
16	Spectral Size	65536

$^{13}C\{^{1}H\}$ NMR Spectrum of 3v

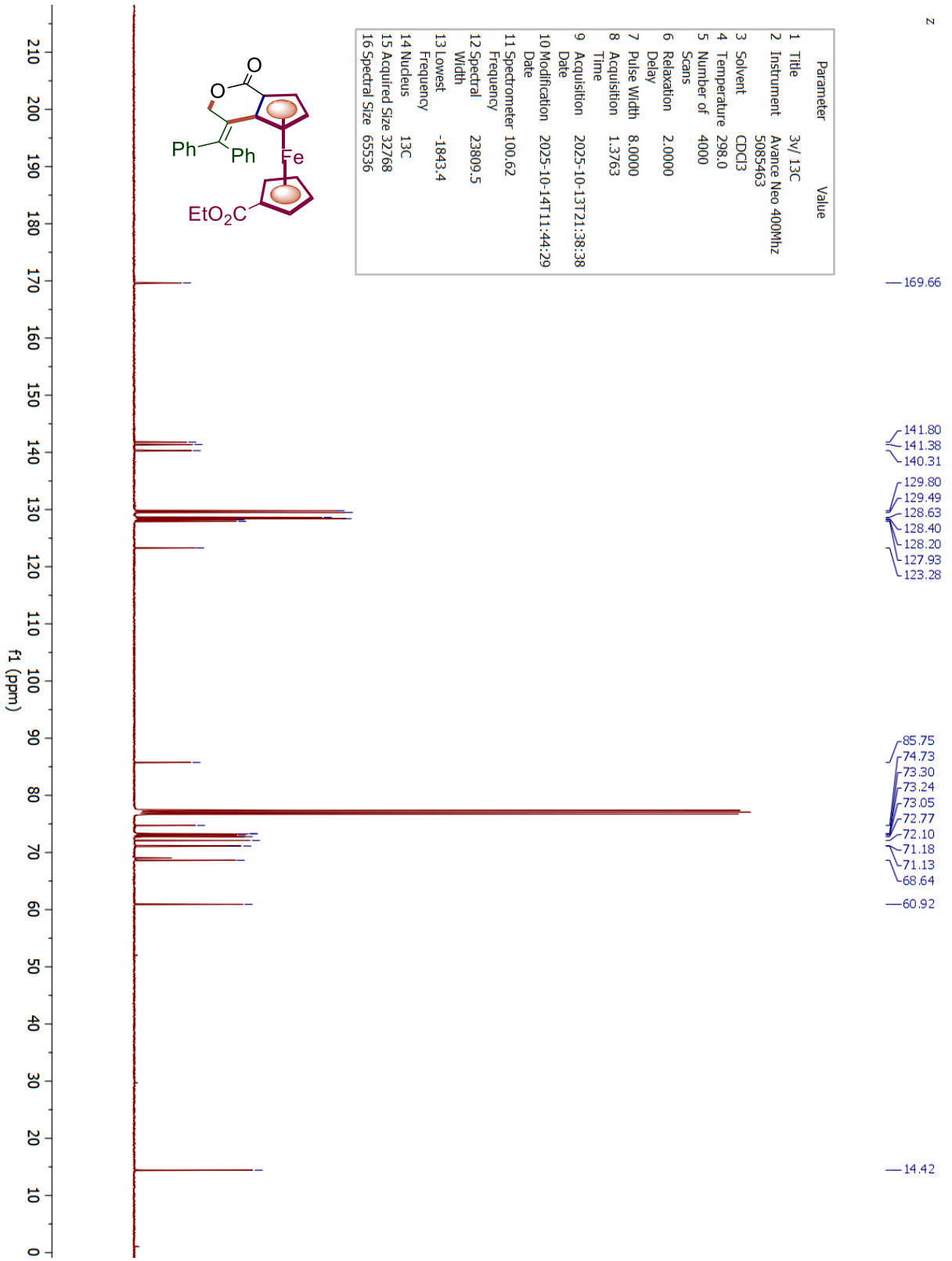

^{1}H NMR Spectrum of 4

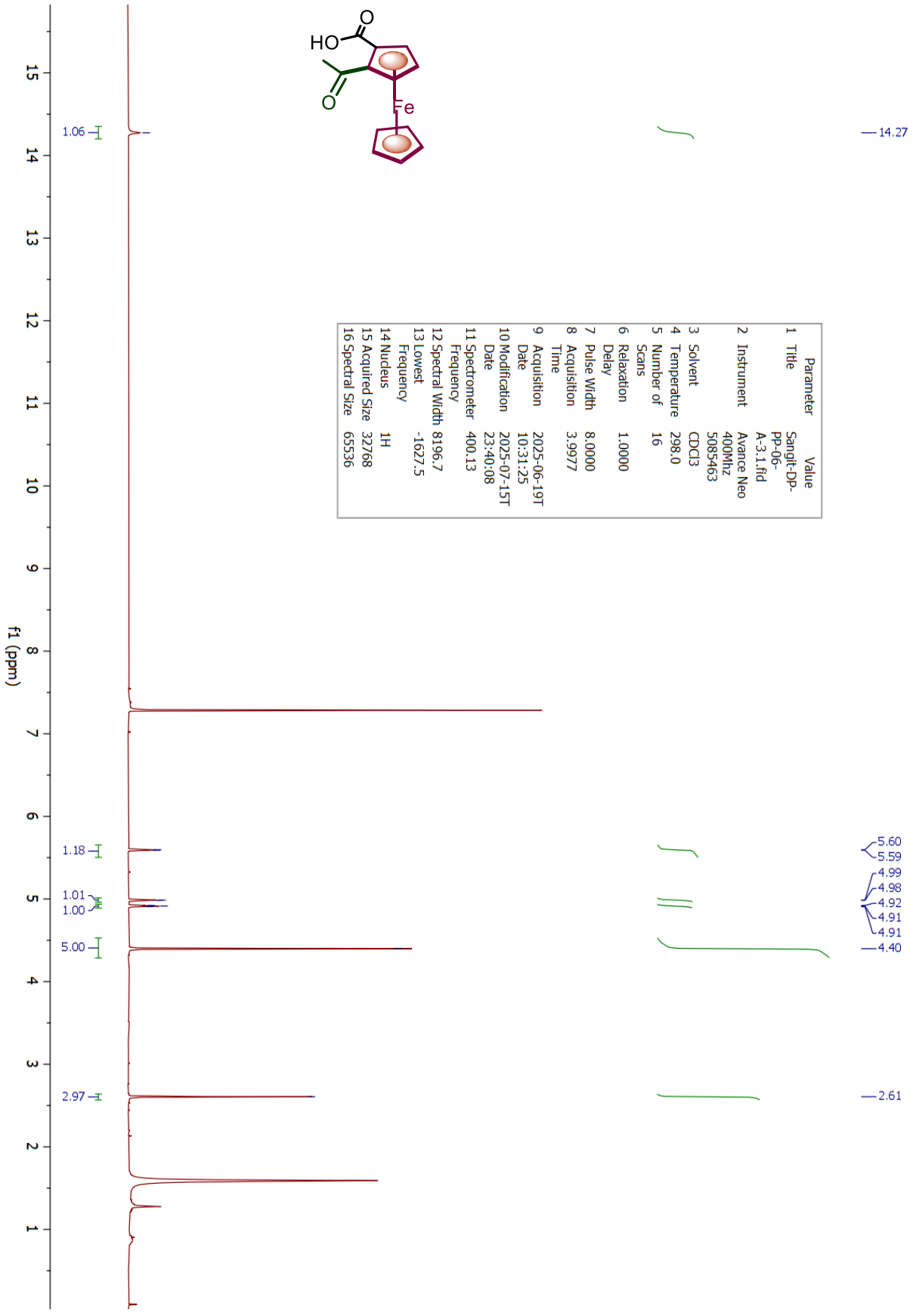

$^{13}C\{^{1}H\}$ NMR Spectrum of 4

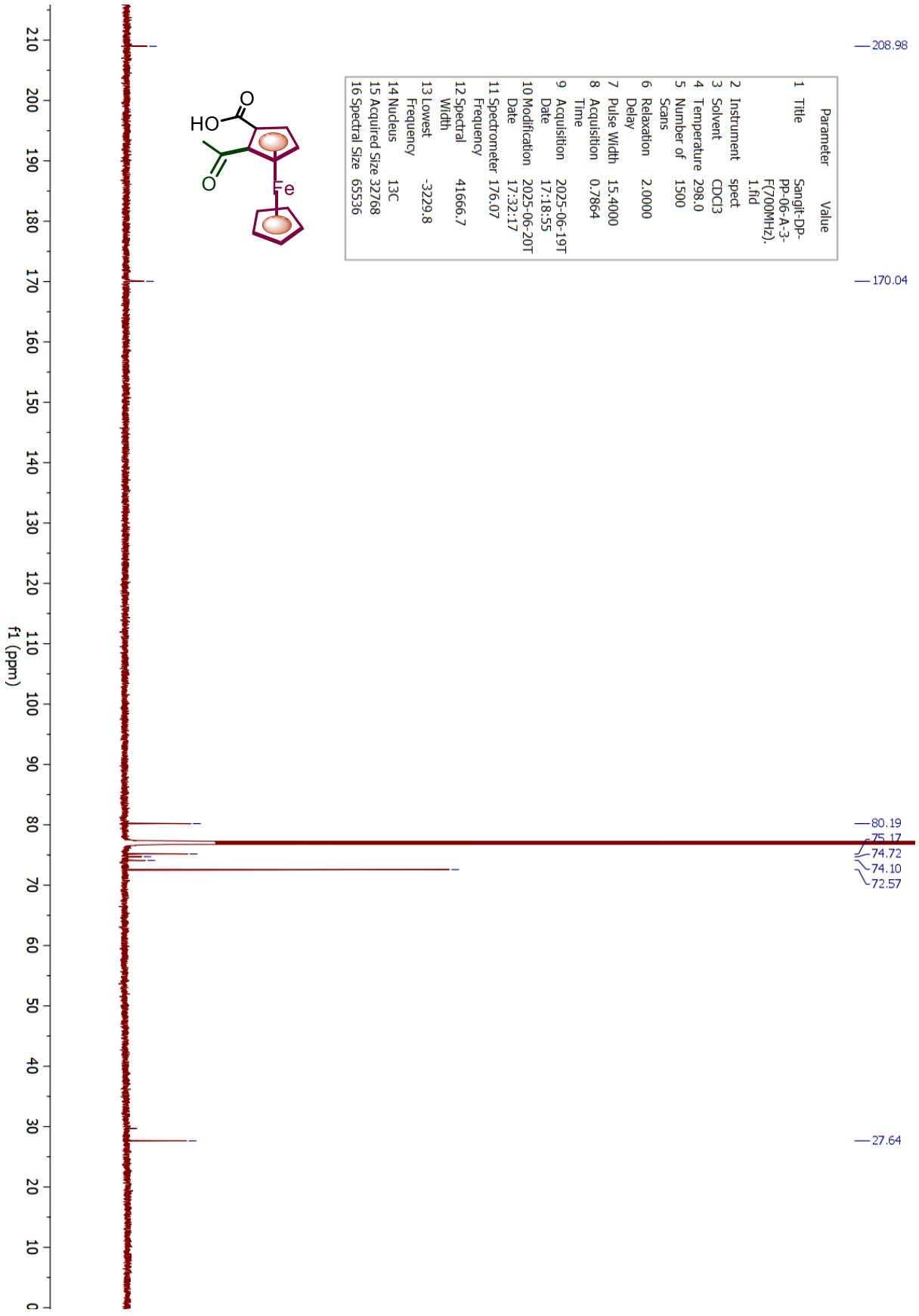

HRMS analysis of the reaction mixture of the synthesis of 1,2-keto ferrocene acid 4

Custom Workflow Report

Agilent Trusted Answers

Spectrum Peaks

m/z	m/z (Calc)	Diff (ppm)	Abund	Height %	Height % (Calc)	Ion Species	Z
410.1171	410.1167	1.00	5197	5.83	6.35	M+	1
411.1204	411.1201	0.77	1486	1.67	1.74	M+	1
412.1128	412.1121	1.84	89124	100.00	100.00	M+	1
413.1157	413.1152	1.24	24143	27.09	29.65	M+	1
414.1193	414.1177	3.88	3945	4.43	4.95	M+	1

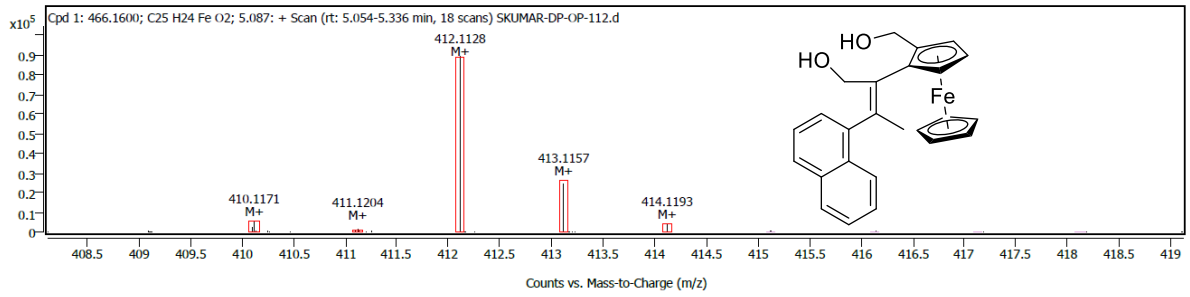

Spectrum Peaks

m/z	m/z (Calc)	Diff (ppm)	Abund	Height %	Height % (Calc)	Ion Species	Z
410.1171	410.1167	1.00	5197	5.83	6.35	M+	1
411.1204	411.1201	0.77	1486	1.67	1.74	M+	1
412.1128	412.1121	1.84	89124	100.00	100.00	M+	1
413.1157	413.1152	1.24	24143	27.09	29.65	M+	1
414.1193	414.1177	3.88	3945	4.43	4.95	M+	1

MassHunter Qual 10.0
(End of Report)

Custom Workflow Report

Agilent Trusted Answers

Spectrum Peaks

m/z	m/z (Calc)	Diff (ppm)	Abund	Height %	Height % (Calc)	Ion Species	Z
394.1217	394.1218	-0.12	5354	5.92	6.35	M+	1
395.1243	395.1252	-2.22	1976	2.19	1.74	M+	1
396.1179	396.1171	1.85	90376	100.00	100.00	M+	1
397.1209	397.1203	1.45	24055	26.62	29.61	M+	1
398.1238	398.1228	2.48	3848	4.26	4.73	M+	1

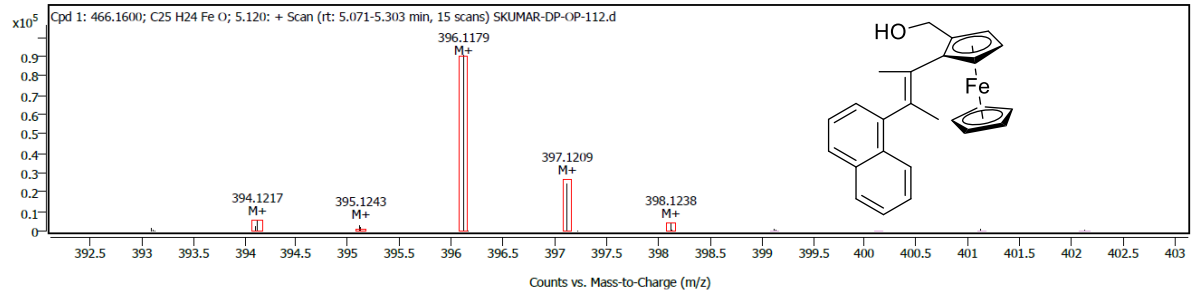

Spectrum Peaks

m/z	m/z (Calc)	Diff (ppm)	Abund	Height %	Height % (Calc)	Ion Species	Z
394.1217	394.1218	-0.12	5354	5.92	6.35	M+	1
395.1243	395.1252	-2.22	1976	2.19	1.74	M+	1
396.1179	396.1171	1.85	90376	100.00	100.00	M+	1
397.1209	397.1203	1.45	24055	26.62	29.61	M+	1
398.1238	398.1228	2.48	3848	4.26	4.73	M+	1

MassHunter Qual 10.0
(End of Report)

Custom Workflow Report

Agilent Trusted Answers

Spectrum Peaks

m/z	m/z (Calc)	Diff (ppm)	Abund	Height %	Height % (Calc)	Ion Species	Z
408.0977	408.1010	-8.21	123	2.37	6.35	M+	1
409.1019	409.1044	-6.28	128	2.46	1.74	M+	1
409.1074	409.1089	-3.49	1545	7.70	6.35	(M+H)+	1
410.0943	410.0964	-5.06	5177	100.00	100.00	M+	1
410.1099	410.1123	-5.84	57	0.28	1.74	(M+H)+	1
411.1046	411.1042	0.87	20067	100.00	100.00	(M+H)+	1

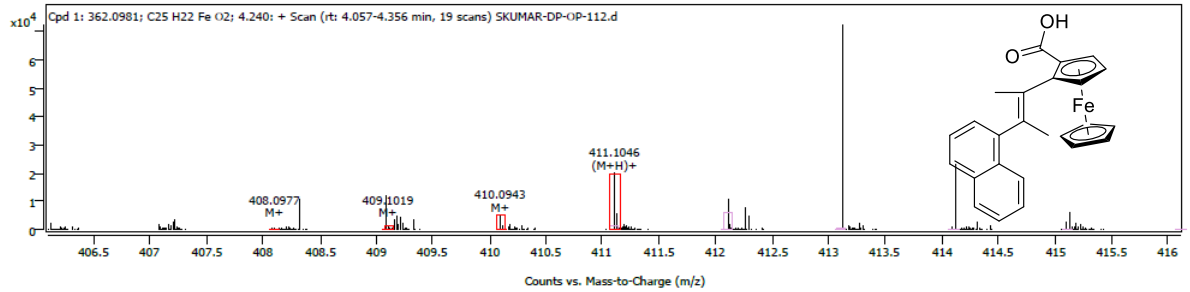

Spectrum Peaks

m/z	m/z (Calc)	Diff (ppm)	Abund	Height %	Height % (Calc)	Ion Species	Z
408.0977	408.1010	-8.21	123	2.37	6.35	M+	1
409.1019	409.1044	-6.28	128	2.46	1.74	M+	1
409.1074	409.1089	-3.49	1545	7.70	6.35	(M+H)+	1
410.0943	410.0964	-5.06	5177	100.00	100.00	M+	1
410.1099	410.1123	-5.84	57	0.28	1.74	(M+H)+	1
411.1046	411.1042	0.87	20067	100.00	100.00	(M+H)+	1

MassHunter Qual 10.0
(End of Report)

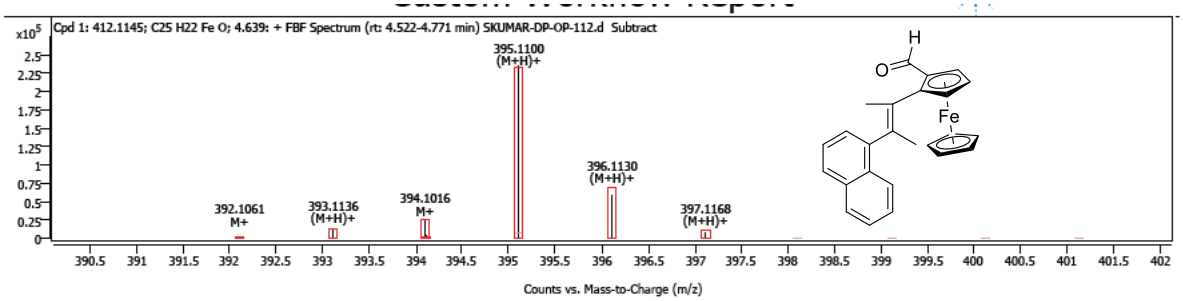

Spectrum Peaks

m/z	m/z (Calc)	Diff (ppm)	Abund	Height %	Height % (Calc)	Ion Species	Z
392.1061	392.1061	-0.05	1980	8.07	6.35	M+	1
393.1136	393.1140	-0.87	12484	5.34	6.35	(M+H)+	1
394.1016	394.1015	0.19	24550	100.00	100.00	M+	1
394.1159	394.1173	-3.70	3628	1.55	1.74	(M+H)+	1
395.1100	395.1093	1.64	233643	100.00	100.00	(M+H)+	1
396.1130	396.1124	1.43	58770	25.15	29.60	(M+H)+	1
397.1168	397.1150	4.57	7439	3.18	4.73	(M+H)+	1

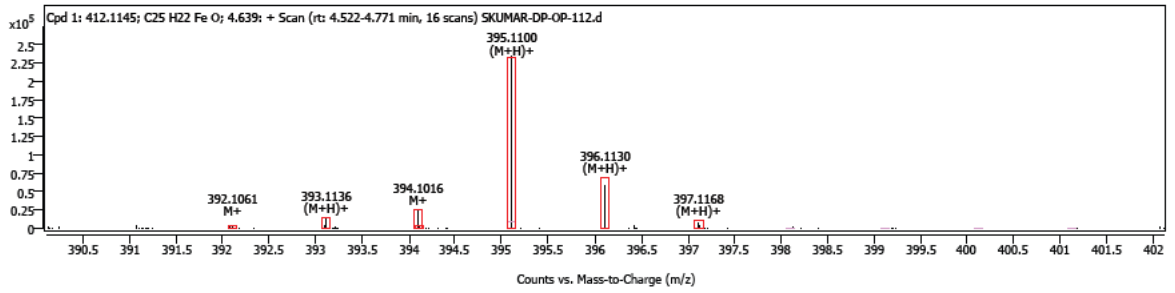

Spectrum Peaks

m/z	m/z (Calc)	Diff (ppm)	Abund	Height %	Height % (Calc)	Ion Species	Z
392.1061	392.1061	-0.05	1980	8.07	6.35	M+	1
393.1136	393.1140	-0.87	12484	5.34	6.35	(M+H)+	1
394.1016	394.1015	0.19	24550	100.00	100.00	M+	1
394.1159	394.1173	-3.70	3628	1.55	1.74	(M+H)+	1
395.1100	395.1093	1.64	233643	100.00	100.00	(M+H)+	1
396.1130	396.1124	1.43	58770	25.15	29.60	(M+H)+	1
397.1168	397.1150	4.57	7439	3.18	4.73	(M+H)+	1

MassHunter Qual 10.0
(End of Report)

Custom Workflow Report

Agilent Trusted Answers

Spectrum Peaks

m/z	m/z (Calc)	Diff (ppm)	Abund	Height %	Height % (Calc)	Ion Species	Z
443.1113	443.1144	-6.80	70	9.10	6.35	(M+H)+	1
444.1028	444.1019	2.11	430	100.00	100.00	M+	1
445.1035	445.1050	-3.44	209	48.58	29.73	M+	1
445.1094	445.1097	-0.70	771	100.00	100.00	(M+H)+	1

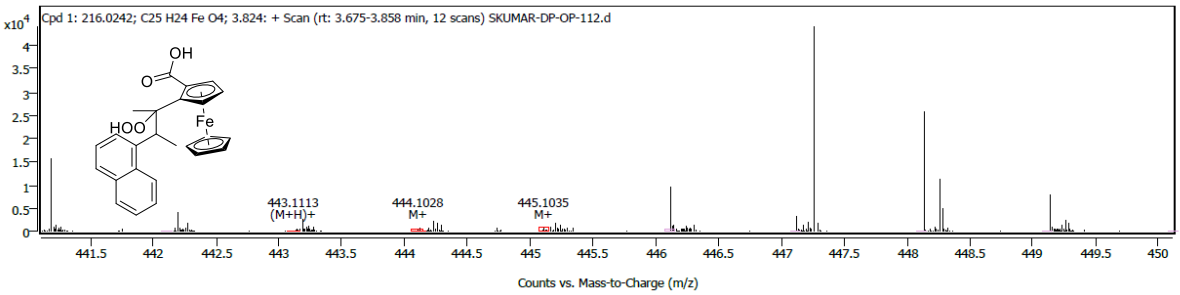

Spectrum Peaks

m/z	m/z (Calc)	Diff (ppm)	Abund	Height %	Height % (Calc)	Ion Species	Z
443.1113	443.1144	-6.80	70	9.10	6.35	(M+H)+	1
444.1028	444.1019	2.11	430	100.00	100.00	M+	1
445.1035	445.1050	-3.44	209	48.58	29.73	M+	1
445.1094	445.1097	-0.70	771	100.00	100.00	(M+H)+	1

MassHunter Qual 10.0
(End of Report)

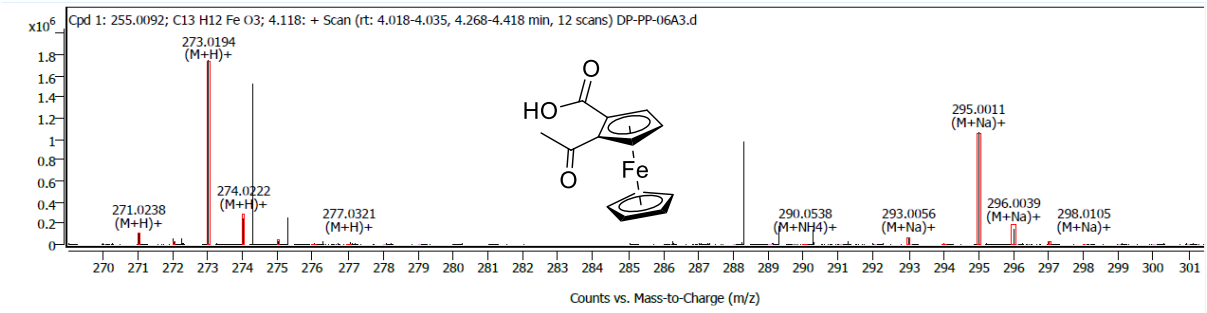

Spectrum Peaks

m/z	m/z (Calc)	Diff (ppm)	Abund	Height %	Height % (Calc)	Ion Species	Z
271.0238	271.0255	-6.46	93224	5.34	6.36	(M+H)+	1
272.0267	272.0289	-8.21	16210	0.93	0.91	(M+H)+	1
273.0194	273.0209	-5.57	1745020	100.00	100.00	(M+H)+	1
274.0222	274.0239	-6.07	241502	13.84	16.63	(M+H)+	1
275.0243	275.0253	-3.66	26635	1.53	2.20	(M+H)+	1
277.0321	277.0294	9.76	402	0.02	0.02	(M+H)+	1
290.0538	290.0474	21.92	77	100.00	100.00	(M+NH4)+	1
293.0056	293.0075	-6.48	59052	5.55	6.36	(M+Na)+	1
294.0089	294.0109	-6.62	8388	0.79	0.91	(M+Na)+	1
295.0011	295.0028	-5.85	1063385	100.00	100.00	(M+Na)+	1
296.0039	296.0058	-6.33	146370	13.76	16.61	(M+Na)+	1
297.0066	297.0073	-2.24	15666	1.47	2.20	(M+Na)+	1
298.0105	298.0094	3.64	876	0.08	0.21	(M+Na)+	1

MassHunter Qual 10.0
(End of Report)

References

(1) Q. Wang, Y. H. Nie, C. X. Liu, W. W. Zhang, Z. J. Wu, Q. Gu, C. Zheng, and S.-L. You, *ACS Catal*., 2022, **12**, 3083−3093.

(2) Z. Zhao, L. Racicot, and G. K. Murphy, *Angew. Chem. Int. Ed*., 2017, **56**, 11620-11623.

(3) (a) B. -F. Shi, N. Maugel, Y. H. Zhang, and J. -Q. Yu, *Angew. Chem. Int. Ed.,* 2008, **47**, 4882–4886. (b) J.-M. Gonzalez, X. Vidal, M.-A. Ortunno, J.-L. Mascarennas, and M. Gulias, *J. Am. Chem. Soc.,* 2022, **144**, 21437−21442.